Chemical Engineering Report Series

Kemian laitetekniikan raporttisarja No. 57

Espoo 2010

# PROCESS EQUIPMENT MODELING USING THE MOMENT METHOD

**Jonas Roininen**

Aalto University
School of Science
and Technology

Chemical Engineering Report Series
Kemian laitetekniikan raporttisarja No. 57
Espoo 2010

# PROCESS EQUIPMENT MODELING USING THE MOMENT METHOD

**Jonas Roininen**

Doctoral dissertation for the degree of Doctor of Science in Technology to be presented with due permission of the Faculty of Chemistry and Materials Sciences for public examination and debate in Auditorium KE2 (Komppa Auditorium) at the Aalto University School of Science and Technology (Espoo, Finland) on the 22nd of October 2010 at 12 noon.

Aalto University
School of Science and Technology
Faculty of Chemistry and Materials Sciences
Department of Biotechnology and Chemical Technology

Aalto-yliopisto
Teknillinen korkeakoulu
Kemian ja materiaalitieteiden tiedekunta
Biotekniikan ja kemian tekniikan laitos

Distribution:
Aalto University
School of Science and Technology
Chemical Engineering
P. O. Box 16100
FI-00076 AALTO
Tel. + 358-9-4702 2634
Fax. +358-9-4702 2694
E-mail: jonas.roininen@tkk.fi



ISBN 978-952-60-3292-4
ISSN 1236-875X

Multiprint Oy
Espoo 2010

## Abstract

Process equipment models are needed in all stages of chemical process research and design. Typically, process equipment models consist of systems of partial differential equations for mass and energy balances and complicated closure models for mass transfer, chemical kinetics, and physical properties. The scope of this work is further development of the moment method for modeling applications that are based on the one-dimensional axial dispersion model. This versatile model can be used for most process equipment, such as chemical reactors, adsorbers and chromatographic columns, and distillation and absorption columns.

The moment method is a numerical technique for partial differential equations from the class of weighted residual methods (WRM). In this work it is shown with examples how the moment method can be applied to process equipment modeling. The examples are: catalyst activity profiles in fixed-bed reactors, dynamic modeling of chemical reactors and fixed-bed adsorbers with axial dispersion, and steady-state and dynamic modeling and simulation of continuous contact separation processes with or without axial dispersion.

An innovative field of application of the moment method is continuous-contact separation processes. The advantage of the moment method, compared to the state-of-the-art nonequilibrium stage model, is that the same level of numerical accuracy can be achieved with fewer variables. In addition, the degree of axial dispersion can be controlled precisely since only physical axial dispersion is introduced via the axial dispersion coefficient.

When using axial dispersion models, special attention has to be paid to the boundary conditions. Using the moment transformation it is shown that the Danckwerts boundary conditions are appropriate for time-dependent models in closed-closed geometries. An advantage of the moment method, compared to other weighted residual methods such as orthogonal collocation on finite elements, is the ease with which boundary conditions are specified. The boundary conditions do not arise as additional algebraic equations. Instead, they simply appear as additive source terms in the moment transformed model equations.

The second part of this thesis deals with the detailed closure models that are needed for process modeling. Relevance of some of the closure models is scrutinized in particular with two test cases. The first test case is gas-liquid mass transfer coefficients in trickle-bed reactors. It is shown that the correlation of Goto and Smith is appropriate for gas-liquid mass transfer coefficients in industrial trickle-bed reactors. The second test case is vapor-liquid equilibrium model parameters for binary systems of *trans*-2-butene and *cis*-2-butene and five alcohols. The Wilson model parameters for all binary systems are fitted against measurements with a total pressure apparatus. The measured pressure-composition profiles are compared against predictions by the UNIFAC and UNIFAC-Dortmund methods.

## Tiivistelmä

Prosessilaitteiden matemaattiset mallit ovat välttämättömiä prosessikehityksen kaikissa vaiheissa. Nämä mallit koostuvat tyypillisesti aine- ja energiataseita kuvaavista osittaisdifferentiaaliyhtälöryhmistä sekä täydentävistä aineensiirto-, reaktiokinetiikka- ja termodynamiikkamalleista. Tämän työn tavoitteena on kehittää momenttimenetelmänä tunnettua osittaisdifferentiaaliyhtälöiden ratkaisumenetelmää erityisesti sellaisia mallinnuskohteita varten, joihin voidaan soveltaa yksiulotteista aksiaalidispersiomallia. Tätä mallia voidaan käyttää lähes kaikkien prosessilaitteiden, kuten reaktoreiden, adsorbereiden, kromatografiakolonnien sekä tislaus- ja absorptiokolonnien, mallitukseen.

Momenttimenetelmä on eräs osittaisdifferentiaaliyhtälöiden numeerinen ratkaisumenetelmä, joka kuuluu painotetun residuaalin menetelmien luokkaan. Tässä työssä on esitetty esimerkein kuinka menetelmää voidaan soveltaa prosessilaitteiden mallitukseen. Esimerkit ovat: katalyytin aktiivisuusprofiilin mallinnus kiintokerrosreaktorissa, aksiaalidispersiota sisältävä dynaaminen reaktori- tai adsorberimalli, sekä tislauskolonnin tasapainotilan ja dynaaminen mallitus ja simulointi, jossa aksiaalidispersio voidaan ottaa huomioon.

Erityisen innovaativinen momenttimenetelmän sovellus on sen käyttö differentiaalikosketuslaitteiden mallituksessa. Momenttimenetelmän etu yleisesti käytettyyn epätasapainoaskelmalliin verrattuna on parempi numeerinen tarkkuus yhdistettynä pienempään muuttujien lukumäärään. Tämän lisäksi aksiaalidispersiota voidaan mallittaa hyvin tarkasti, koska malliin sisältyy ainoastaan fysikaalista diffuusiota, jota voidaan säädellä aksiaalidispersiokertoimen avulla.

Aksiaalidispersiomallien yhteydessä on kiinnitettävä erityistä huomiota reunaehtojen määrittelyyn. Momenttimenetelmän avulla osoitetaan, että Danckwertsin reunaehtoja voidaan soveltaa aikariippuviin tapauksiin suljetussa geometriassa. Momenttimenetelmän etu muihin painotetun residuaalin menetelmiin, esimerkiksi ortogonaaliseen kollokaatioon, verrattuna on reunaehtojen määrittelemisen helppous. Reunaehdot eivät esiinny malleissa algebrallisina lisäyhtälöinä, vaan additiivisina lähdetermeinä, jotka lisätään momenttimuunnettuihin malliyhtälöihin.

Väitöskirjan toinen osa käsittelee eräitä lisämalleja, jotka ovat välttämättömiä prosessilaitteiden mallinnuksen kannalta. Näiden mallien merkitystä tarkastellaan kahden esimerkin avulla. Ensimmäinen esimerkki käsittelee kaasu-nesteaineensiirtokertoimia triklekerrosreaktorissa, ja siinä osoitetaan että Goton ja Smithin aineensiirtokorrelaatio soveltuu käytettäväksi teollisen mittakaavan triklekerrosreaktoreissa. Toinen esimerkki käsittelee höyry-nestetasapainoa binäärisysteemeissä, jotka koostuvat *trans*-2- tai *cis*-2-buteenista ja viidestä eri alkoholista. Wilsonin mallin parametrit sovitetaan kokonaispainelaitteistolla kerätyn mittausaineiston avulla. Mitattuja koostumus-paineprofiileja verrataan UNIFAC- ja UNIFAC-Dortmund-menetelmillä laadittuihin ennustuksiin.

## Preface

I did the research for this dissertation as a member of the Chemical Engineering Research Group at the Department of Biotechnology and Chemical Technology at Aalto University School of Science and Technology (former Helsinki University of Technology) between November 2007 and March 2010. I thank all people and organizations who have contributed to this thesis, and especially those listed below.

First and foremost, I thank my supervisor Professor Ville Alopaeus for his guidance during the years. He has not only been a teacher to me, but also a mentor, a co-author, a colleague, and a friend. Without his contribution, this work would not have been possible. Despite being very busy, he had always time to listen to my concerns and he constantly encouraged me to come up with own ideas for research topics.

I also thank our former Professor of Chemical Engineering Juhani Aittamaa, who encouraged me to join his research group in the first place. He continued to give me advice and guidance even after he left the university.

I express my gratitude to all of my other co-authors, namely Dr. Sami Toppinen, Gijsbert Wierink, Dr. Petri Uusi-Kyyny, Dr. Juha-Pekka Pokki, and Minna Pakkanen for their contributions to this thesis. I thank all the other staff at the Chemical Engineering and Plant Design Research Groups for their support and companionship, and especially Lasse Westerlund and Sirpa Aaltonen for their help with administrative issues.

This work was for the most part funded by the Graduate School of Chemical Engineering, and I warmly thank them for the financial support. Their funding made it possible for me to maintain academic freedom and focus on research topics from my own fields of interest.

And last but not least, I thank my parents and my sisters for their everlasting support and encouragement during this project.

Otaniemi, Espoo, September 8, 2010

Jonas Roininen

## List of Publications

This thesis is based on the following publications (Appendices I – VI), which are referred to in the text by their Roman numerals.

[I] Roininen, J., Alopaeus, V., 2008. Modeling of Catalyst Activity Profiles in Fixed-Bed Reactors with a Moment Transformation Method. *Industrial & Engineering Chemistry Research,* 47, 8192-8196.

[II] Roininen, J., Alopaeus, V., 2010. The Moment Method for One-Dimensional Dynamic Reactor Models with Axial Dispersion. *Computers & Chemical Engineering,* in press, 11 pages.

[III] Roininen, J., Alopaeus, V., 2010. Dynamic Simulation of Continuous-Contact Separation Processes with the Moment Transformation Method. *Industrial & Engineering Chemistry Research,* 49, 3365-3373.

[IV] Roininen, J., Alopaeus, V., Toppinen, S., Aittamaa, J., 2009. Modeling and Simulation of an Industrial Trickle-Bed Reactor for Benzene Hydrogenation: Model Validation against Plant Data. *Industrial & Engineering Chemistry Research,* 48, 1866-1872.

[V] Roininen, J., Uusi-Kyyny, P., Pokki, J.-P., Pakkanen, M., Alopaeus, V, 2008. Vapor–Liquid Equilibrium for the Systems trans-2-Butene + Methanol, + 1-Propanol, + 2-Propanol, + 2-Butanol, and + 2-Methyl-2-propanol at 364.5 K. *Journal of Chemical & Engineering Data,* 53, 607-612.

[VI] Wierink, G., Roininen, J., Uusi-Kyyny, P., Pokki, J.-P., Pakkanen, M., Alopaeus, V, 2008. Vapor−Liquid Equilibrium for the cis-2-Butene + Methanol, + 2-Propanol, + 2-Butanol, + 2-Methyl-2-propanol Systems at 364.5 K. *Journal of Chemical & Engineering Data,* 53, 1539-1544.

## Author's Contributions to the Appended Publications

[I] The author participated in the model development, chose the example system, performed the calculations, analyzed the results with the co-author, and wrote the paper.

[II] The author developed the model, performed the calculations, analyzed the results with the co-author, and wrote the paper.

[III] The author developed the model, performed the calculations, analyzed the results with the co-author, and wrote the paper.

[IV] The author performed the calculations, analyzed the results with the co-authors, and wrote the paper.

[V] The author fitted the model parameters against the data, analyzed the results with the co-authors, and wrote the paper.

[VI] The author fitted the model parameters against the data, analyzed the results with the co-authors, and assisted in writing the paper.

## Table of Contents

# 1 Introduction

Present-day chemical engineering is not imaginable without mathematical models for the various pieces of process equipment that are used in chemical processing. Models are needed in all stages of chemical engineering research and design, from the earliest concepts to process control and retrofitting. Mathematical models are, by definition, an abstraction of the physical world and always a compromise between accuracy and usability. However, with the exponential increase of computing power in the last decades, process modeling has taken giant leaps towards increasingly complex models that can represent the physical world more and more realistically. For example, computational fluid dynamics (CFD) has become a viable tool in process equipment design, and it is often used for analyzing the flow patterns in column internals and providing pseudo-experimental data for parameter fitting. This development has led to significant acceleration of process research and design, as time-consuming experiments can be more often replaced with modeling and simulation.

Still, until the present day, modeling concepts are being taught and used that are at least inaccurate and in the worst case plain wrong. Such concepts are for example the plug-flow assumption, the equilibrium stage, and the continuous stirred tank (CSTR) and CSTR-in-series models. (Churchill, 2007) These concepts may still have their justified fields of application, but their limitations should be known and understood, and advanced, more realistic models should be preferred. For example, plug-flow-reactor and CSTR or CSTR-in-series models can be replaced with the general axial dispersion model, of which the plug-flow reactor and the CSTR are the two limiting cases. The idea of the axial dispersion model is to parameterize the complex physical processes that cause back mixing and model them with a diffusion-like second-order term. Despite its relative simplicity, the axial dispersion model is a very good model for reasons that are discussed in this thesis.

The limitations of the equilibrium stage model for distillation and absorption are already widely accepted, and many simulation tools that are based on the nonequilibrium stage concept are available nowadays. This is certainly an improvement compared to the equilibrium stage model, since the nonequlibrium stage model is based on actual interphase mass transfer rates, whereas the equilibrium stage model is based only on phase equilibrium. It must be kept in mind, though, that the double film model of mass transfer, which is a central element of the nonequilibrium stage model, is also an abstraction that relies on empirical correlations for mass transfer coefficients. In addition, the nonequilibrium stage model still contains the unjustified CSTR-in-series approximation that brings along a high degree of numerical diffusion. Although numerical diffusion can be exploited for modeling physical axial dispersion, the problem still remains that it depends on the numerical solution of the model rather than on the physics of the system.

The motivation for the use of those simplified methods is of course the relative ease of their solution. Generally speaking, the more realistic but complicated models cannot be readily solved with the standard methods available in mathematical packages. However, alternative mathematical methods are available that can be implemented in many process

simulators. One class of these methods is the class of Weighted Residual Methods (WRM). One particular WRM is the moment method that is the main subject of this thesis.

The starting point for this thesis is the paper by Alopaeus *et al.* (2008) that presents the moment method in the form in which it is applied here. Naturally, the idea of the moment method is older, but its applications in chemical engineering have been few. (Finlayson, 1980) So far, probably the most important application of the moment method in the realm of chemical engineering is in population balances. (Alopaeus *et al.*, 2006b)

Three of the six publications that constitute this thesis, namely [I] – [III], present refinements and further applications of the moment method. Publication [I] discusses a special application, namely the modeling of catalyst activity profiles in fixed-bed reactors. Publication [II] presents the general formulation of the moment method for axial dispersion models with some examples and a discussion of the boundary conditions. Publication [III] shows how the moment method can be used for dynamic modeling of continuous-contact separation processes.

It must be kept in mind that with increasing complexity of the models used, more physical and chemical data is needed. For example, the equilibrium stage model requires only an accurate VLE model, whereas the nonequilibrium stage model requires mass and heat transfer correlations, physical property correlations, and other physical data and technical specifications. Publications [IV] – [VI] concern the complicated closure models and the data that are necessary for using detailed process equipment models. Publication [IV] deals with the validation of mass transfer correlations for trickle-bed reactors, and Publications [V] and [VI] deal with vapor-liquid equilibria in some $C_4$-alkene + alcohol systems, a class of components that is encountered for example in the synthesis of methyl-*tert*-butyl-ether by reactive distillation.

# 2 Modeling of Process Equipment

## 2.1 Chemical Engineering Models

The grand unifying concept that has shaped the chemical engineering profession more than anything else is the concept of unit operations: the commonality of heat transfer, fluid flow, evaporation, distillation, etc. as elements of design for all chemical plants irrespective of the process or products. (Churchill, 2007) Traditionally, chemical engineering education and design has been characterized by the use of dedicated unit operation models, probably the most prominent examples being the equilibrium stage model for distillation and the ideal reactor models for chemical reactors. Common to these simple models is a high degree of abstraction that tends to obscure the commonality of the physical principles, such as fluid flow, mass transfer, and chemical kinetics, which apply to each of the unit operations.

An idea that has fundamentally transformed the chemical engineering view of modeling of process equipment is the transport phenomena approach, which was promoted in a seminal book of the same name by Bird *et al.* (1960). This book first presented the idea that all process equipment could be modeled with a unified approach that was governed by the principles of mass, heat, and momentum transfer. (Churchill, 2007) A major shortcoming at the time of the book's first publication was the limited scope of the problems that was mathematically tractable with the mainly analytical methods it presented, since powerful numerical methods were still unavailable at the time. However, in the decades to follow the situation changed dramatically due to the unforeseen increase in computational power and the rapid development in numerical methods. Following the transport phenomena approach, the universal principles common to different process equipment models are further explored in the sections to follow, beginning with the convection-dispersion equation.

## 2.2 The Convection-Dispersion Equation

The basis for all modeling approaches based on the transport phenomena concept is a partial differential equation of the form:

$$\underset{\text{accumulation}}{\frac{\partial \Psi}{\partial t}} = \underset{\text{convection}}{-\left(\nabla \cdot \Psi \vec{U}\right)} + \underset{\text{dispersion}}{\left(\nabla \cdot D \nabla \Psi\right)} + \underset{\text{source}}{S\left(\Psi, \vec{r}\right)} \tag{2.1}$$

$\Psi$ is the concentration of some property, $D$ is the axial dispersion coefficient, and $S$ is a general source term. If we insert $\Psi \equiv C$ we obtain a mass balance based on concentration, and if we insert $\Psi \equiv \rho C_p T$ we obtain an energy balance based on enthalpy. Strictly speaking, this is an approximation of the energy balance in liquid systems when the physical properties can be assumed constant. Here, this form of the energy balance should be understood as a model equation, rather than a design equation. In this work, only one-dimensional models are considered. In one-dimensional form, eq (2.1) becomes:

$$\frac{\partial \Psi}{\partial t} = -\frac{\partial (u\Psi)}{\partial z} + \frac{\partial}{\partial z}\left( D \frac{\partial \Psi}{\partial z} \right) + S(\Psi, z) \tag{2.2}$$

Eq (2.2) is the basic model equation that can be used for almost all process equipment, such as chemical reactors, adsorbers, and absorption and distillation columns.

In this work, eq (2.2) is understood as a macroscopic model for convection, dispersion, and generation in chemical process equipment. These phenomena usually take place in a catalyst bed or a column packing. Formally, eq (2.2) is identical with the convection-diffusion equation for a species in a mixture in microscopic scale. The difference is that in microscopic scale the diffusion of a species is based on diffusion laws that are exact natural laws, whereas the dispersion term in the macroscopic convection-dispersion equation should be understood as a model for the various physical phenomena that cause dispersion, such as molecular diffusion, turbulence, and residence time distribution. Therefore, the axial dispersion coefficient $D$ in eq (2.2) is not a physical property, but a model parameter that is dependent on factors such as the packing type, flow regime, and physical properties of the fluid.

Two common assumptions are: constant velocity $u$ and constant axial dispersion coefficient $D$. In this case, eq (2.2) can be simplified to:

$$\frac{\partial \Psi}{\partial t} = -u \frac{\partial \Psi}{\partial z} + D \frac{\partial^2 \Psi}{\partial z^2} + S(\Psi, z) \tag{2.3}$$

Eq (2.3) is a linear partial differential equation, since it is linear with respect to the partial derivatives of $\Psi$. If the axial dispersion coefficient is zero, eq (2.3) is a hyperbolic partial differential equation. Otherwise, eq (2.3) is a parabolic partial differential equation. The two limiting cases of the model are plug-flow for $D \rightarrow 0$ and complete backmixing for $D \rightarrow \infty$.

A different approach to axial dispersion and residence time distribution problems is stochastic modeling, in which the movement of fluid elements through the domain is treated as a series of probabilistic events. (e.g., Krambeck *et al.*, 1967, Fan *et al.*, 1995, Alopaeus *et al.,* 2006a) Those models are outside the scope of this thesis.

## 2.3 Boundary Conditions

The boundary conditions are an important part of the axial dispersion model. As mentioned above, eq (2.3) is a parabolic partial differential equation when $D > 0$. This means that boundary conditions must be specified at every spatial boundary (inflow and outflow boundary in the one-dimensional case). There are two cases that need to be considered: boundary conditions for closed vessels and boundary conditions for open vessels. (Fogler, 1999) By the definition used here, a closed vessel is one where there is no axial dispersion either upstream or downstream of the reactive section (or catalyst bed, column packing, etc.). In an open vessel, axial dispersion is present upstream and downstream of the reactive section. Figure 1 shows a schematic representation of these two cases.

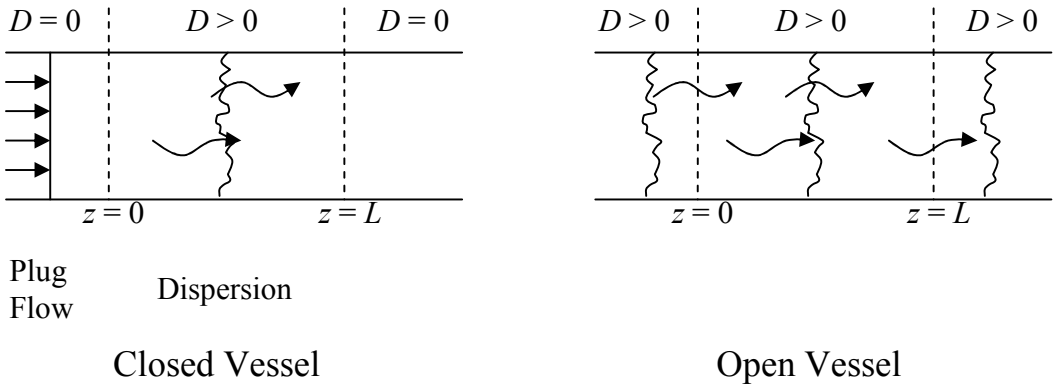


**Figure 1. Types of boundary conditions.**

From a mathematical viewpoint, there are three types of boundary conditions. They can be easily associated with physical boundary conditions for example in the case of heat transfer. The three types of boundary conditions are (in the parenthesis the physical interpretation for heat transfer is given): Dirichlet boundary condition, the function value is given at the domain boundary (constant temperature of the boundary); Neumann boundary condition, the derivative is given at the boundary (constant heat flux across the boundary); And Robin boundary condition, which is a linear combination of the Dirichlet and Neumann boundary conditions (convection at the boundary, the heat flux depends linearly on the temperature of the boundary).

The appropriate boundary conditions for the convection-dispersion model are not so straightforward. The famous Danckwerts (1953) boundary conditions for closed-closed geometries are: a Robin-type boundary condition at the inflow boundary, and a Neumann-type boundary condition at the outflow boundary:[1]

Inflow:

$$\Psi_0 = \Psi\left(z = 0^+, t\right) - \frac{D}{u}\left(\frac{\partial \Psi}{\partial z}\right)_{z=0^+} \tag{2.4}$$

Outflow:

$$\left(\frac{\partial \Psi}{\partial z}\right)_{z=L} = 0 \tag{2.5}$$

The physical implication of the Danckwerts boundary conditions is that the dispersive flux across the domain boundaries is zero. This depicts an idealized physical case where the mechanics that cause axial dispersion vanish immediately before the reactor entrance and after the reactor exit. The characteristic feature of the Danckwerts boundary conditions is the discontinuity at the domain entrance. The effects of the Dankwerts boundary conditions are shown in Figure 2.

[1] The same boundary conditions were already suggested by Langmuir (1908).

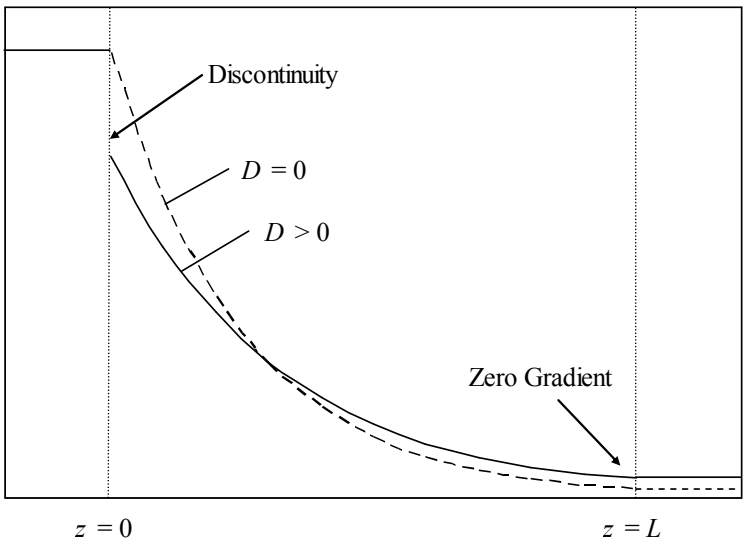


**Figure 2. The effects of Danckwerts boundary conditions.**

Originally, Danckwerts derived his boundary conditions based on intuition rather than on physics. The Danckwerts boundary conditions were derived for the steady-state case in papers by Wehner and Wilhelm (1956) and Bischoff (1961). A note by Acrivos in the paper of Wehner and Wilhelm (1956) suggests that the Danckwerts boundary conditions would also apply for the unsteady case in closed-closed vessels. Parulekar and Ramkrishna (1984a, 1984b, 1984c) analyzed systematically different types of boundary conditions in dynamic systems using integral transforms. They found that the Danckwerts boundary conditions are a special case when the axial dispersion coefficient before and after the domain is zero (closed-closed-conditions).

In open-open vessels, the boundary condition at either boundary is:

$$\Psi\left(z = L^{-}, t\right) - \frac{D^{-}}{u}\left(\frac{\partial \Psi}{\partial z}\right)_{z=L^{-}} = \Psi\left(z = 0^{+}, t\right) - \frac{D^{+}}{u}\left(\frac{\partial \Psi}{\partial z}\right)_{z=0^{+}} \tag{2.6}$$

Publication [II] contains a derivation of the boundary conditions using the moment transformation method, similar to the analysis of Parulekar and Ramkrishna (1984a).

Golz and Dorroh (2001) and Golz (2003) discuss the time-variant boundary conditions of the convection-diffusion equation and argue that the Danckwerts exit boundary condition should be replaced with a Robin-type condition similar to the one at the inlet. However, in lack of observations there can be no information about the exit concentration *a priori*, and the best guess that can be made is the zero-gradient exit proposed by Danckwerts. Golz and Dorroh (2001) suggest a method for estimating the exit concentration that can be used in the case of a linear source term. In chemical engineering applications, however, the source term is nonlinear in most cases, since it is usually a reaction rate expression or an interfacial mass transfer flux.

Although it appears that the issue of the Danckwerts boundary conditions still remains unresolved, it can be said at least that they are a very good approximation of the physical boundary conditions in closed-closed geometries, even in time-dependent cases. According to Golz and Dorroh (2001), the error caused by using the Danckwerts boundary conditions is inversely proportional to time and Péclet number. This implies that the Danckwerts boundary conditions apply exactly at a) steady state, when time $t \rightarrow \infty$, and b) when the Péclet number is large. Condition b) is fulfilled in most chemical engineering applications, as opposed to, for example, flow in underground reservoirs, where the slow convective velocity results in a rather low Péclet number.

## 2.4 Chemical Reactors with a Single Fluid Phase

### *2.4.1 Reactor Model*

The model equation for a chemical reactor with a single fluid phase is obtained directly from eq (2.2) by substituting the concentration of species *i* for Ψ:

$$\frac{\partial C_i}{\partial t} = -\frac{\partial (uC_i)}{\partial z} + \frac{\partial}{\partial z}\left( D\frac{\partial C_i}{\partial z} \right) + \nu_i R \tag{2.7}$$

In deriving eq (2.7), it is assumed that the reaction takes place in the fluid and the concentration is expressed as moles per fluid volume. If the reaction takes place in the catalyst phase and the reaction rate is expressed per catalyst mass, then the source term becomes, by this definition:

$$S = \frac{1-\varepsilon}{\varepsilon} R \tag{2.8}$$

For elementary chemical reactions, the reaction rate term is of the form:

$$R = k_0 \exp\left( -\frac{E_a}{RT} \right) \prod_{i=1}^{nc} C_i^{\alpha_i} \tag{2.9}$$

The order of the reaction $\alpha$ is usually not higher than two. Often the kinetic expression for a catalytic reaction is far more complicated than eq (2.9). If mass transfer to the catalytic material is taken into account, then the source term in eq (2.7) is replaced with the fluid-solid mass transfer flux $N_{FSi} a_S$. If the reactor is a packed-bed reactor that is filled with a porous material, then the velocity *u* in eq (2.7) is the interstitial velocity that can be defined as:

$$u = \frac{\dot{V}}{\varepsilon A} \tag{2.10}$$

The interstitial velocity is the average velocity of the fluid in the interstices of the packing material. The true local velocity of a fluid element depends on the local flow conditions in the interstices of the bed and can be very different from $u$.

In the case of linear reaction rate term $R = kC$ an analytical steady-state solution is given by Danckwerts (1953):

$$\frac{C}{C_0} = \exp\left(\frac{uz}{2D}\right)\left[\frac{2(1+a)\exp\left(\frac{ua(L-z)}{2D}\right) - 2(1-a)\exp\left(\frac{ua(z-L)}{2D}\right)}{(1+a)^2\exp\left(\frac{uaL}{2D}\right) - (1-a)^2\exp\left(-\frac{uaL}{2D}\right)}\right] \tag{2.11}$$

where

$$a = \sqrt{1+\frac{4kD}{u^2}} \tag{2.12}$$

Zheng and Gu (1996) derived an analytical solution for the time-dependent case, but unfortunately they used the Dirichlet boundary condition at the inlet instead of the more appropriate Danckwerts boundary condition.

For the plug-flow reactor ($D = 0$) the steady-state solution is:

$$\frac{C}{C_0} = \exp\left(-\frac{kz}{u}\right) \tag{2.13}$$

And for a continuous stirred tank reactor (CSTR) with complete backmixing ($D \to \infty$):

$$\frac{C}{C_0} = \frac{1}{1+\frac{kL}{u}} \tag{2.14}$$

The plug-flow and CST reactors are two types of ideal reactors (the third being the batch reactor). Figure 3 shows the effect of increasing $D$ on the concentration profile with the two ideal reactors as limiting cases.

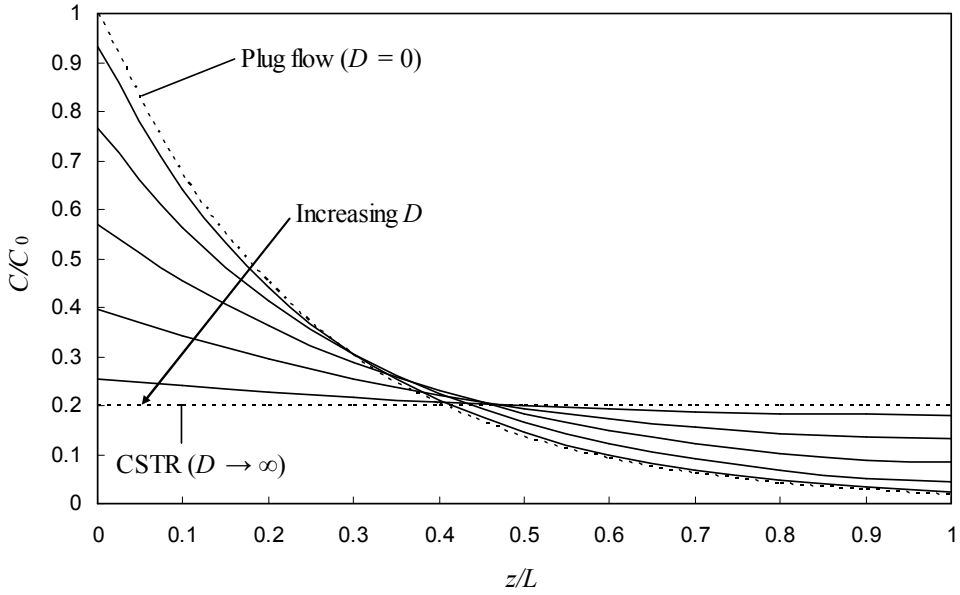


**Figure 3. Steady-state concentration profiles for different values of *D* with the two ideal reactors as limiting cases.**

### *2.4.2 Axial Dispersion Coefficient*

The major diffusion-type mixing mechanisms that cause axial dispersion are molecular diffusion and turbulent eddies. Both can be modeled with the second-order term in eqs (2.2) and (2.7). But the axial dispersion model can also be used to take into account radial mixing and other nonflat velocity profiles. (Fogler, 1999) When the flow profile is laminar, the concentration profiles along the streamlines can be integrated analytically. The result is the Aris-Taylor dispersion coefficient for laminar flow in a pipe:

$$D = D_{AB} + \frac{u^2 R^2}{48 D_{AB}} \tag{2.15}$$

The Aris-Taylor dispersion coefficient includes the distribution of residence times, as well as the molecular diffusion along a streamline and between streamlines. Correlations for the axial dispersion coefficient for turbulent flow in pipes and flow through packed beds can be found for example in Levenspiel (1972).

The axial dispersion coefficient can be determined experimentally by injecting a tracer into the reactor at some time $t = 0$ and measuring the tracer concentration in the effluent stream $C(t)$ as a function of time. The tracer can be injected either as a pulse or a step input. (Fogler, 1999) The residence time distribution (RTD) function $E(t)$ is defined as:

$$E(t) = \frac{C(t)}{\int_0^\infty C(t)dt} \tag{2.16}$$

The residence time distribution function can be used to detect nonidealities in reactor behavior, such as short-circuiting, channeling, and dead volumes.

The mean residence time $t_m$ can be calculated as the 1st moment of the RTD function: (Fogler, 1999)

$$t_m = \int_0^\infty tE(t)dt \tag{2.17}$$

In a closed system, the mean residence time is equal to the space-time:

$$t_m = \tau_S = \frac{V_r}{\dot{V}} \tag{2.18}$$

The variance of the dimensionless tracer concentration function of a pulse tracer input can be related to the axial dispersion coefficient. The formulas are: (Fogler, 1999)

For closed-closed systems:

$$\frac{\sigma^2}{t_m^2} = \frac{2}{\mathrm{Pe}} - \frac{2}{\mathrm{Pe}^2}\left(1 - e^{-\mathrm{Pe}}\right) \tag{2.19}$$

For open-open systems:

$$\frac{\sigma^2}{t_m^2} = \frac{2}{\mathrm{Pe}} + \frac{8}{\mathrm{Pe}^2} \tag{2.20}$$

Where:

$$t_m = \left(1 + \frac{2}{\mathrm{Pe}}\right)\tau_S \tag{2.21}$$

Using eqs (2.19) – (2.21), it is possible to determine the axial dispersion coefficient when experimental data for the residence time distribution is available.

### *2.4.3 Packed-Bed Adsorber and Chromatographic Separation*

Modeling of a packed bed adsorber or a chromatographic column requires that, in addition to the fluid phase, the state of the stationary phase as a function of time is taken into account as well. In the reactor model above it was assumed that the state of the catalyst depends directly on the state of the surrounding fluid without hysteresis effect.

For the concentration of species in the stationary phase, the variable $q$ is introduced. $q$ is a function of both the axial coordinate and time, but it is not affected by convection or diffusion like the concentration of species in the fluid, $C$.

A packed-bed adsorber or a chromatography column can be modeled using the same equation as a chemical reactor, with modification of the source term. Assuming uniform concentration inside the particles, the source term in the adsorber model is:

$$S = -\frac{\partial q}{\partial t} \tag{2.22}$$

This can be written as:

$$\frac{\partial q}{\partial t} = k_1\left(C - k_2 q\right) \tag{2.23}$$

$$k_1 = \frac{k_c a}{\varepsilon} \tag{2.24}$$

$$k_2 = \frac{\varepsilon}{K\left(1-\varepsilon\right)} \tag{2.25}$$

$k_c a$ is an effective mass transfer coefficient, and $K$ is the adsorption equilibrium coefficient between the fluid and the solid phase. Analytical solutions for systems without axial dispersion are given by Rice and Do (1995) for step input (packed-bed adsorber) and pulse input (chromatographic separation).

If it is assumed that there is no film resistance between the surface of the adsorbent and the fluid phase, the mass balance can be written as: (Liao and Shiau, 2000)

$$\frac{\partial C}{\partial t} = -u\frac{\partial C}{\partial z} + D\frac{\partial^2 C}{\partial z^2} - \frac{\rho_s K\left(1-\varepsilon\right)}{\varepsilon}\frac{\partial C}{\partial t} \tag{2.26}$$

Eq (2.26) can be simplified to:

$$R_d\frac{\partial C}{\partial t} = -u\frac{\partial C}{\partial z} + D\frac{\partial^2 C}{\partial z^2} \tag{2.27}$$

With a change of variables, eq (2.27) can be reduced to the linear convection-dispersion equation (cf. Section 5.2). The constant $R_d$ is a "retardation factor":

$$R_d = 1 + \frac{\rho_s K\left(1-\varepsilon\right)}{\varepsilon} \tag{2.28}$$

With certain assumptions, the equilibrium constant $K$ can also be modified to include the effect of nonuniform concentration within the adsorbent particles. (Liao and Shiau, 2000)

An analytical solution to the problem with Dirichlet boundary conditions at the inlet is available. (ibid)

## 2.5 Two- and Three-Phase Systems: Separations and Multiphase Reactors

### *2.5.1 Separation Processes*

Models for separation processes that are based on the equations of mass transfer rather than on the concept of the equilibrium stage are called rate-based models. A detailed discussion of the equilibrium stage model can be found, for example, in King (1980). Especially in academia, rate-based models have become state-of-the-art. Probably the most popular and well-known rate based model is the nonequilibrium stage model of Krishnamurthy and Taylor (1985a, 1985b), which is discussed in detail in Section 3.4.3. Historically, the nonequilibrium stage model is an evolution of the equilibrium stage model, in which the nonequilibrium stage is understood as a model for a distillation tray. The nonequilibrium stage model for packed columns (Krishnamurthy and Taylor, 1985b) is actually a discretized form of the continuous-contact separation process model, which is written in the form of partial differential equations.

Following the trend of process intensification, many separation processes are nowadays conceived as reactive separations. (Krishna, 2002, Noeres *et al.*, 2003) In principle, the equations for reactive systems are the same as for nonreactive systems, plus terms for the reaction rate and heat generation. For the sake of completeness, the model equations below are written with the reaction terms for the liquid phase. Then the rate-based model comprises the following equations:

Total buildup (i.e. the amount of vapor or liquid in moles per unit volume of column packing) in either phase (continuity equations):

$$\frac{\partial B_L}{\partial t} = -\frac{\partial L}{\partial z} + \sum_{i=1}^{nc} N_{iVL} a + \varepsilon h_L \sum_{i=1}^{nc} \nu_i R_L \tag{2.29}$$

$$\frac{\partial B_V}{\partial t} = -\frac{\partial V}{\partial z} - \sum_{i=1}^{nc} N_{iVL} a \tag{2.30}$$

Individual component buildup in either phase (with component dispersion):

$$\frac{\partial b_{iL}}{\partial t} = -\frac{\partial (x_i L)}{\partial z} + \frac{\partial}{\partial z}\left( D_L B_L \frac{\partial x_i}{\partial z} \right) + N_{iVL} a + \varepsilon h_L \nu_i R_L \tag{2.31}$$

$$\frac{\partial b_{iV}}{\partial t} = -\frac{\partial (y_i V)}{\partial z} + \frac{\partial}{\partial z}\left( D_V B_V \frac{\partial y_i}{\partial z} \right) - N_{iVL} a \tag{2.32}$$

Heat balances (in terms of enthalpy, with heat dispersion):

$$\frac{\partial(B_L H_L)}{\partial t} = -\frac{\partial(LH_L)}{\partial z} + \frac{\partial}{\partial z}\left(\alpha_L B_L \frac{\partial H_L}{\partial z}\right) + q_{VL}a + \varepsilon h_L \Delta H_R \sum_{i=1}^{nc} \nu_i R_L \tag{2.33}$$

$$\frac{\partial(B_V H_V)}{\partial t} = -\frac{\partial(VH_V)}{\partial z} + \frac{\partial}{\partial z}\left(\alpha_V B_V \frac{\partial H_V}{\partial z}\right) - q_{VL}a \tag{2.34}$$

The only difference between the equations for the $V$ and $L$ phases is the sign of the interfacial mass and heat transfer fluxes and the reaction rate $R$ in the reactive case. In countercurrent operation, the flow rate in one of the phases is given a negative sign. It is important to note that although the bulk phase mass and energy balances are written with the time derivatives, the vapor-liquid interface and the vapor and liquid films are assumed to be at equilibrium, meaning that there is no accumulation of mass or energy at the interface or in the films. For details on the calculation of the interphase mass and heat transfer fluxes, see Section 6.1.

It is assumed here that the reaction takes place in the liquid phase in a section of the column that is filled with catalytic packing. It is further assumed that the reaction takes place on the catalyst surface, yet the reaction is modeled as pseudohomogeneous. If the reaction is fast and takes place in the liquid phase, then the reaction in the liquid film must be taken into account as well. (Taylor and Krishna, 2000, Higler *et al.*, 1998)

Since the flow rates $V$ and $L$ are not constant along the axial coordinate, additional equations are needed to complete the set of partial differential equations (2.29) – (2.34). One possibility is to write the momentum conservation equations for both phases and solve them along with eqs (2.29) – (2.34). The momentum equations are nonlinear partial differential equations that require special solution algorithms, such as SIMPLE (Semi-Implicit Method for Pressure Linked Equations). Such methods have been developed especially for the simulation of fluid flows. (e.g., Fletcher, 1991, Ferziger and Perić, 2002)

An approach that is often used in chemical engineering is to use empirical correlations for liquid holdup and pressure drop. Liquid holdup is defined as the fraction of the interstitial volume of the packing that is occupied by liquid. Correlations for liquid holdup and pressure drop are of the form:

$$h_{L,corr} = f(V, L, x, y, T) \tag{2.35}$$

$$\frac{dP}{dz} = f(V, L, x, y, T) \tag{2.36}$$

Typical correlations are for example those of Buchanan (1969) for random packings and Rocha *et al.* (1993) for structured packings. Properties of many packing types can be found for example in Kister *et al.* (2008). The correlations of Buchanan that are used in [III] are:

$$\frac{h_L}{\varepsilon} = 2.2\left(\frac{\mathrm{Fr}_L}{\mathrm{Re}_L}\right)^{0.333} + 1.8\mathrm{Fr}_L^{0.5} \tag{2.37}$$

$$\left(\frac{d_p\left(dP/dz\right)}{\rho_t^V u_{SV}^2}\right) = 7.8\left(1 + 52\frac{\mu_V}{u_{SV} d_p \rho_t^V}\right)\left[1 - 2.0\left(\frac{h_L}{\varepsilon} - 0.01\right)\right]^{-5} \tag{2.38}$$

$B_L$ and $B_V$ are related to $h_L$ in the following way:

$$h_L = \frac{B_L}{c_{TL}\varepsilon} \tag{2.39}$$

$$h_V = 1 - h_L = \frac{B_V}{c_{TV}\varepsilon} \tag{2.40}$$

When the value calculated from the liquid holdup correlation (2.35) or (2.37) is substituted for the liquid holdup in eqs (2.39) and (2.40), two additional algebraic equations are obtained that have to be satisfied along with eqs (2.29) – (2.34):

$$0 = 1 - \frac{B_L}{h_{L,corr} c_{TL}\varepsilon} \tag{2.41}$$

$$0 = 1 - \frac{B_V}{(1 - h_{L,corr}) c_{TV}\varepsilon} \tag{2.42}$$

Although holdup and pressure drop correlations apply strictly in steady-state only, they are frequently used for dynamic simulations as well. (Srivastava and Joseph, 1984, Hitch *et al.*, 1987, Gunaseelan and Wankat, 2002, Ruivo *et al.*, 2004) It can be assumed that the changes in holdup and pressure drop during the transients are so small that the correlations still apply with good accuracy. This is the case during transients from one steady state to another, but not necessarily during startup and shutdown periods as the column may be initially completely dry.

*Axial Dispersion*

Axial dispersion in absorption and distillation columns is a phenomenon that has been neglected in most studies so far. Clearly, axial dispersion is only hardly tangible within the frameworks of the classical equilibrium and nonequilibrium stage models because of their inherent numerical diffusion. A short discussion of the effects of axial dispersion on separation efficiency can be found in King (1980). In tall industrial columns, axial dispersion is rarely a problem, but it can become important in small laboratory columns and microdistillation devices. There are a few studies that address axial dispersion in column packings, e.g., Dunn *et al.* (1977), Ellenberger and Krishna (1999), Macías-Salinas and Fair (2000), Baten *et al.* (2001), and Zhang *et al.* (2008).

### 2.5.2 Multiphase Reactors

Multiphase reactors are modeled in a very similar fashion as separation processes, and eqs (2.29) – (2.34) apply as well. The mass and heat balance equations are complemented by terms for the liquid-solid and gas/vapor-solid mass transfer, and additional equations are needed for the state of the solid catalyst phase. The set of equations can also include intraparticle unsteady-state mass and energy balances.

An important type of multiphase reactor is the trickle-bed reactor. Trickle-bed reactors are fixed-bed reactors with concurrent gas-liquid flow at low superficial velocities. They are commonly used for hydrotreating operations in oil refining, for example hydrogenation of aromatics and desulfurization. Early models of trickle-bed reactors were based on pseudohomogenous kinetics. (Henry and Gilbert, 1973, Iannibello *et al.*, 1985) Nowadays, models with rigorous interphase mass transfer are state-of-the-art. (e.g., Korsten and Hoffmann, 1996, Toppinen *et al.*, 1996, Avraam and Vasalos, 2003, Bhaskar *et al.*, 2004) The mass transfer rates are calculated using the Maxwell-Stefan method or an appropriate simplification of it. A trickle-bed reactor operating in countercurrent mode can also be regarded as a reactive distillation unit. (Taylor and Krishna, 2000)

The hydrodynamics of trickle-bed reactors can be fairly complicated including phenomena like liquid maldistribution, poor catalyst wetting, and multiple flow regimes. These phenomena can be studied for example with CFD simulations. (Lappalainen, 2009) Although a cell-network model has been suggested for combining the hydrodynamic and reactor models, (Guo *et al.*, 2008) the plug-flow assumption is still made in most cases. The plug-flow assumption is often justified in large industrial reactors, where the diameter of the catalyst particles is small compared to the height of the reactor, since the phenomena that cause axial dispersion take place on the scale of the catalyst particles. However, smaller laboratory reactors often need to be modeled with the axial dispersion term.

In steady-state, a trickle-bed reactor can be modeled with the equations given below. (Toppinen *et al.*, 1996) Here, the same notation as in Section 2.5.1 is used, but since the light phase in a trickle bed reactor is usually gas rather than vapor, the symbol $G$ is used instead of $V$. The equations are:

Mass balances for gas and liquid phases:

$$\frac{d(x_i L)}{dz} = N_{GLi} a_{GL} - N_{LSi} a_S \tag{2.43}$$

$$\frac{d(y_i G)}{dz} = -N_{GLi} a_{GL} \tag{2.44}$$

Energy balances:

$$\frac{d(LH_L)}{dz} = q_{GL} a_{GL} - q_{LS} a_S - q_W a_W \tag{2.45}$$

$$\frac{d\left(GH_G\right)}{dz} = -q_{GL}a_{GL} \tag{2.46}$$

Pressure drop is usually calculated using a correlation:

$$\frac{dP}{dz} = f(L, G, T_L, T_G, P). \tag{2.47}$$

The steady-state mass balance for the solid catalyst phase is

$$N_{LSi}a_S + R_i = 0. \tag{2.48}$$

In addition to pressure drop, correlations are needed for mass transfer coefficients and hydrodynamic parameters such as liquid holdup and wetting efficiency.

The reaction rate $R_i$ is assumed to be a function of the temperature of and the concentrations at the catalyst surface. In the model presented here, diffusion or heat transfer limitations inside catalyst particles are ignored or they are assumed to be included in the kinetic relations. It is further assumed that there is no direct mass transfer from the gas to the solid phase, implying that the catalyst is completely wetted. This is usually the case when the reactor operates in the so-called high interaction, or pulsing flow regime. In principle, gas-solid mass transfer could also be included in the equations. (e.g., Avraam and Vasalos, 2003)

# 3 Numerical Methods for Solving Process Equipment Models

## 3.1 Introduction to Numerical Methods

Chemical engineering models of process equipment, such as those discussed in Section 2, are characterized by relatively simple, often one-dimensional spatial domains, algebraic constraints, and complicated closure models for mass transfer, chemical kinetics, and thermodynamics. Consequently, a number of numerical methods that are especially suitable for this kind of problems have been developed. (e.g., Finlayson, 1980, Rice and Do, 1995)

In opposition to chemical engineering and process equipment models, computational fluid dynamics (CFD) is characterized by complex geometry and relatively simple physics. Sophisticated methods, based on the finite volume philosophy, have been developed especially with those problems in mind. Those methods are discussed in detail in dedicated textbooks, for example by Fletcher (1991) and Ferziger and Perić (2002).

For a while, it seemed that CFD would be the philosopher's stone that would ultimately resolve all modeling problems in chemical engineering. However, the development has not been as rapid as initially thought and the use of CFD in chemical engineering is still limited because of the highly complex flow patterns in chemical process equipment and the lack of accurate closure models. Nowadays, then, CFD is often used to generate pseudo-experimental data that is then used in the development of correlations for simplified but more practical models. (Kenig, 2008) However, many of the ideas and principles behind CFD methods are also directly applicable to process modeling in chemical engineering.

There are two conceptually different methods that can be used for the numerical solution of partial differential equations: Finite difference and Weighted Residual Methods (WRM). Finite difference methods replace the continuous derivatives with discretized equations, and the solution is only defined at the nodal points of the grid. Weighted residual methods assume that the solution can be represented analytically, in the form:

$$\Psi = \sum_{j=1}^{J} a_j(t)\phi_j \tag{3.1}$$

In eq (3.1), $a_j(t)$ are unknown coefficients and $\phi_j$ are known analytic functions called trial functions. (Fletcher, 1991) A comprehensive overview of weighted residual methods with many applications is given by Finlayson (1972). The finite volume method can also be interpreted as a weighted residual method, although it is similar in implementation to the finite difference method. (Fletcher, 1991)

In the following sections, some of the most important and most frequently used numerical methods are presented briefly.

## 3.2 Finite Difference Method

The finite difference method is probably the oldest method for solving partial differential equations, as old as calculus itself. Finite difference methods are discussed in detail by Fletcher (1991) and Ferziger and Perić (2002), and from a chemical engineering viewpoint by Finlayson (1980). The idea behind finite difference approximation can be seen clearly in the definition of a derivative:

$$\frac{\partial \Psi}{\partial x} = \lim_{\Delta x \to 0} \frac{\Psi(x + \Delta x) - \Psi(x)}{\Delta x} \tag{3.2}$$

From this definition, three approximations of the first spatial derivative that use the neighboring points can be derived instantly. They are:

Forward difference:

$$\left.\frac{d\Psi}{dx}\right|_i \approx \frac{\Psi_{i+1} - \Psi_i}{\Delta x} \tag{3.3}$$

Backward difference:

$$\left.\frac{d\Psi}{dx}\right|_i \approx \frac{\Psi_i - \Psi_{i-1}}{\Delta x} \tag{3.4}$$

Central difference:

$$\left.\frac{d\Psi}{dx}\right|_i \approx \frac{\Psi_{i+1} - \Psi_{i-1}}{2\Delta x} \tag{3.5}$$

2nd derivatives can be approximated with:

$$\left.\frac{d^2\Psi}{dx^2}\right|_i \approx \frac{\Psi_{i+1} - 2\Psi_i + \Psi_{i-1}}{\Delta x^2} \tag{3.6}$$

Higher-order schemes, both symmetric and asymmetric, can be derived easily from Taylor series expansions. (Fletcher, 1991) The sum of the terms in the Taylor series that is dropped from the discrete representation of the derivative is called the truncation error of the method. The highest power of $\frac{\partial \Psi}{\partial z}$ in the part of the series that is retained is called the method order. The forward and backward difference schemes are first-order accurate. The central difference scheme and other three-point schemes are second-order accurate. (The third point, $\Psi_i$, cancels out in eq (3.5) but it is used in deriving the equation.) If all the grid points are used to calculate the derivative at one point, then one speaks of the spectral method. (Trefethen, 2000) Spectral methods are especially well suited for problems with periodic boundary conditions. A variant for rectangular domains exists as

well, in which case the spectral method resembles the orthogonal collocation method (Section 3.3.3).

The choice of the differencing scheme for the advection term influences directly the numerical behavior of the system and the numerical difficulties that can be expected. First-order schemes suffer from numerical diffusion, whereas higher-order schemes suffer from spurious oscillations in the vicinity of steep gradients. The problems and the ways to mitigate them are very similar for both finite difference and finite volume methods, and they are discussed in more detail in Section 3.4.1. In simple geometries (Cartesian, cylindrical, spherical) the finite difference and finite volume formulations can be reduced to the exactly same equations, and thus the same methods to improve the numerical solution can be applied to both. The finite volume method is more versatile in the sense that it can be adopted more easily for irregular and complicated geometries.

Finite difference schemes require a calculation grid, which is a discrete representation of the continuous domain. Preferably, the grid is designed so that the outermost points coincide with the domain boundaries. The boundary conditions are then easily set. Dirichlet boundary conditions are enforced by simply setting the solution at the boundary point to the desired value. Neumann and Robin boundary conditions can be set by substituting the boundary condition into the discretized eq (3.5), and solving for the "imaginary" gridpoint outside the domain. For example, the following Robin-type boundary condition is commonly encountered in heat or mass transfer with boundary convection:

$$\left.\frac{\partial \Psi}{\partial z}\right|_{z=0} = \alpha\left[\Psi_0 - \Psi(z=0)\right] \tag{3.7}$$

Using the central difference, eq (3.7) is substituted into eq (3.5):

$$\alpha\left(\Psi_0 - \Psi_N\right) = \frac{\Psi_{N+1} - \Psi_{N-1}}{2\Delta z} \tag{3.8}$$

This can be solved for $\Psi_{N+1}$:

$$\Psi_{N+1} = 2\Delta z\alpha\left(\Psi_0 - \Psi_N\right) + \Psi_{N-1} \tag{3.9}$$

When the value calculated from (3.9) is used for the "imaginary" gridpoint $\Psi_{N+1}$ outside the boundary, the boundary condition is satisfied automatically.

For the discrete representation of the time derivative $\frac{\partial \Psi}{\partial t}$, in principle the same methods are applicable as for the spatial discretization. However, because time proceeds only in positive direction, information from time levels $n + 1$ and higher is not available. Using the backward difference for time discretization, the Euler methods can be constructed:

$$\frac{\partial \Psi}{\partial t} \approx \frac{\Psi^{n+1} - \Psi^{n}}{\Delta t} \tag{3.10}$$

If the spatial derivatives are expressed at time level $n$, then the method is called explicit Euler method. In this case the solution at time level $n + 1$ can be calculated directly. If the spatial derivatives are expressed at time level $n + 1$, then the method is called implicit Euler method, and obtaining the solution at $n + 1$ requires solving a system of equations. Both the explicit and implicit Euler method are first-order accurate, but the explicit Euler method has a strict stability limit, whereas the implicit Euler method is unconditionally stable.

For this reason implicit or partially implicit schemes are preferred, since they allow for longer time steps than explicit schemes. The implicit Euler scheme is often used for obtaining a steady-state solution in the so-called relaxation method. The Crank-Nicolson scheme and the three-level implicit scheme are used for transient problems.

The finite difference method involves the construction of a discrete grid, the replacement of the continuous derivatives in the partial differential equation with equivalent finite difference approximations, and the rearrangement of the resulting algebraic equation into an algorithm. (Fletcher, 1991) The various steps in applying the finite difference method are shown schematically in Figure 4.

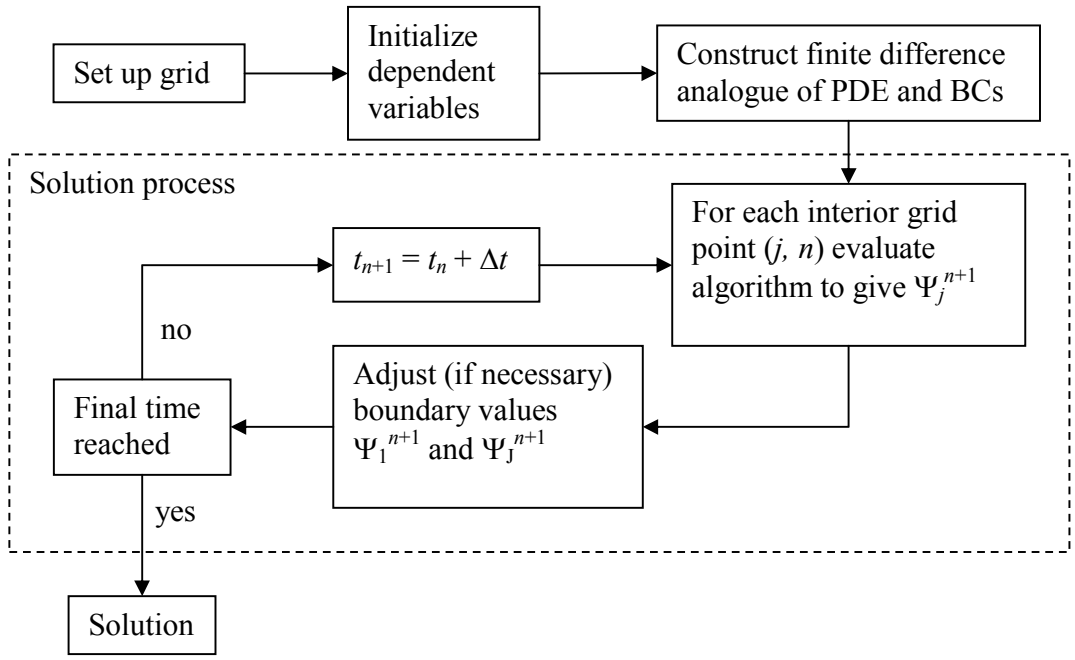


**Figure 4. Schematic of the finite difference solution process according to Fletcher (1991).**

An alternative philosophy of the finite difference representation is to discretize only the spatial term in the partial differential equation, and reduce the partial differential equation to a system of ordinary differential equations at the nodal points. This system can then be integrated with common integration techniques. This method is known as the method of

lines. However, the construction of the semi-discrete form introduces an error associated with the spatial discretization, and consequently the best choice for solving the resulting system is an algorithm that is of lower order than for a system without approximation. (Fletcher, 1991, chapter 7.4) The method of lines is particularly attractive because the various techniques that are used for systems of ordinary differential equations can be used to solve the semi-discrete form of the partial differential equations. Consequently, the method can be easily implemented in software packages like MATLAB.

In chemical engineering, the finite difference method has been used for the simulation of distillation and absorption processes. The SIMCAL and DYNCAL models of Hitch *et al.* (1986, 1987) fall into this category. They used the implicit Euler method (Hitch *et al.*, 1987) for time integration and Newton's method for solving the algebraic equations.

## 3.3 Weighted Residual Methods

### *3.3.1 General Formulation*

This section explains the fundamentals of weighted residual methods. It follows the outlines of the corresponding chapters in Finlayson (1972, 1980) and Fletcher (1991, chapter 5). In order to apply the weighted residual method, it is assumed that an approximate solution in form of eq (3.1) exists:

$$\Psi(z,t) \equiv \sum_{j=1}^{J} a_j(t)\phi_j(z) \tag{3.11}$$

$a_j(t)$ are unknown coefficients and $\phi_j$ are known analytic functions, often called trial functions. The number of the coefficients $a_j$ is the method order. Another way to define the approximate solution is:

$$\Psi(z,t) \equiv \Psi_0 + \sum_{j=1}^{J} a_j(t)\phi_j(z) \tag{3.12}$$

$\Psi_0$ is chosen to satisfy the initial and boundary conditions, whereas the functions $\phi_j$ satisfy the homogenous boundary conditions. Definition (3.12) is used mainly for collocation methods, in which the trial function is constructed as a series of orthogonal polynomials with known properties of the solution.

The trial functions may be polynomials or trigonometric functions. Some methods require trial functions that satisfy the boundary conditions inherently. The unknown coefficients $a_j$ are determined by solving a system of equations generated from the governing equation. If the problem is time-dependent, a system of ordinary differential equations will be obtained. To obtain a steady-state solution, a system of algebraic equations will have to be solved.

For example eq (2.2) can be written as:

$$L(\overline{\Psi}) = \frac{\partial \overline{\Psi}}{\partial t} + \frac{\partial (u\overline{\Psi})}{\partial z} - \frac{\partial}{\partial z}\left( D \frac{\partial \overline{\Psi}}{\partial z} \right) - S(\overline{\Psi}, z) \tag{3.13}$$

The overbar in eq (3.13) denotes the exact solution. If the approximate solution (3.12) is substituted into eq (3.13), it will not be identically zero. Instead, a residual remains:

$$L(\Psi) = R \tag{3.14}$$

The residual $R$ is a continuous function of $z$ and $t$. If $J$ is made sufficiently large, then the coefficients $a_j(t)$ can be chosen such that $R$ approaches zero over the computational domain. The coefficients $a_j(t)$ are determined by requiring that the integral of the weighted residual over the computational domain be zero:

$$\int W_m(z) R(z) dz = 0 \tag{3.15}$$

By letting $m = 1 \ldots J$ a system of equations for the unknown coefficients $a_j$ is obtained. Different choices for the weighting function $W(z)$ result in different methods within the class of methods of weighted residuals. Figure 5 shows a schematic classification of weighted residual methods. The different methods are explained in more detail in the sections to follow.

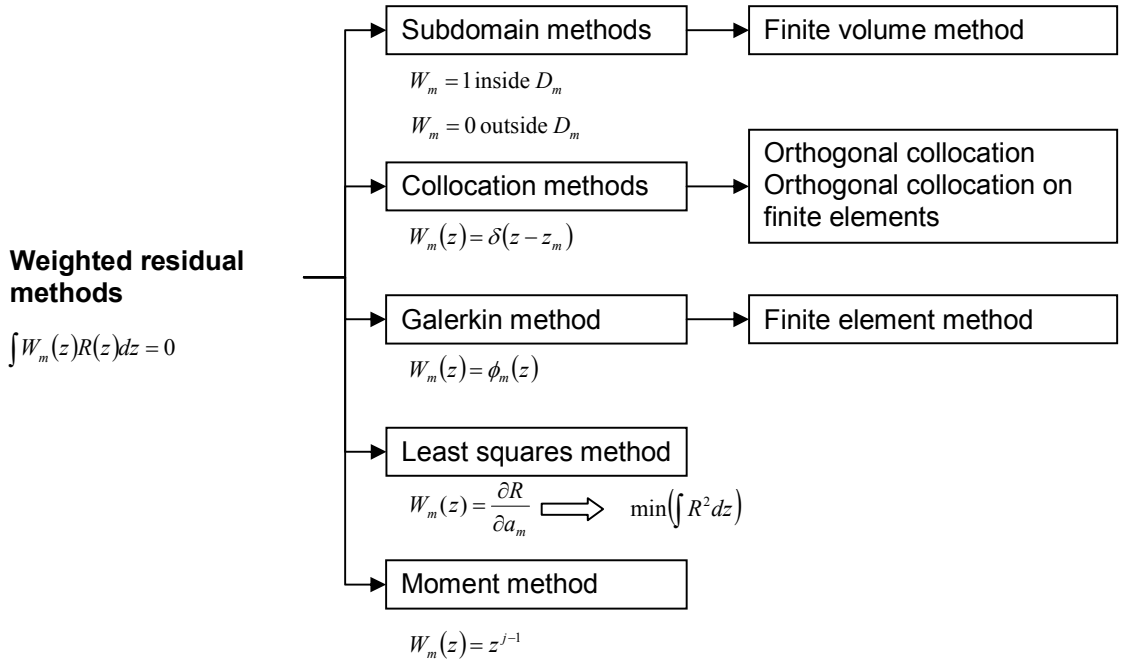


**Figure 5. Classification of weighted residual methods according to the weighting function.**

### *3.3.2 Subdomain Method*

The residual is forced to zero in a subdomain $D_m$:

$W_m = 1$ in $D_m$

$W_m = 0$ outside $D_m$

The finite volume method can be interpreted as a subdomain method. The finite volume method is discussed in more detail below.

### 3.3.3 Collocation Method

The residual is forced to zero at discrete points $z_m$ that are called the collocation points:

$$W_m(z) = \delta(z - z_m) \tag{3.16}$$

In eq. (3.16), $\delta$ is the Dirac delta function. If the trial functions are a series of orthogonal polynomials and the roots of an orthogonal polynomial are chosen as the collocation points $z_m$, then the method is called orthogonal collocation. If the domain is divided into subdomains and orthogonal collocation is applied to each subdomain separately, then the method is called orthogonal collocation on finite elements. The orthogonal polynomials used as trial functions must be chosen such that they satisfy the boundary conditions, since the boundary conditions are not inherently satisfied by the collocation equation.

Orthogonal polynomials are defined as:

$$P_m(z) = \sum_{j=0}^{m} c_j z^j \tag{3.17}$$

With the orthogonality condition:

$$\int_a^b w(z) P_k(z) P_m(z) dz = 0, \; k = 0...m-1 \tag{3.18}$$

This procedure specifies the polynomials within a multiplicative constant, which is determined by setting the first coefficient equal to one. The orthogonality condition may include a weighting function $w(z) \geq 0$. The polynomials $P(z)$ can be constructed such that they have additional convenient properties. For second-order partial differential equations that are defined in $0 \leq z \leq 1$ and have no special symmetry properties, the following trial function can be used: (Finlayson, 1972, p. 105)

$$y(z) = b + cz + z(1-z)\sum_{i=1}^{N} a_i P_{i-1}(z) \tag{3.19}$$

For a problem where the solution is defined in $0 \leq z \leq 1$ and is symmetric around $z = 0$, it is favorable to use only even powers of $z$ and exclude the odd powers. A possible choice of trial function is, assuming Dirichlet boundary conditions (value specified at the boundary):

$$y(z) = y(1) + (1 - z^2)\sum_{i=1}^{N} a_i P_{i-1}(z^2) \tag{3.20}$$

$N$ is the number of interior collocation points, and the polynomials are defined to be orthogonal with the condition

$$\int_0^1 W(z^2) P_k(z^2) P_m(z^2) z^{a-1} dz = 0, \; k = 0...m-1 \tag{3.21}$$

$a$ = 1, 2, or 3 for planar, cylindrical, or spherical geometry, respectively.

Orthogonal collocation and orthogonal collocation on finite elements are widely used methods in chemical engineering. A typical textbook problem is reaction and diffusion in a spherical catalyst particle. (Finlayson, 1972, 1980, Villadsen and Michelsen, 1978, Rice and Do, 1995) Cho and Joseph (1983) and Srivastava and Joseph (1984) used the orthogonal collocation method for dynamic simulation of separation processes. An advantage of the orthogonal collocation method is that it can be written in a compact matrix notation. The method is preferably written in a form where, instead of the weights for the trial functions, the function values at the collocation points are obtained directly. Then the collocation equations are written for the inner collocation points, and the values of the two endpoints are solved from algebraic equations that arise from the boundary conditions. In writing the equations for orthogonal collocation on finite elements, similar algebraic equations are needed at the interior element boundaries to achieve continuity of the solution between the elements. In the time-dependent case, this leads to a system of differential-algebraic equations. This problem can be avoided if Hermite polynomials are used. Hermite polynomials are inherently continuous at the element boundaries, so that additional algebraic equations are not needed. (Finlayson, 1980)

### 3.3.4 Least Squares Method

The least squares method is obtained when the following weighting function is used:

$$W_m(z) = \frac{\partial R}{\partial a_m} \tag{3.22}$$

This is equivalent to minimizing the function $\int R^2 dz$. The least squares method is not widely used in chemical engineering, but it has some applications for example in nuclear engineering. (Finlayson, 1972) It has also been used for solving population balance problems. (Dorao and Jakobsen, 2006)

### 3.3.5 Galerkin Method

The idea behind the Galerkin method is to choose the weighting functions from the same family of functions as the trial functions:

$$W_m(z) = \phi_m(z) \tag{3.23}$$

The trial functions must be members of a complete set of functions. A set of functions is complete if any function of a given class can be expanded in terms of the set: (Finlayson, 1972)

$$f = \sum a_i \phi_i \tag{3.24}$$

Polynomials, for example, satisfy this condition. A continuous function is zero if it is orthogonal to every member of a complete set. Two functions $f_1$ and $f_2$ are orthogonal if the integral of their product (inner product) is zero:

$$\int_0^1 f_1 f_2 dz = 0 \tag{3.25}$$

The Galerkin method forces the residual to be zero by making it orthogonal to each member of a complete set as $J \to \infty$.

Linear or quadratic functions that are nonzero in parts of the domain (called elements) are usually used as trial functions. (But in principle, polynomials of any degree can be used.) Figure 6 shows a typical configuration of linear approximating functions.

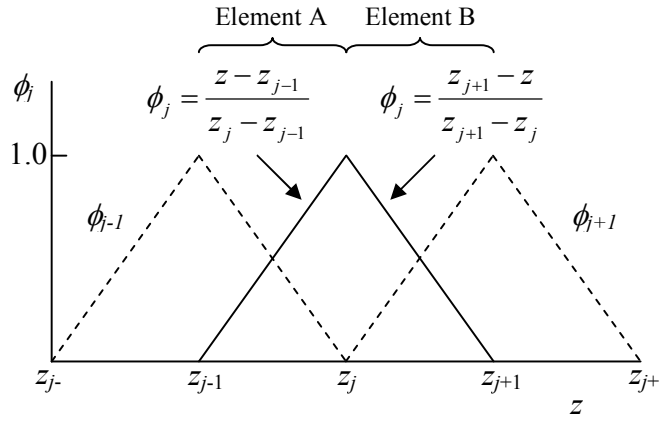


**Figure 6. One-dimensional linear approximating functions.**

The Galerkin method is the basis for a family of techniques known as finite element methods. (Fletcher, 1991) One variant of the finite element method is the moving finite element method (MFEM) that can be used for tracking of sharp concentration fronts. (Sereno *et al.*, 1991, 1992)

### *3.3.6 Moment Method*

The moment method is obtained when the first $J$ powers of $z$ are used as the weighting functions:

$$W_m(z) = z^{j-1} \quad j = 1...J \tag{3.26}$$

The moment method is based on the same orthogonality principle as the Galerkin method. The moment method is the main subject of this thesis and is discussed in more detail in Section 4.

## 3.4 Finite Volume Method

### *3.4.1 General Formulation*

Both the finite volume method and the finite difference method are very similar in implementation, but the former is better suitable for complicated geometries. Finite volume methods have been developed to a high degree of sophistication for computational fluid dynamics purposes. Fluid dynamics problems are characterized by two- and three-dimensional domains, complex geometries, and nonlinearity. The central idea behind the finite volume method is Gauss' theorem, which is used to transform a volume integral into a surface integral:

$$\iiint_V \left(\nabla \cdot \vec{F}\right) dV = \oiint_S \vec{F} \cdot \vec{n} dS \tag{3.27}$$

Finite volume methods employ a cell grid, on which the volume integral is applied. Figure 7 shows a one-dimensional grid with the numbering of the cell nodes and the cell faces. A single cell within the grid is called a control volume. The net flux through the control volume boundary is the sum of integrals over the control volume faces:

$$\oiint_S f dS = \sum_k \int_{S_k} f dS \tag{3.28}$$

In discrete form eq (3.28) is:

$$\Delta V \frac{\Delta \Psi}{\Delta t} = \sum_{i=1}^{N} F_i S_i + \Delta V S \tag{3.29}$$

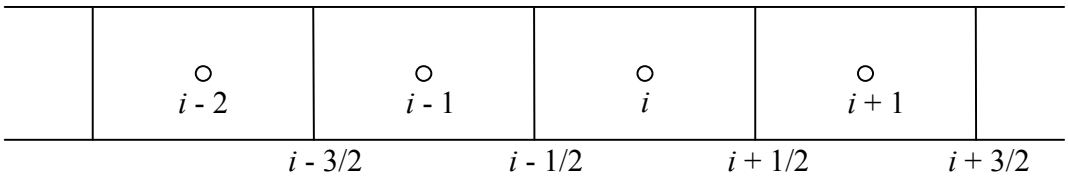


**Figure 7. One-dimensional calculation grid with cell nodes and faces for the finite volume method.**

The convective flux through the cell boundary is the convective velocity times the concentration at the cell boundary:

$$F_{i+1/2,conv} = u_{i+1/2} \Psi_{i+1/2} \tag{3.30}$$

The diffusive flux is easily calculated by approximating the gradient at the cell boundary with a central difference scheme:

$$F_{i+1/2,diff} = D\frac{\Psi_{i+1} - \Psi_{i-1}}{\Delta z} \tag{3.31}$$

The main problem of the finite volume method is the interpolation of the function values at the cell boundaries, since the solution is only given at the cell nodes. Patankar (1980) promoted the first-order upwind method in his seminal book. The first-order upwind scheme assumes simply that the value of the variable at the boundary is equal to its value at the center of the control volume located upstream:

$$\Psi_{i+1/2} = \Psi_i \tag{3.32}$$

The first-order upwind scheme is stable and yields always physically meaningful solutions. Unfortunately, it also results in heavy numerical diffusion, and thus a very dense grid is required (and even then, accuracy is poor). Higher-order methods, such as central difference or QUICK (quadratic interpolation scheme, both second-order), are more accurate, but they tend to generate oscillations in the vicinity of steep gradients and discontinuities. In fluid dynamics, such discontinuities arise as shockwaves in supersonic flow. In chemical engineering models, contact discontinuities are more common. A contact discontinuity is for example the concentration front that travels down a reactor during its startup. Methods have been developed to eliminate the oscillations that arise from the use of the high-order schemes. Such methods are for example flux-corrected transport (FCT), total variation diminishing (TVD), and essentially non-oscillatory and weighted essentially non-oscillatory (ENO and WENO) schemes. (Ferziger and Perić, 2002, chapter 10.3.1)

The specification of boundary conditions is very much the same in both the finite volume method and the finite difference method. Next to the domain boundary, one or two (dependent on the discretization scheme) “virtual” control volumes are added, where the boundary conditions are inserted as extrapolated cell values. (Figure 8)

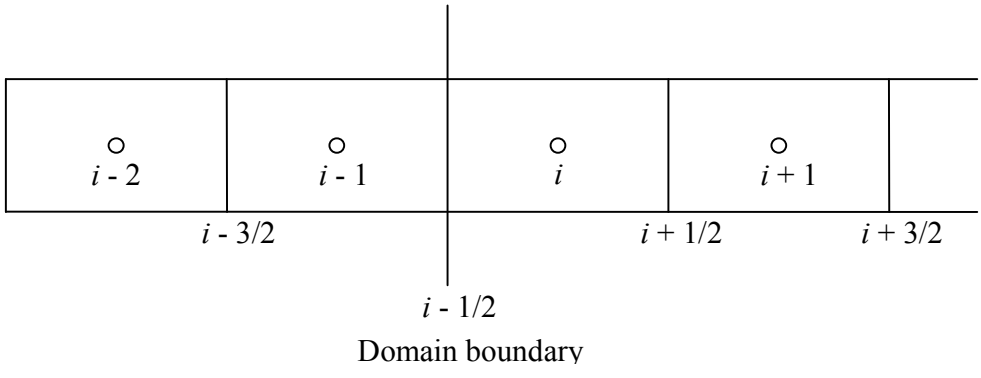


**Figure 8. “Virtual” control volumes at the domain boundary. Cell *i* is the first control volume in the domain.**

Following the success of the finite volume method in the field of computational fluid dynamics, the same principles are becoming more popular in chemical engineering modeling, as well. Cruz *et al.* (2005) for example used a finite volume model with high-order discretization and flux limiters to model some separation processes.

### *3.4.2 CSTR-in-Series Model*

A common implementation of the finite volume model in chemical engineering is the CSTR-in-series model, in which a tubular reactor or other process equipment is approximated as a series of continuous stirred tanks. (Figure 9) Actually, this model originates from a technical reactor concept called a cascade. From a mathematical viewpoint, the CSTR-in-series model can be regarded as a control volume model with first-order upwind discretization.

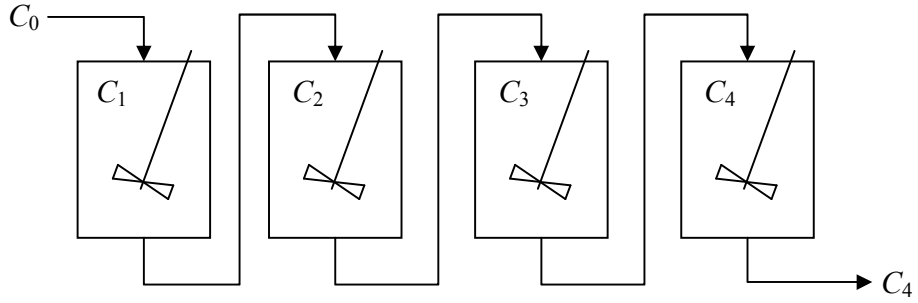


**Figure 9. Schematic representation of a CSTR-in-series model.**

The first-order upwind scheme results in heavy numerical diffusion, but in this case the numerical diffusion is desired since it is used to model axial dispersion. The apparent dispersion coefficient due to the first-order upwind discretization can be estimated with:

$$D \approx \frac{u\Delta z}{2} \tag{3.33}$$

Figure 10 shows a comparison between the axial dispersion model and the CSTR-in-series model for different Péclet numbers.

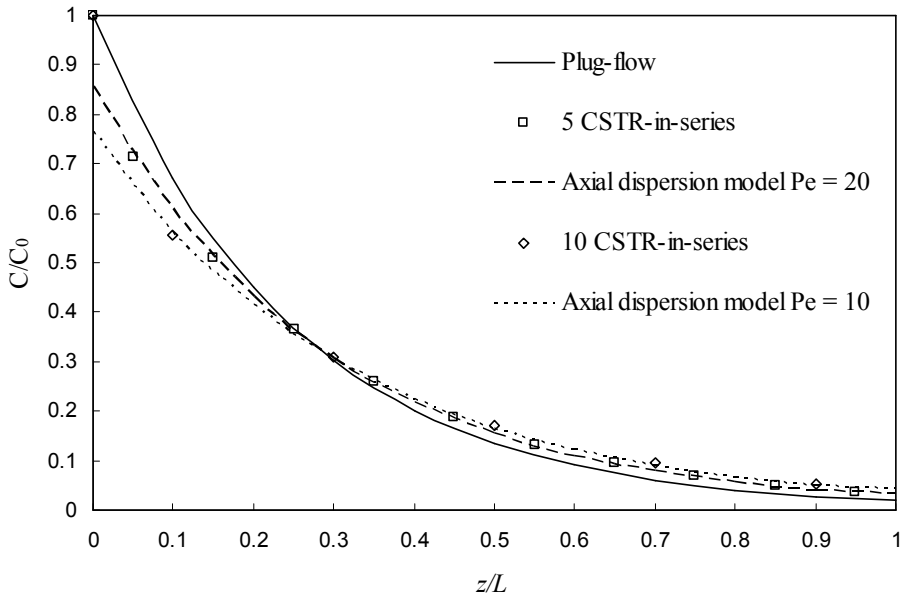


**Figure 10. Comparison of the CSTR-in-series model and the axial dispersion model.**

The important difference between the CSTR-in-series model and the finite volume model with first-order upwind discretization lies in the treatment of the diffusive flux: The user of a CSTR-in-series model uses the intrinsic numerical diffusion for modeling physical axial dispersion, whereas the user of a finite volume model tries to eliminate the numerical diffusion by using a dense grid. The physical diffusive flux, if present, is then added on top of the numerical diffusion.

In textbooks, e.g., Fogler (1999), the CSTR-in-series model is suggested for modeling of nonideal tubular reactors such that the number of tanks is adjusted to yield the same residence time distribution as measured in an experiment. The residence time distribution function for CSTR-in-series is: (Fogler, 1999)

$$E(t) = \frac{t^{n-1}}{(n-1)!\,\tau_{si}^{n}} \exp\left(-\frac{t}{\tau_{si}}\right) \tag{3.34}$$

The number of tanks in series can be calculated using the dimensionless variance obtained from a tracer experiment:

$$n = \frac{\tau_s^2}{\sigma^2} \tag{3.35}$$

The CSTR-in-series model has some advantages in chemical engineering applications. For example, the steady-state conversion for first-order reactions can be calculated directly from:

$$X = 1 - \frac{1}{(1+\tau_i k)^n} \tag{3.36}$$

Generally speaking, however, there is no real advantage to using the CSTR-in-series model instead of the axial dispersion model, eq (2.2), for tubular reactors; especially since tools for solving second-degree differential equations are available in software packages such as MATLAB. An important exception, however, are multiphase processes where the flow directions are countercurrent (distillation, absorption, counter-current trickle-bed reactors). In those cases, a direct solution algorithm results in a trial-and-error method that is computationally expensive. (Feintuch and Treybal, 1978) For this reason, the nonequilibrium stage method has gained such large popularity. Alternative, but little used methods are weighted residual methods, such as orthogonal collocation (Srivastava and Joseph, 1984) and the moment method, the subject of this thesis. (cf. Section 5)

### *3.4.3 Nonequilibrium Stage Model*

An important application of the finite volume method is the nonequilibrium stage model for separation processes. Figure 11 shows a schematic representation of a nonequilibrium stage. The nonequilibrium stage model was first conceived as an evolution of the equilibrium stage model for tray columns. (Krishnamurthy and Taylor, 1985a, Taylor and Krishna, 1993) The need for such a model emerged from the fact that the equilibrium stage model combined with the concept of stage efficiency proved unsatisfactory for multicomponent systems. (Taylor and Krishna, 1993) The nonequilibrium stage model for continuous-contact separation processes (Krishnamurthy and Taylor, 1985b) that followed the nonequilibrium stage model for tray columns (Krishnamurthy and Taylor, 1985a) is actually a finite volume model with first-order upwind discretization for the equations presented in Section 2.5.1. In tray columns, the liquid holdup on a tray forms a natural control volume. In order to apply the method to continuous-contact processes, the column is divided into finite slices. All variables, hydrodynamic parameters, and mass and heat transfer coefficients are assumed constant within these slices.

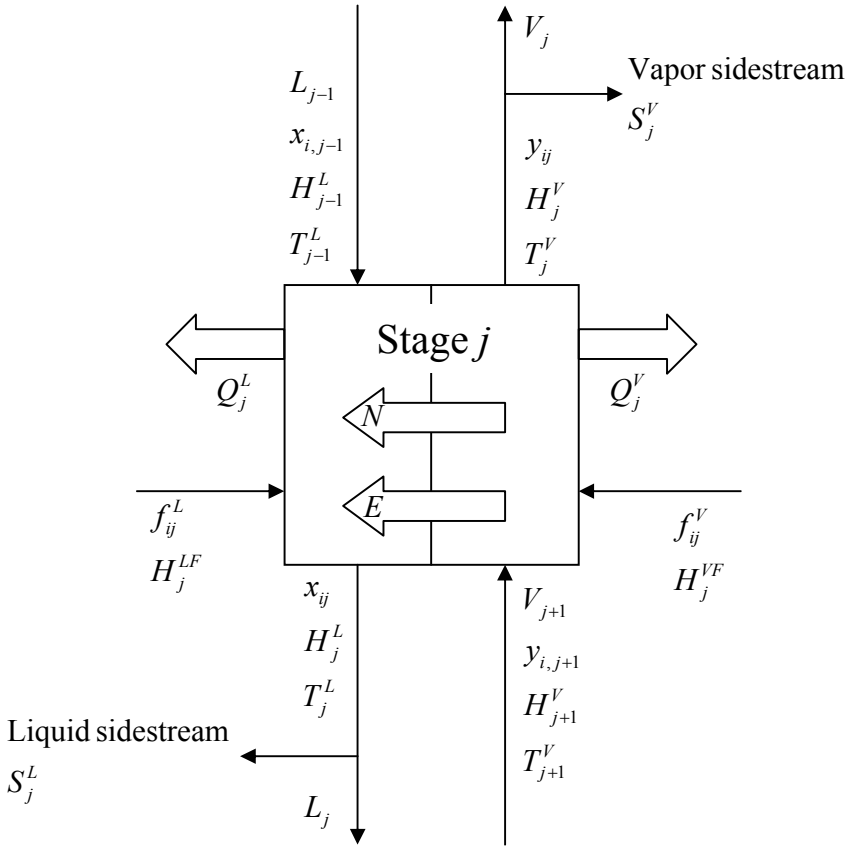


**Figure 11. Schematic diagram of a nonequilibrium stage. This stage represents a single tray in a tray column or a section of packing in a packed column. (after Taylor & Krishna, 1993)**

The model equations for stage *j* in steady-state are given below (after Taylor & Krishna, 1993). Reaction rate terms are not included in the equations but can be easily added.

Total material balances for the vapor and liquid phases:

$$M_{tj}^V \equiv \left(1 + r_j^V\right)V_j - V_{j+1} - F_j^V + \sum_{i=1}^{nc} N_{ij} a_j = 0 \tag{3.37}$$

$$M_{tj}^L \equiv \left(1 + r_j^L\right)L_j - L_{j+1} - F_j^L - \sum_{i=1}^{nc} N_{ij} a_j = 0 \tag{3.38}$$

Component material balances in the vapor and liquid phases:

$$M_{ij}^V \equiv \left(1 + r_j^V\right)V_j y_{ij} - V_{j+1} y_{i,j+1} - f_{ij}^V + N_{ij} a_j = 0\,, \qquad i = 1 \ldots nc \tag{3.39}$$

$$M_{ij}^L \equiv \left(1 + r_j^L\right)L_j x_{ij} - L_{j-1} x_{i,j-1} - f_{ij}^L - N_{ij} a_j = 0\,, \qquad i = 1 \ldots nc \tag{3.40}$$

Energy balances for the vapor and liquid phases:

$$E_j^V \equiv \left(1 + r_j^V\right) V_j H_j^V - V_{j+1} H_{j+1}^V - F_j^V H_j^{VF} + Q_j^V + E_j^V = 0 \tag{3.41}$$

$$E_j^L \equiv \left(1 + r_j^L\right) L_j H_j^L - L_{j-1} H_{j-1}^L - F_j^L H_j^{LF} + Q_j^L - E_j^L = 0 \tag{3.42}$$

Interface energy balance:

$$E_j^I \equiv h_j^V a_j \left(T_j^V - T_j^I\right) - h_j^L a_j \left(T_j^I - T_j^L\right) + \sum_{i=1}^{nc} N_{ij} a_j \left(\overline{H}_{ij}^V - \overline{H}_{ij}^L\right) = 0 \tag{3.43}$$

Mass transfer rate equations:

$$R_{ij}^V \equiv N_{ij} a_j - N_{ij}^V a_j = 0, \qquad i = 1 \ldots nc\text{-}1 \tag{3.44}$$

$$R_{ij}^L \equiv N_{ij} a_j - N_{ij}^L a_j = 0, \qquad i = 1 \ldots nc\text{-}1 \tag{3.45}$$

Phase equilibrium relations at the interface:

$$Q_{ij}^I \equiv K_{ij} x_{ij}^I - y_{ij}^I = 0, \quad i = 1 \ldots nc \tag{3.46}$$

Summation equations:

$$S_j^{VI} \equiv \sum_{i=1}^{nc} y_{ij}^I - 1 = 0 \tag{3.47}$$

$$S_j^{LI} \equiv \sum_{i=1}^{nc} x_{ij}^I - 1 = 0 \tag{3.48}$$

Pressure equation:

$$P_j \equiv P_j - P_{j-1} - \left(\Delta P_{j-1}\right) = 0 \tag{3.49}$$

The $5nc + 6$ independent variables and equations are ordered into vectors:

$$\left(x_j\right) \equiv \left(V_j \quad y_{ij} \quad T_j^V \quad y_{ij}^I \quad x_{ij}^I \quad T_j^I \quad L_j \quad x_{ij} \quad T_j^L \quad N_{ij} \quad P_j\right)^T \tag{3.50}$$

$$\left(F_j\right) \equiv \left(M_{tj}^V \quad M_{ij}^V \quad E_j^V \quad R_{ij}^V \quad S_j^{VI} \quad Q_{ij}^I \quad E_j^I \quad M_{tj}^L \quad M_{ij}^L \quad E_j^L \quad R_{ij}^L \quad S_j^{LI} \quad P_j\right)^T \tag{3.51}$$

For simple columns, the system of equations for all stages forms a block tridiagonal matrix. The system of nonlinear equations represented by the vector in eq (3.51) is usually solved with Newton's method. (Taylor and Krishna, 1993) Naturally, the nonequilibrium stage method suffers from the same extent of numerical diffusion that is characteristic of all first-order methods. This is clearly shown in the example in Section 5.3, in which the moment method is compared against the nonequilibrium stage method.

To overcome this shortcoming, a very large number of nonequilibrium stages are needed for the model to be accurate.

For the purpose of dynamic simulation, the balance equations (3.37) – (3.42) can be written with the time derivatives. Then, some information on the tray holdup or liquid holdup in the packing is needed. In tray columns, the vapor and liquid holdups in the froth on the tray, the vapor holdup above the tray, and the liquid holdup in the downcomer may be considered separately. (Kooijman and Taylor, 1995) In dynamical modeling of packed columns, a holdup correlation can be used. (e.g., Gunaseelan and Wankat, 2002) The use of holdup correlations in dynamic simulation was already discussed in Section 2.5.1. It is important to note, however, that even when the bulk material balances are dynamic, the vapor and liquid films and the interface are still assumed to be at equilibrium, i.e., there is no accumulation of material or energy in the vapor and liquid films or at the interface.

# 4 Moment Transformation: General Formulation

The main purpose of this thesis is to demonstrate how to use the moment method for chemical engineering modeling and simulation. This section deals with the general formulation of the moment transformation. First, recall eq (3.12) that is the approximate solution in a weighted residual method:

$$\Psi(z,t) = \Psi_0 + \sum_{j=1}^{J} a_j(t)\phi_j(z) \tag{3.12}$$

Again, the convection-dispersion equation is used as an example:

$$\frac{\partial\overline{\Psi}}{\partial\theta} + \frac{\partial\overline{\Psi}}{\partial\zeta} - \frac{1}{\mathrm{Pe}}\frac{\partial^2\overline{\Psi}}{\partial\zeta^2} - S = 0 \tag{4.1}$$

Here, too, the overbar denotes the exact solution, and the physical domain $z$ is replaced with the dimensionless domain $\zeta \in [0,1]$. This is no restriction, since any physical domain can be transformed into the dimensionless domain by simple change of variables. Time can be either physical time $t$ or dimensionless time $\theta$, and latter is used in this section. The residual is obtained by substituting the approximate solution (3.12) into the differential equation (4.1):

$$R = \frac{\partial\Psi}{\partial\theta} + \frac{\partial\Psi}{\partial\zeta} - \frac{1}{\mathrm{Pe}}\frac{\partial^2\Psi}{\partial\zeta^2} - S \tag{4.2}$$

The residual is then substituted into eq (3.15), with the weighting function being the $j^{\text{th}}$ power of $\zeta$:

$$0 = \int_0^1 R\zeta^j d\zeta = \int_0^1 \left( \frac{\partial\Psi}{\partial\theta} + \frac{\partial\Psi}{\partial\zeta} - \frac{1}{\mathrm{Pe}}\frac{\partial^2\Psi}{\partial\zeta^2} - S \right)\zeta^j d\zeta \tag{4.3}$$

Since integration is a linear operation, each term can be integrated separately. Rearranging eq (4.3) yields:

$$\int_0^1 \frac{\partial\Psi}{\partial\theta}\zeta^j d\zeta = \int_0^1 \left( -\frac{\partial\Psi}{\partial\zeta} + \frac{1}{\mathrm{Pe}}\frac{\partial^2\Psi}{\partial\zeta^2} + S \right)\zeta^j dz \tag{4.4}$$

According to Leibniz' rule, the differential operator on the left hand side of the equation can be moved outside of the integral:

$$\int_0^1 \frac{\partial\Psi}{\partial\theta}\zeta^j d\zeta = \frac{\partial}{\partial\theta}\int_0^1 \Psi\zeta^j d\zeta = \frac{\partial m_j}{\partial\theta} \tag{4.5}$$

The term $m_j = \int_0^1 \Psi(\zeta)\zeta^j d\zeta$ is called the $j^{th}$ moment of $\Psi$.

Eq (4.4) can then be rewritten as:

$$\frac{dm_j}{d\theta} = \int_0^1 \left( -\frac{\partial \Psi}{\partial \zeta} + \frac{1}{\mathrm{Pe}} \frac{\partial^2 \Psi}{\partial \zeta^2} + S \right) \zeta^j d\zeta \tag{4.6}$$

Integration by parts gives the moment transformed equation with boundary conditions:

$$\frac{dm_j}{d\theta} = \int_0^1 \left( \zeta^j S + j\zeta^{j-1} \left[ \Psi - \frac{1}{\mathrm{Pe}} \frac{\partial \Psi}{\partial \zeta} \right] \right) d\zeta - \Psi\big|_{\zeta=1} + \delta(0, j)\Psi\big|_{\zeta=0} \tag{4.7}$$

It is assumed that the state profiles can be approximated by a set of basis functions $P(\zeta)$ that are linear in terms of the coefficients: (Alopaeus *et al.,* 2008)

$$\Psi(\zeta, \theta) = \sum_{i=0}^{n} w_i(\theta) P_i(\zeta) \tag{4.8}$$

In many cases, it is preferable to improve the accuracy of the solution by dividing the domain into a number of sub-intervals, and apply the state profile approximation to each of these sub-intervals individually. The equations given in this section apply equally in that case, but all dimensionless variables and quantities must be defined with respect to the sub-interval length.

The simplest choice of basis functions is the first *n* powers of *ζ:*

$$P_n(\zeta) = \zeta^n \tag{4.9}$$

The key idea of the method is to follow the time evolution of the state profile moments. The moments can be calculated from the basis functions as:

$$m_j(\theta) = \int_0^1 \Psi(\zeta, \theta)\zeta^j d\zeta = \sum_{i=0}^{n} w_i(\theta) \int_0^1 P_i(\zeta)\zeta^j d\zeta, \qquad j = 0...k \tag{4.10}$$

Eq (4.10) can be written in matrix form as:

$$(m) = [A](w) \tag{4.11}$$

Where

$$A_{i,j} = \int_0^1 P_{i-1}(\zeta)\zeta^{j-1} d\zeta, \qquad i = 1\ldots n+1, \quad j = 1\ldots k+1 \tag{4.12}$$

Now the weights ($w$) can be calculated from the moments by a simple matrix inversion:

$$(w) = [A]^{-1}(m) \tag{4.13}$$

If the first integer powers of $\zeta$ are chosen as the basis functions, then the following transformation is obtained:

$$m_j(\theta) = \int_0^1 \Psi(\zeta,\theta)\zeta^j d\zeta = \int_0^1 \sum_{i=0}^{n} w_i(\theta)\zeta^i \zeta^j d\zeta = \sum_{i=0}^{n} \frac{w_i(\theta)}{i+j+1}, j = 0\ldots k \tag{4.14}$$

The transformation matrix is:

$$A_{i,j} = \frac{1}{i+j-1}, \qquad i,j = 1\ldots n+1 \tag{4.15}$$

This is actually the Hilbert matrix, which is a famous example of ill-conditioned matrices. The inverse of the Hilbert matrix can be calculated analytically:

$$A^{-1}_{i,j} = (-1)^{i+j}(i+j-1)\binom{n+i-1}{n-j}\binom{n+j-1}{n-i}\binom{i+j-2}{i-1}^2, \qquad i,j = 1\ldots k+1 \tag{4.16}$$

Unfortunately, numerical instabilities that occur with the inverse Hilbert matrix prevent the use of polynomials of degree higher than about 10, even when using double precision accuracy. The numerical behavior of the transformation can be improved to some extent by using other trial functions such as Chebyshev polynomials. For polynomials of degree lower than 10, it is actually immaterial which set of polynomials is used. For more information on the use of Chebyshev polynomials as trial functions, see Alopaeus *et al.* (2008).

The transformation matrix depends only on the choice of number of moments and the trial functions. Therefore, the matrix for a chosen set of trial functions can be constructed and inverted before the actual simulation. Although the initial condition is usually not given as a polynomial profile, any given set of polynomial coefficients that represent the initial conditions can be transformed into initial moments by simple matrix multiplication: $(m) = [A](w)$.

Similar to the OC, OCFE, and Galerkin methods, the moment method can be written in a compact matrix notation. The details can be found in the Appendix of Publication [I].

Eq (4.7) is actually a set of $n + 1$ ordinary differential equations in time that can be integrated with well-known techniques such as Runge-Kutta or Adams methods. (e.g., Finlayson, 1980) The application of the moment method requires the evaluation of the integral on the right hand side of eq (4.7). Simple source terms can be integrated analytically, but in the general case a quadrature rule is used to approximate the integral. A quadrature rule with $N$ quadrature points integrates exactly a polynomial function of

degree $2N - 1$. For linear source terms, the sufficient number of quadrature points can be determined by this rule. Some experimentation may be needed to make the error resulting from inaccurate quadrature inferior to the error resulting from an insufficient number of variables. The degree of the quadrature rule used must be at least high enough to ensure that the trial function with the highest degree is integrated exactly.

A discrete form of the moment method has been widely used for solving population balance models. (Alopaeus *et al.*, 2006b, 2007) In population balance modeling, the moments themselves bear a physical meaning, e.g., total surface area and total mass. In the axial dispersion model, some physical meaning can be attributed to the moments as well, although the relations are not as clear as in the population balance case. For example, the first moment can be associated with the location of a concentration front and the second moment can be associated with the standard deviation of a pulse.

# 5 Applications of the Moment Method in Process Modeling

## 5.1 Catalyst Activity Profiles in Fixed-Bed Reactors

The application of the moment transformation method to the modeling of catalyst activity profiles in fixed-bed reactors is the subject of Publication [I]. Deactivation is a chemical reaction that changes the properties of the catalyst and results in the loss of catalytic activity. Deactivation can occur due to a number of reasons, such as sintering, coking, or poisoning. (Fogler, 1999) Often, a model with separable reaction kinetics is used: (Levenspiel, 1972)

$$R(\zeta,t) = a(t)R_0(\zeta) \tag{5.1}$$

$R_0$ is the reaction rate on fresh catalyst, and $a$ is catalyst activity that represents the state of the catalyst at time $t$ relative to fresh catalyst. In this way, the time-dependent behavior of the catalyst can be separated from the reaction kinetics.

The rate of catalyst deactivation can be modeled with a kinetic expression similar to the main chemical reactions. It is usually a function of temperature and concentrations, and often also of the catalyst activity itself. It is important to note that all the factors affecting the deactivation rate of the catalyst can be formulated as function of the reactor axial coordinate alone:

$$\frac{\partial a}{\partial t} = r_d(C,T,a) = r_d(C(\zeta),T(\zeta),a(\zeta)) = r_d(\zeta) \tag{5.2}$$

Applying the moment transformation equation (4.3) to eq (5.2) yields:

$$\frac{dm_j}{dt} = \int_0^1 r_d(\zeta)\zeta^j d\zeta \tag{5.3}$$

Since the catalyst phase is stationary, no convection or dispersion terms are present in eq (5.2), although it would be easy to introduce a convection term in order to model a moving bed reactor. The assumption of stationary catalyst phase means that no boundary conditions are needed, only an initial condition that is usually full catalytic activity of the whole catalyst bed: $a(0,\zeta) = 1$. With eq (5.3), the time rate of change for each moment can be calculated simultaneously as the reactor model is solved by integration along the axial coordinate. Since the time rate of change of the moments does not appear in the reactor model because of the pseudo-steady-state assumption, this does not complicate the reactor model solution.

Among the models presented in this thesis, the catalyst activity profile model is a special case, since it combines a dynamic model that is solved with the moment transformation method with a steady-state reactor model. If the residence time in the reactor is negligible compared to the timescale of catalyst deactivation, then the reactor state variables may be integrated as a set of ordinary differential equations (ODE) only with respect to the axial

coordinate at any given time. This pseudo-steady-state approach has been proven valid for many industrial applications of fixed-bed reactors, where catalyst deactivation is typically slow compared to residence time in the reactor. (Ogunye and Ray, 1970, Buzzi-Ferraris *et al.*, 1984) With this approach, the reactor model can be completely separated from the dynamic model for catalyst deactivation. Only the information from the reactor model is used to calculate the rates of catalyst deactivation, and the catalyst activity profile from the dynamic part of the model is used in turn for solving the reactor model at any given timestep. In some applications catalyst deactivation is so rapid that the pseudo-steady-state assumption is not valid anymore. In those cases a fully dynamic model must be used.

Naturally, the polynomial approximation model is best suitable for catalyst activity profiles that suggest a polynomial formulation. This is usually the case for complex profiles that result from coke formation or physical changes of the catalyst or the support material at hot zones in the catalyst bed. (Birtill, 2007) In principle, the method can also be applied for modeling other slow time-dependent phenomena, such as fines deposition and changing hydrodynamic conditions in trickle-bed reactors. (Iliuta *et al.*, 2003)

In Publication [I], the features of the model are demonstrated with an example of a vinyl chloride monomer reactor. This example was chosen because the reactor model with the kinetics of catalyst deactivation is available in a convenient form, and the resulting catalyst activity profile is well suited for the polynomial approximation method. The reactor model of Ogunye and Ray (1970) is used in the form as presented in Buzzi-Ferraris *et al.* (1984). The model equations are shown in Table 1 of Publication [I]. The vinylation of hydrogen chloride takes places on a $HgCl_2$ catalyst according to the following equation:

$$HC \equiv CH + HCl \rightarrow H_2C = CHCl \qquad \Delta H_r = -99\,kJ/mol \qquad (5.4)$$

Due to the highly exothermic reaction, hot spots appear in the catalyst bed and cause the mercuric chloride to sublime, leaving the inactive carbon support. Together with the highly temperature-dependent deactivation kinetics this results in a complex catalyst activity profile. A reference solution was calculated with a finite difference method with 300 grid points. This solution was regarded as an “exact solution”, to which the polynomial approximation solutions were compared. Figure 12 shows catalyst activity profiles modeled with polynomials of different degrees compared to the reference solution. Figure 13 shows the difference between the reference solution and the polynomial approximation solutions. Figure 14 shows the time-dependent conversion and temperature profiles in the reactor. Due to the numerical limitations that arise from the use of the inverse Hilbert matrix the polynomial degree was limited to 10. In this case, even a seventh-degree polynomial is sufficient to model the catalyst activity profile with good accuracy, although only a single polynomial is used in the whole domain.

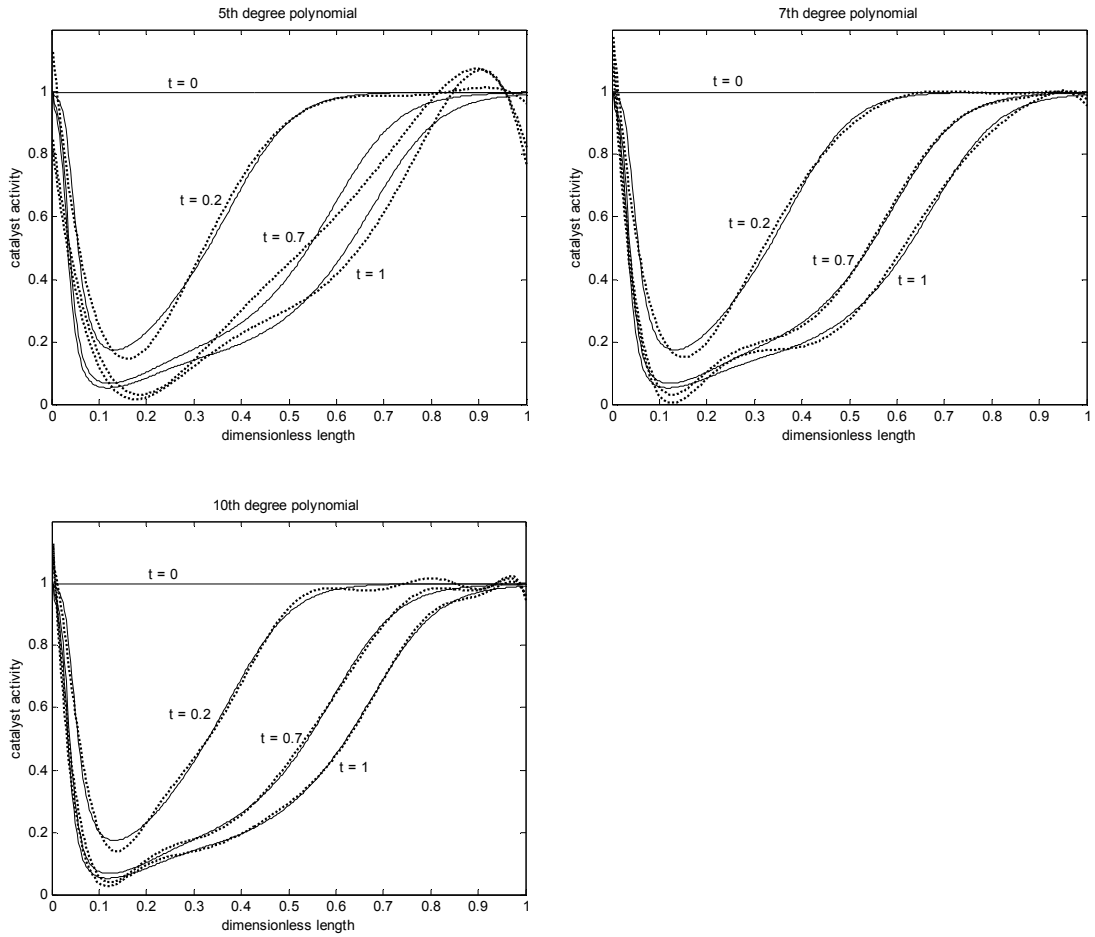


**Figure 12. Catalyst activity profiles in the vinyl chloride monomer reactor, modeled with 5$^{th}$, 7$^{th}$, and 10$^{th}$ degree polynomials. — exact profile; ···· polynomial approximation. (*t* = dimensionless time)**

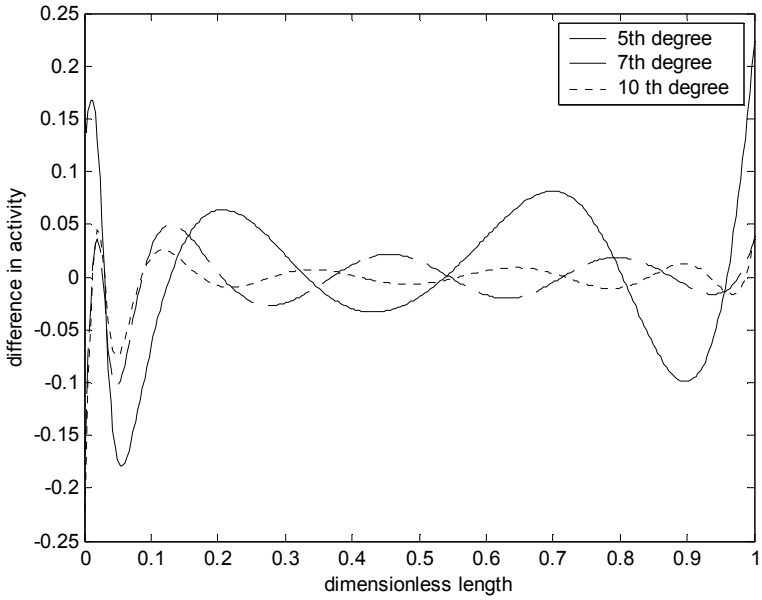


**Figure 13. Deviation of the polynomial approximation profiles to the reference solution for 5$^{th}$, 7$^{th}$, and 10$^{th}$ degree polynomials.**

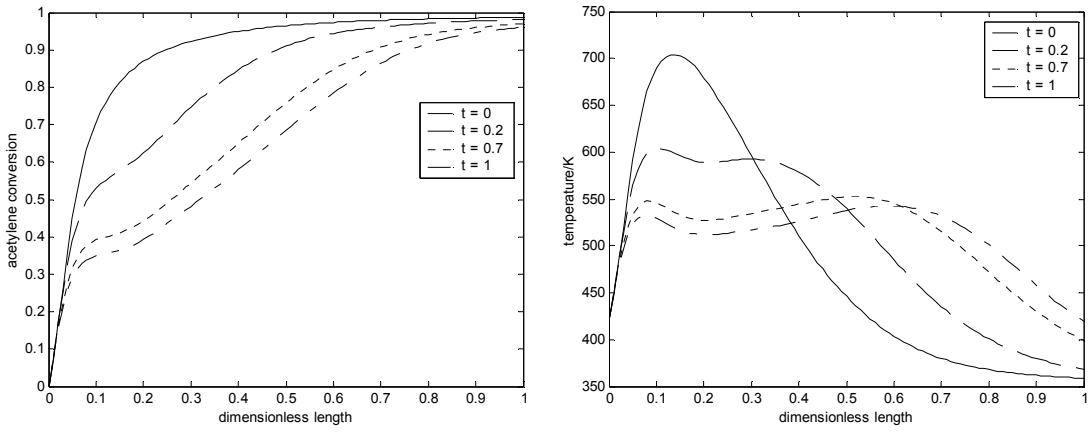


**Figure 14. Conversion (left) and temperature (right) in the vinyl chloride monomer reactor with the underlying catalyst activity profile approximated as 10$^{th}$ degree polynomial.**

## 5.2 Chemical Reactor with Axial Dispersion

### *5.2.1 Reactor model*

The application of the moment transformation method to chemical reactors with axial dispersion is the subject of Publication [II]. The basis of the analysis to follow is the model equation (2.3). By defining the dimensionless variables $\psi = \frac{C}{C_{ref}}$, $\zeta = \frac{z}{L}$, and $\theta = \frac{ut}{L}$ eq (2.3) can be written in the form:

$$\frac{\partial \psi}{\partial \theta} = -\frac{\partial \psi}{\partial \zeta} + \frac{\partial}{\partial \zeta}\left(\frac{1}{\mathrm{Pe}}\frac{\partial \psi}{\partial \zeta}\right) + S(\psi, \zeta) \tag{5.5}$$

The dimensionless number $\mathrm{Pe} = \frac{uL}{D}$ that appears in eq (5.5) is the Péclet number that can be regarded as the ratio of rate of transport by convection to rate of transport by dispersion or diffusion. (Fogler, 1999) Some authors prefer the Bodenstein number $\mathrm{Bo} = \frac{D}{uL}$, which is the inverse of the Péclet number. The advantage of the Bodenstein number over the Péclet number is that it is finite when $D = 0$. The Péclet number, however, is used in most textbooks and this convention is retained here.

The moment transformation of eq (5.5) is done by substituting it into eq (4.4) and integrating:

$$\frac{dm_j}{d\theta} = \int_0^1 \frac{\partial \psi}{\partial \theta}\zeta^j dz = \int_0^1 \left( -\frac{\partial \psi}{\partial \zeta} + \frac{\partial}{\partial \zeta}\left(\frac{1}{\mathrm{Pe}}\frac{\partial \psi}{\partial \zeta}\right) + S(\psi, \zeta)\right)\zeta^j d\zeta \tag{5.6}$$

Since integration is a linear operation, each term can be integrated separately:

$$\left.\frac{dm_j}{d\theta}\right|_{convection} = j\int_0^1 \psi \zeta^{j-1} d\zeta + \delta(0, j)\psi\big|_{\zeta=0} - \psi\big|_{\zeta=1} \tag{5.7}$$

$$\left.\frac{dm_j}{d\theta}\right|_{source} = \int_0^1 S(\psi, \zeta)\zeta^j d\zeta \tag{5.8}$$

$$\left.\frac{dm_j}{d\theta}\right|_{diffusion} = -j\int_0^1 \zeta^{j-1}\frac{1}{\mathrm{Pe}}\frac{\partial \psi}{\partial \zeta} d\zeta - \delta(0, j)\frac{1}{\mathrm{Pe}}\frac{\partial \psi}{\partial \zeta}\bigg|_{\zeta=0} + \frac{1}{\mathrm{Pe}}\frac{\partial \psi}{\partial \zeta}\bigg|_{\zeta=1} \tag{5.9}$$

Collecting all terms gives the full moment transformation with boundary conditions:

$$\frac{dm_j}{d\theta} = \int_0^1 \left( S(\psi,\zeta)\zeta^j + j\zeta^{j-1}\left(\psi - \frac{1}{\mathrm{Pe}}\frac{\partial\psi}{\partial\zeta}\right)\right)d\zeta$$
$$+\delta(0,j)\left(\psi\big|_{\zeta=0} - \frac{1}{\mathrm{Pe}}\frac{\partial\psi}{\partial\zeta}\bigg|_{\zeta=0}\right) - \left(\psi\big|_{\zeta=1} - \frac{1}{\mathrm{Pe}}\frac{d\psi}{d\zeta}\bigg|_{\zeta=1}\right) \qquad (5.10)$$
$$= \int_0^1 \left( S(\psi,\zeta)\zeta^j + j\psi\zeta^{j-1} - \frac{j}{\mathrm{Pe}}\zeta^{j-1}\frac{\partial\psi}{\partial\zeta}\right)d\zeta + \delta(0,j)R_0 - R_1$$

The last two terms in eq (5.10) are the boundary conditions at the inflow and outflow boundaries, respectively. The Kronecker delta means that the inflow boundary condition is added as a source term only to the zeroth moment. The shorthand notations

$$R_0 \equiv \psi\big|_{\zeta=0} - \frac{1}{\mathrm{Pe}}\frac{\partial\psi}{\partial\zeta}\bigg|_{\zeta=0} \qquad (5.11)$$

and

$$R_1 \equiv \psi\big|_{\zeta=1} - \frac{1}{\mathrm{Pe}}\frac{d\psi}{d\zeta}\bigg|_{\zeta=1} \qquad (5.12)$$

are introduced for the boundary conditions. Unlike in the orthogonal collocation method, in the moment method the boundary conditions do not yield additional equations that have to be solved along with the differential equations; the boundary conditions are simply added to the equations. This reduces the number of equations to be solved. The moment method also allows for easy construction of both high-order and low-order methods, also on finite elements.

The Danckwerts boundary conditions discussed in Section 2.2 are, in their dimensionless form:

$$\psi\big|_{\zeta=0} = \psi_0 - \frac{1}{\mathrm{Pe}}\frac{\partial\psi}{\partial\zeta}\bigg|_{\zeta=0} \qquad (5.13)$$
$$\psi\big|_{\zeta=1} = 0$$

In the moment transformation equation (5.10), they are specified simply by setting

$$R_0 = \psi_0 \qquad (5.14)$$
$$R_1 = \hat{\psi}\big|_{\zeta=1}$$

where the overhead sign ^ means the value of the variable calculated from the approximating polynomial in that section. At the sub-interval boundaries, the physical boundary condition is given by eq (2.6). Different formulas can be used for the numerical

boundary condition. Since convection carries information in the downstream direction only, the convective contribution is always calculated from the polynomial in the upstream section. The diffusive contribution at the boundary can be calculated either as the arithmetic average of the derivatives of the polynomial on both sides of the element boundary:

$$R_{1,i} = R_{0,i+1} \equiv \widehat{\psi}\Big|_{\zeta=1}^{i} - \frac{1}{2}\left( \frac{1}{\mathrm{Pe}_i} \frac{\partial \widehat{\psi}}{\partial \zeta}\bigg|_{\zeta=1}^{i} + \frac{1}{\mathrm{Pe}_{i+1}} \frac{\partial \widehat{\psi}}{\partial \zeta}\bigg|_{\zeta=0}^{i+1} \right) \tag{5.15}$$

Or the diffusive contribution can be calculated using only the polynomial in the downstream section:

$$R_{1,i} = R_{0,i+1} \equiv \widehat{\psi}\Big|_{\zeta=1}^{i} - \frac{1}{\mathrm{Pe}_{i+1}} \frac{\partial \widehat{\psi}}{\partial \zeta}\bigg|_{\zeta=0}^{i+1} \tag{5.16}$$

### 5.2.2 Examples

Publication [II] contains two examples of applications of the moment transformation method to systems with axial dispersion: startup of a tubular reactor and a packed-bed adsorber. Concentration profiles from the reactor startup example are shown in Figure 15 and Figure 16 for two different systems with different Péclet numbers. The number of variables in the approximations was kept constant at 12, and the accuracy was varied by changing the polynomial degree and the number of sub-intervals.

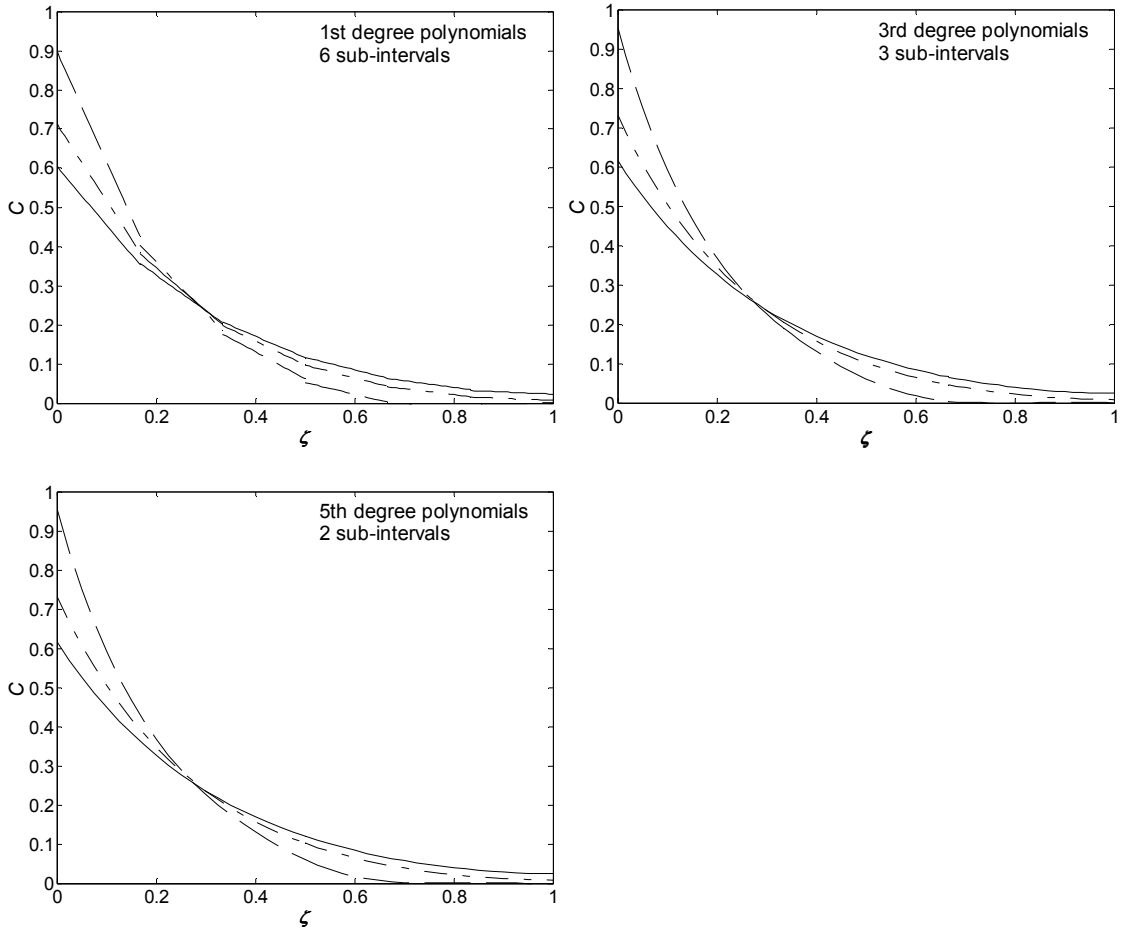


**Figure 15. Concentration profiles at $\theta_L$ = 0.5 for a 1st order reaction with $Da_L$ = 5 for different Péclet numbers using 12 variables and polynomials of different degree. ( — $Pe_L$ = 5; –·– $Pe_L$ = 10; –– $Pe_L$ = 100)**

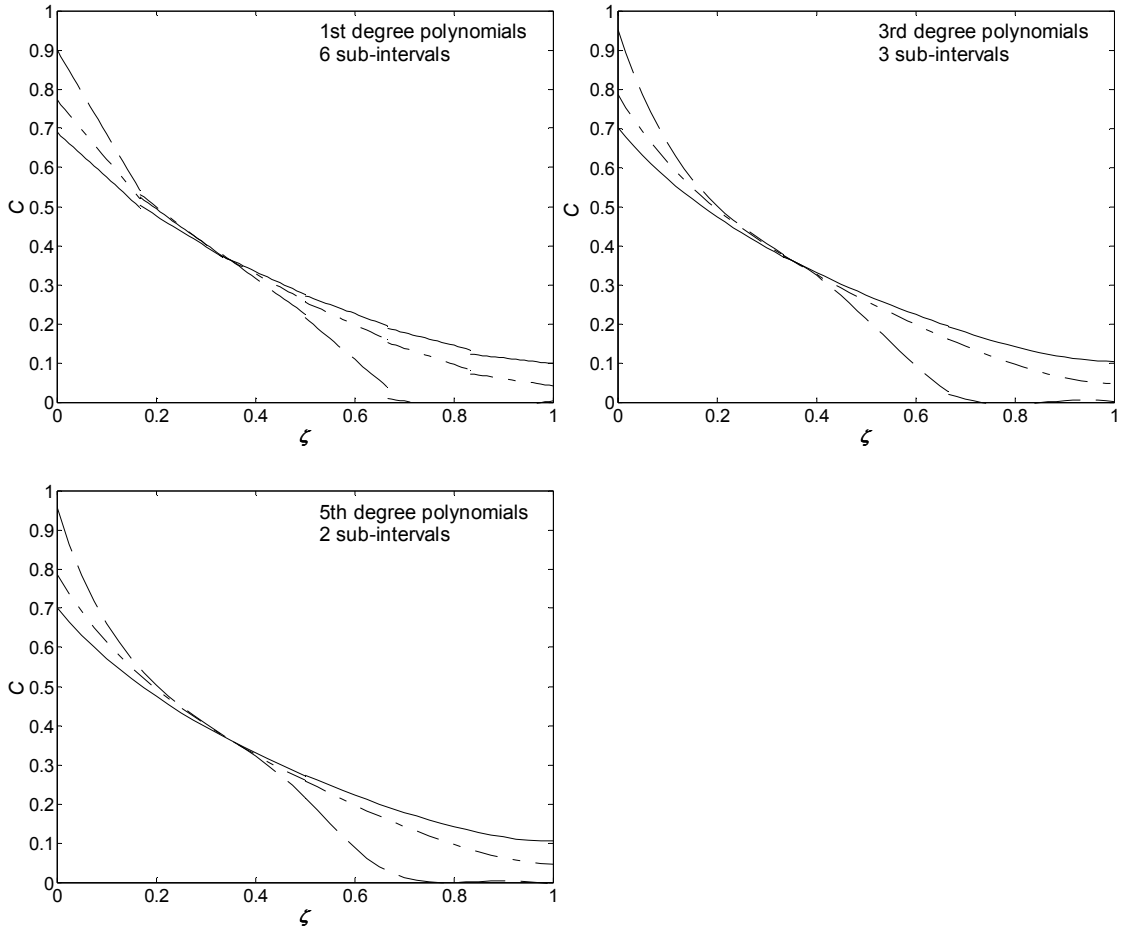


**Figure 16. Concentration profiles at $\theta_L$ = 0.5 for a 2nd order reaction with $Da_L$ = 5 for different Péclet numbers using 12 variables and polynomials of different degree. ( — $Pe_L$ = 5; –·–· $Pe_L$ = 10; –– $Pe_L$ = 100) Notice the concentration front at $\zeta$= 0.5 that is barely visible in the 1st order polynomials (linear profiles).**

### *5.2.3 Error Analysis*

To obtain an error estimate for the method, an error analysis similar to the one in Alopaeus *et al.* (2008) was done. A finite volume (finite difference) model solution with 500 variables and first-order discretization was used as a reference, to which the solution obtained with the moment method was compared. A discrete approximation of the root mean squared (RMS) error was used as the error estimate. Figure 17 shows the error for the solution of a tubular reactor model with first-order reaction and high axial dispersion at steady-state. Figure 18 shows the error in the numerically more challenging case of a reactor with little axial dispersion and second-order reaction.

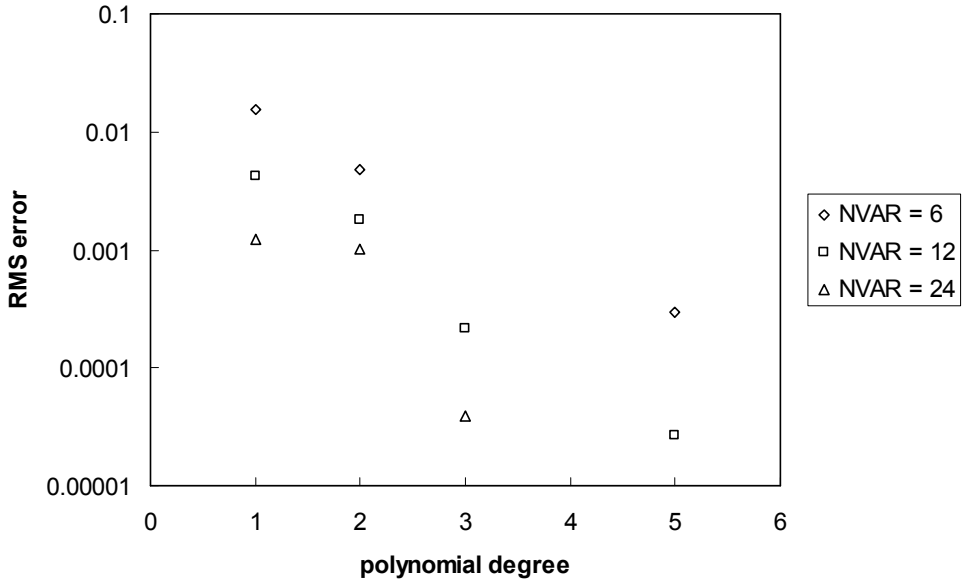


**Figure 17. RMS errors in the steady-state solution of the reactor case, compared to the reference solution with 500 control volumes, with $Pe_L = 10$, $Da_L = 5$ (1st order reaction), and $\theta_L = 2$.**

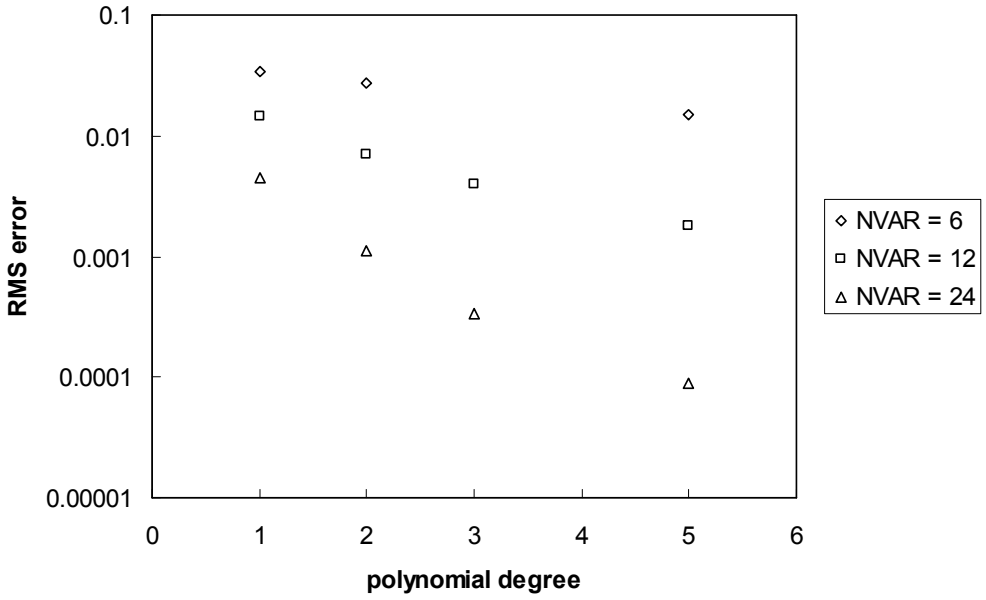


**Figure 18. RMS errors in the reactor case at $\theta_L = 0.5$, compared to the reference solution with 500 control volumes. $Pe_L = 100$, $Da_L = 5$ (2nd order reaction).**

## 5.3 Continuous-Contact Distillation and Absorption

The application of the moment transformation method to the simulation of continuous-contact distillation and absorption processes is the subject of Publication [III]. Continuous-contact distillation and absorption processes are modeled with eqs (2.29) – (2.34). In order to apply the moment transformation method, eqs (2.29) – (2.34) are first transformed into their nondimensional forms. This is done by introducing the dimensionless variables shown in Table 1. In the analysis to follow, the reaction term is ignored, but in principle it can be included as well. The dimensionless forms of eqs (2.29) – (2.34) are:

$$\frac{\partial B_L^*}{\partial \theta} = -\frac{\partial L^*}{\partial \zeta} + \sum_{i=1}^{nc} \left(N_{iVL} a\right)^* \tag{5.17}$$

$$\frac{\partial B_V^*}{\partial \theta} = -\frac{\partial V^*}{\partial \zeta} - \sum_{i=1}^{nc} \left(N_{iVL} a\right)^* \tag{5.18}$$

$$\frac{\partial b_{iL}^*}{\partial \theta} = -\frac{\partial \left(x_i L^*\right)}{\partial \zeta} + \frac{1}{\mathrm{Pe}_{m,L}} \frac{\partial}{\partial \zeta}\left( B_L^* \frac{\partial x_i}{\partial \zeta} \right) + \left(N_{iVL} a\right)^* \tag{5.19}$$

$$\frac{\partial b_{iV}^*}{\partial \theta} = -\frac{\partial \left(y_i V^*\right)}{\partial \zeta} + \frac{1}{\mathrm{Pe}_{m,V}} \frac{\partial}{\partial \zeta}\left( B_V^* \frac{\partial y_i}{\partial \zeta} \right) - \left(N_{iVL} a\right)^* \tag{5.20}$$

$$\frac{\partial E_L^*}{\partial \theta} = -\frac{\partial \left(L^* H_L^*\right)}{\partial \zeta} + \frac{1}{\mathrm{Pe}_{h,L}} \frac{\partial}{\partial \zeta}\left( B_L^* \frac{\partial H_L^*}{\partial \zeta} \right) + \left(q_{VL} a\right)^* \tag{5.21}$$

$$\frac{\partial E_V^*}{\partial \theta} = -\frac{\partial \left(V^* H_V^*\right)}{\partial \zeta} + \frac{1}{\mathrm{Pe}_{h,V}} \frac{\partial}{\partial \zeta}\left( B_V^* \frac{\partial H_V^*}{\partial \zeta} \right) - \left(q_{VL} a\right)^* \tag{5.22}$$

**Table 1. Dimensionless variables and quantities in eqs (5.17) – (5.22). The same reference values are used for vapor and liquid phases.**

| Dimensionless variables | Definition |
|---|---|
| Axial coordinate | $\zeta = \dfrac{z}{\Delta h}$ |
| Time | $\theta = \dfrac{t}{\tau}$ |
| Total buildup | $B^* = \dfrac{B}{c_{ref}}$ |
| Component buildup | $b_i^* = \dfrac{b_i}{c_{ref}}$ |
| Energy buildup | $E^* = \dfrac{BH}{c_{ref} H_{ref}} = B^* H^*$ |
| Enthalpy | $H^* = \dfrac{H}{H_{ref}}$ |
| Liquid flowrate | $L^* = \dfrac{L}{c_{ref} u_{ref}}$ |
| Vapor flowrate | $V^* = \dfrac{V}{c_{ref} u_{ref}}$ |
| **Dimensionless quantities** | |
| Volumetric interfacial mass transfer flux | $\left(N_i a\right)^* = \dfrac{N_i a \tau}{c_{ref}}$ |
| Volumetric interfacial heat transfer flux | $\left(qa\right)^* = \dfrac{qa\tau}{c_{ref} H_{ref}}$ |
| Mass Péclet number | $\mathrm{Pe}_m = \dfrac{u_{ref}\Delta h}{D}$ |
| Heat Péclet number | $\mathrm{Pe}_h = \dfrac{u_{ref}\Delta h}{\alpha}$ |
| Reference time (s) | $\tau = \dfrac{\Delta h}{u_{ref}}$ |

When the moment transformation equation (4.4) is applied to eqs (5.17) – (5.22), the following transformed equations are obtained:

$$\frac{dm_j^{BL}}{d\theta} = \int_0^1 \left( \zeta^j \sum_{i=1}^{nc} \left(N_{iVL} a\right)^* + j\zeta^{j-1} L^* \right) d\zeta + \delta(0,j) L^*_{\zeta=0} - L^*_{\zeta=1} \tag{5.23}$$

$$\frac{dm_j^{BV}}{d\theta} = \int_0^1 \left( \zeta^j \sum_{i=1}^{nc} \left(-N_{iVL} a\right)^* + j\zeta^{j-1} V^* \right) d\zeta + \delta(0,j) V_{\zeta=0}^* - V_{\zeta=1}^* \tag{5.24}$$

$$\begin{aligned} \frac{dm_j^{biL}}{d\theta} &= \int_0^1 \left[ \zeta^j \left(N_{iVL} a\right)^* + j\zeta^{j-1} \left( L^* - \frac{B_L^*}{\mathrm{Pe}_{m,L}} \frac{\partial x_i}{\partial \zeta} \right) \right] d\zeta \\ &+ \delta(0,j) \left( x_i L^* - \frac{B_L^*}{\mathrm{Pe}_{m,L}} \frac{\partial x_i}{\partial \zeta} \right)_{\zeta=0} - \left( x_i L^* - \frac{B_L^*}{\mathrm{Pe}_{m,L}} \frac{\partial x_i}{\partial \zeta} \right)_{\zeta=1} \end{aligned} \tag{5.25}$$

$$\begin{aligned} \frac{dm_j^{biV}}{d\theta} &= \int_0^1 \left[ \zeta^j \left(-N_{iVL} a\right)^* + j\zeta^{j-1} \left( V^* - \frac{B_V^*}{\mathrm{Pe}_{m,V}} \frac{\partial y_i}{\partial \zeta} \right) \right] d\zeta \\ &+ \delta(0,j) \left( y_i V^* - \frac{B_V^*}{\mathrm{Pe}_{m,V}} \frac{\partial y_i}{\partial \zeta} \right)_{\zeta=0} - \left( y_i V^* - \frac{B_V^*}{\mathrm{Pe}_{m,V}} \frac{\partial y_i}{\partial \zeta} \right)_{\zeta=1} \end{aligned} \tag{5.26}$$

$$\begin{aligned} \frac{dm_j^{HL}}{d\theta} &= \int_0^1 \left[ \zeta^j \left(q_{VL} a\right)^* + j\zeta^{j-1} \left( L^* H_L^* - \frac{B_L^*}{\mathrm{Pe}_{h,L}} \frac{\partial H_L^*}{\partial \zeta} \right) \right] d\zeta \\ &+ \delta(0,j) \left( L^* H_L^* - \frac{B_L^*}{\mathrm{Pe}_{h,L}} \frac{\partial H_L^*}{\partial \zeta} \right)_{\zeta=0} - \left( L^* H_L^* - \frac{B_L^*}{\mathrm{Pe}_{h,L}} \frac{\partial H_L^*}{\partial \zeta} \right)_{\zeta=1} \end{aligned} \tag{5.27}$$

$$\begin{aligned} \frac{dm_j^{HV}}{d\theta} &= \int_0^1 \left[ \zeta^j \left(-q_{VL} a\right)^* + j\zeta^{j-1} \left( V^* H_V^* - \frac{B_V^*}{\mathrm{Pe}_{h,V}} \frac{\partial H_V^*}{\partial \zeta} \right) \right] d\zeta \\ &+ \delta(0,j) \left( V^* H_V^* - \frac{B_V^*}{\mathrm{Pe}_{h,V}} \frac{\partial H_V^*}{\partial \zeta} \right)_{\zeta=0} - \left( V^* H_V^* - \frac{B_V^*}{\mathrm{Pe}_{h,V}} \frac{\partial H_V^*}{\partial \zeta} \right)_{\zeta=1} \end{aligned} \tag{5.28}$$

The holdup discrepancy functions, eq (2.41) and eq (2.42), are transformed similarly:

$$F_j^L = 0 = \int_0^1 \left( 1 - \frac{B_L}{h_{L,corr} c_{TL} \varepsilon} \right) \zeta^j d\zeta \tag{5.29}$$

$$F_j^V = 0 = \int_0^1 \left( 1 - \frac{B_V}{\left(1 - h_{L,corr}\right) c_{TV} \varepsilon} \right) \zeta^j d\zeta \tag{5.30}$$

The system defined by eqs (5.23) – (5.30) is a system of differential algebraic equations. In vector form the system can be represented as:

$$\overline{F} = \left( \frac{dm_j^{BL}}{d\theta} \quad \frac{dm_j^{biL}}{d\theta} \quad \frac{dm_j^{Bv}}{d\theta} \quad \frac{dm_j^{biV}}{d\theta} \quad \frac{dm_j^{HL}}{d\theta} \quad \frac{dm_j^{HV}}{d\theta} \quad F_j^L \quad F_j^V \right)^T \tag{5.31}$$

The solution vector is defined as:

$$\overline{S} = \left( m_j^{BL} \quad m_j^{biL} \quad m_j^{BV} \quad m_j^{biV} \quad m_j^{HL} \quad m_j^{HV} \quad m_j^L \quad m_j^V \right)^T \tag{5.32}$$

The steady-state solution can be obtained by solving the system of nonlinear equations:

$$\overline{F}\left(\overline{S}\right) = 0 \tag{5.33}$$

Dynamic solutions are obtained by adding the discretized time derivatives to the residuals on the RHS of the balance eqs (5.23) – (5.28). The same implicit methods that are used for time integration in the finite difference method can be applied here. The three practical methods for the discretization of the time derivative are: the implicit Euler method, the three-level implicit method, and the Crank-Nicolson scheme (Ferziger and Perić, 2002), of which the former two are the easiest to implement. In principle higher order methods could be used as well but in practice second-order accuracy is sufficient for most purposes.

The three-level implicit method is stable at all time steps and is second-order accurate.

$$0 = \frac{dm_j^{k,n+1}}{d\theta} - \left( \frac{\frac{3}{2} m_j^{k,n+1} - 2m_j^{k,n} + \frac{1}{2} m_j^{k,n-1}}{\Delta\theta} \right) \tag{5.34}$$

The implicit Euler method is also stable at all time steps but is only first-order accurate.

$$0 = \frac{dm_j^{k,n+1}}{d\theta} - \left( \frac{m_j^{k,n+1} - m_j^{k,n}}{\Delta\theta} \right) \tag{5.35}$$

Both time integration schemes lead eventually to the same steady-state solution, but if exact transients are important, then the three-level implicit scheme should be preferred.

The system of nonlinear equations consists of totally (2 × nc + 2 + 2) × (degree + 1) × (number of subintervals) equations. In Publication [III], the Newton-Raphson method was used to solve the system.

In Publication [III], the method is demonstrated with an example of ternary distillation of the system benzene-*m*-xylene-toluene. A description of the simulated column is given in Publication [III]. The design specifications were fixed reflux ratio and fixed bottom product flow rate. Simulations were done for systems with and without axial dispersion. Figure 19 shows the steady-state composition profiles in the column, calculated with different method orders (degree of the approximating polynomials) and constant number of 24 variables. This is achieved by combining polynomial degree and number of

elements in the following ways, remembering that the number of variables for a profile within an element is (*degree* + 1): $0^{th}$ degree and 24 elements; $1^{st}$ degree and 12 elements; $2^{nd}$ degree and 8 elements; and $3^{rd}$ degree and 6 elements. The approximation with $0^{th}$ degree polynomials is equivalent to the nonequilibrium stage model. Figure 20 shows more profiles calculated with the nonequilibrium stage model with increasing number of elements in comparison to a reference solution ($3^{rd}$ degree polynomials, 10 elements, 40 variables) and to a solution with $3^{rd}$ degree polynomials and 2 elements (8 variables). The comparison shows that even with a large number of elements, the nonequilibrium stage model converges only slowly towards the reference solution, whereas with high-degree polynomial profiles, even approximations with a low number of variables are already very accurate. A more profound error analysis, similar to the reactor case in the previous section, is given in Publication [III]. The figures clearly show that the numerical diffusion in the nonequilibrium stage model has the same effect on the column profiles and the predicted column performance as physical axial dispersion.

This can be seen especially when Figure 20 is compared to Figure 21, which shows the same simulations in a case with axial dispersion, with all axial dispersion coefficients set to 0.005 $m^2\ s^{-1}$. Figure 22 demonstrates the dynamic simulation feature of the model. It shows the dynamic response of both systems (with and without axial dispersion) to a sudden change of the reflux ration from 8 to 2 (at constant bottom product flow rate).

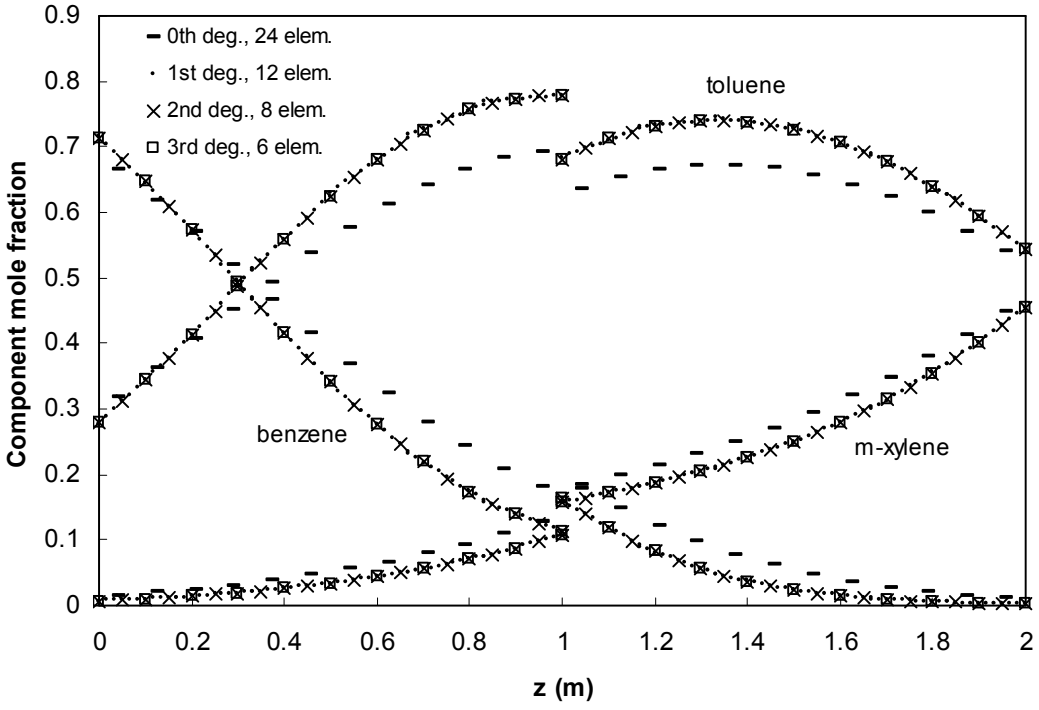


**Figure 19. Steady-state liquid composition profiles in the column without axial dispersion. Profiles calculated with 24 variables/profile and increasing polynomial degree. Approximation with $0^{th}$ degree polynomials is equivalent to the nonequilibrium stage model. Condenser at $z$ = 0, bottom of the packing at $z$ = 2 m, feed point at $z$ = 1 m, reboiler not shown.**

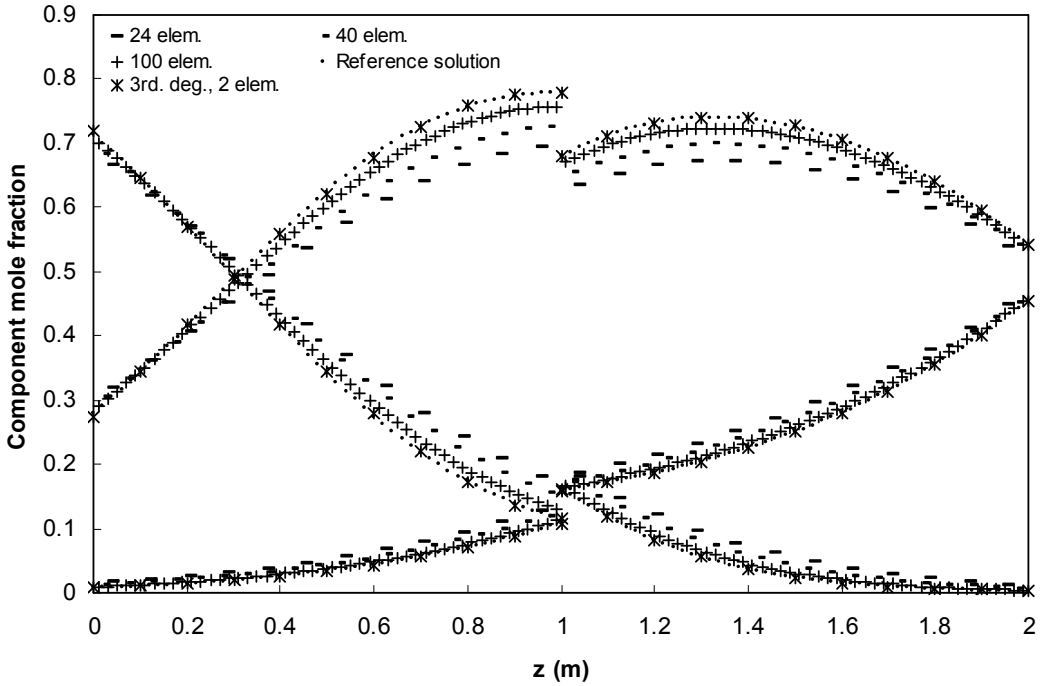


**Figure 20. Comparison of steady state liquid composition profiles calculated with $0^{th}$ degree polynomials and increasing number of elements (equivalent to nonequilibrium stage model) to polynomial approximations.**

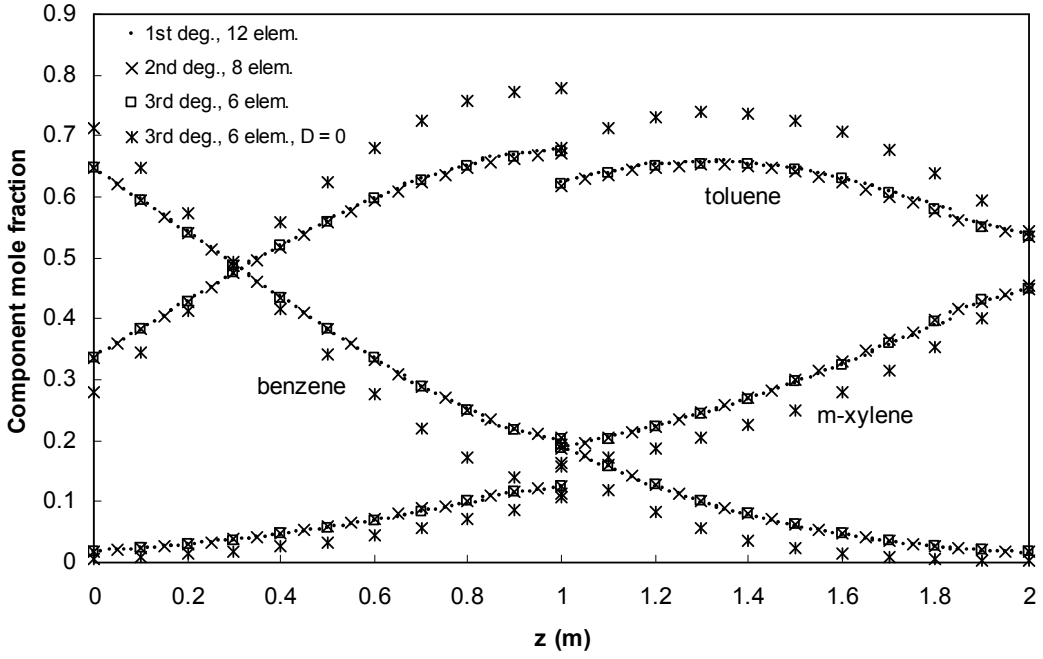


**Figure 21. Steady-state liquid composition profiles in the column with axial dispersion ($D_L = D_V = \alpha_L = \alpha_V = 0.005$ m$^2$ s$^{-1}$). Condenser at $z = 0$, bottom of the packing at $z = 2$ m, feed point at $z = 1$ m, reboiler not shown. Profiles calculated with 24 variables/profile and increasing polynomial degree.**

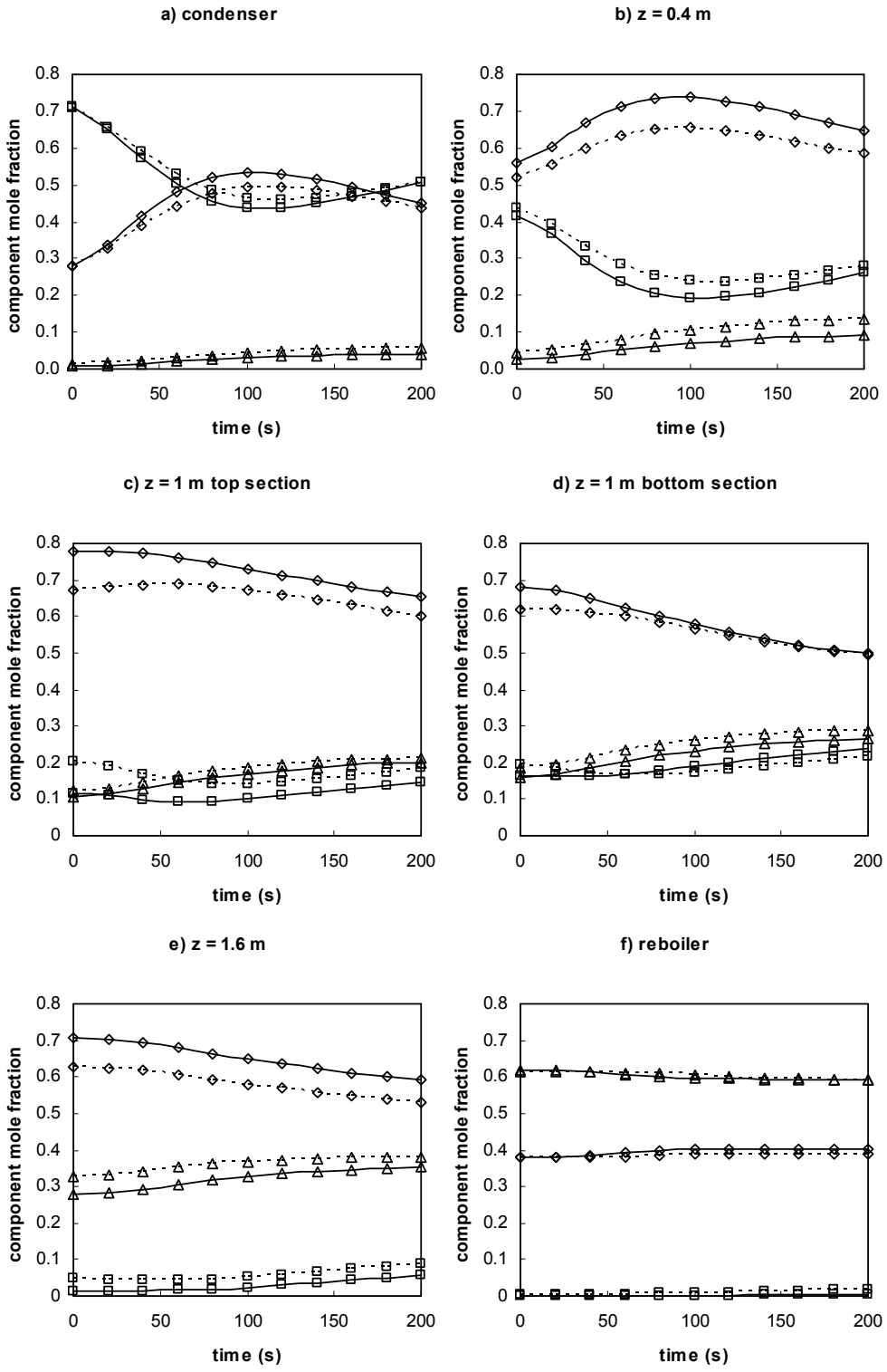


**Figure 22. Dynamic response of the column to a change of the reflux ratio from 8 to 2 at $t = 0$ s. Solid line: no axial dispersion. Dashed line: $D_L = D_V = \alpha_L = \alpha_V = 0.005$ m$^2$ s$^{-1}$. □: benzene; ◊: toluene; Δ: m-xylene.**

## 5.4 Computational Effort and CPU Time

The computational effort that is reflected in CPU time required by the various methods is interesting to the user. However, a fair comparison between methods of different order is often difficult. In many cases, the number of variables needed to achieve a certain level of accuracy is a good measure of the computational effort. A first-order method requires the use of far more variables to achieve a certain level of accuracy than a high-order method. If the number of variables is kept constant, the first-order method will require less CPU time but the solution will be by far more inaccurate.

Such a comparison was done in Publication [II], where the orthogonal collocation on finite elements (OCFE) method and the moment method were compared to the finite volume method. Figure 23 shows a comparison of relative CPU times for a particular test problem (dynamic plug-flow reactor) between the OCFE method, the moment method, and the finite volume method with 2nd order discretization. The results were obtained using MATLAB's ode15s solver that can handle both ordinary differential and differential-algebraic equations. Cubic polynomials were used for both WRM. The number of variables was chosen such that the same level of accuracy was obtained with all methods. When the WRM are compared, it is seen that the moment method requires approximately twice the CPU time compared to the collocation method. This is due to the additional computational effort that arises from the numerical evaluation of the definite integral by quadrature. This holds also for other integral methods such as the finite element or the Galerkin method. The time required to obtain a comparably accurate solution with the finite volume method is much higher.

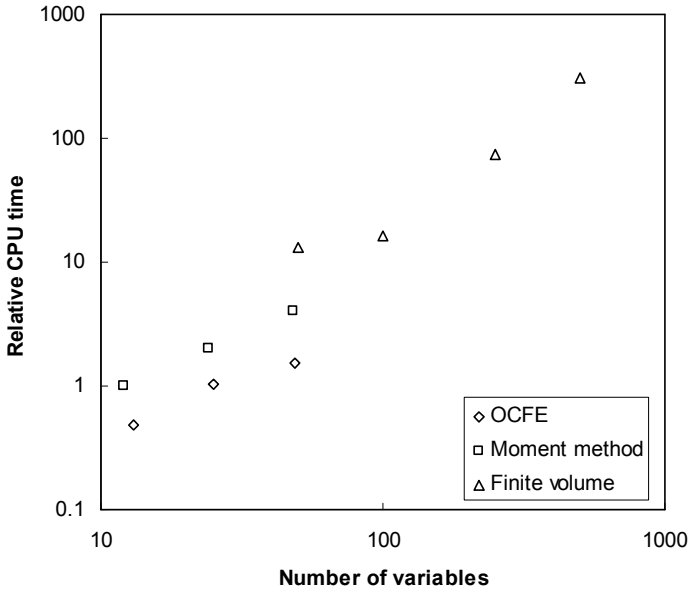


**Figure 23. Comparison of CPU times between the orthogonal collocation on finite elements (OCFE), moment, and finite volume methods.**

The moment method and other WRM offer two means to increase the number of variables: increasing the number of elements and increasing the degree of the approximating polynomials. Generally speaking, the effect on CPU time of these two strategies is roughly the same. If the problem is very large, it can be argued that increasing the number of elements is the better strategy since it keeps the number of non-diagonal elements of the differentiation matrix low. When using the moment method, of course, the degree of the polynomials is limited anyway by the inverse of the moment transformation matrix. Sometimes the calculation can be sped up significantly by applying certain numerical tricks. The best example is the spectral method, where Fast Fourier Transform (FFT) can be used instead of full matrix multiplication. (Trefethen, 2000)

A factor that significantly affects the computational effort needed for dynamic simulation is the choice of time integration method. If the problem is not stiff, then explicit methods such as Runge-Kutta are favorable. If the problem is stiff, then implicit methods such as backward differencing formulae (BDF) have to be used due to reasons of stability. (Davis, 1984) Advanced integrators can automatically judge the stiffness of the system and adjust time step and integration method accordingly.

Implicit methods involve the solution of a system of equations, linear or non-linear, at every time step. They can be easily adopted for solving differential-algebraic equations, while explicit methods cannot be generally used for the task. This means that explicit methods cannot be used for time integration in conjunction with WRM that produce differential-algebraic equations, the most prominent example being collocation methods that include the boundary conditions as algebraic equations. In some cases, especially when modeling multiphase systems, the moment method can also lead to a system of differential-algebraic equations. Then implicit methods have to be used as well. An example is the continuous-contact separation model in Publication [III].

# 6 Closure Models

## 6.1 Mass Transfer Models

### *6.1.1 Maxwell-Stefan Model and Effective Diffusivity Methods*

The Maxwell-Stefan model and the full matrix method associated with it are state-of-the-art for calculating multicomponent mass and heat transfer. The basic idea behind the Maxwell-Stefan model is the force balance on a molecule of species *i* in a mixture. A detailed development of the equations can be found in chapter 8 of Taylor and Krishna's (1993) book.

With the full matrix method, the diffusive fluxes in a film of finite thickness are calculated as:

$$\left(J_B\right) = c_t \left[k^\bullet\right]\left(x_B - x_I\right) \tag{6.1}$$

$\left[k^\bullet\right] = [k][\Xi]$ is the matrix of finite mass transfer coefficients, where the matrix of low-flux mass transfer coefficients [*k*] and the high-flux correction matrix $[\Xi]$ are defined as:

$$[k] = [R_B]^{-1}[\Gamma] \tag{6.2}$$

$$[\Theta] = [\Gamma]^{-1}[\Phi]$$

$$[\Xi] = [\Theta]\{\exp[\Theta] - [I]\}^{-1} \tag{6.3}$$

The elements of the square matrices [*R*] and [Φ] are:

$$R_{ii} = \frac{x_i}{\kappa_{in}} + \sum_{\substack{k=1 \\ k \neq i}}^{n} \frac{x_k}{\kappa_{ik}} \tag{6.4}$$

$$R_{ij} = -x_i\left(\frac{1}{\kappa_{ij}} - \frac{1}{\kappa_{in}}\right) \tag{6.5}$$

$$\Phi_{ii} = \frac{N_i}{c_t \kappa_{in}} + \sum_{\substack{k=1 \\ k \neq i}}^{n} \frac{N_k}{c_t \kappa_{ik}} \tag{6.6}$$

$$\Phi_{ij} = -N_i\left(\frac{1}{c_t \kappa_{ij}} - \frac{1}{c_t \kappa_{in}}\right) \tag{6.7}$$

The binary mass transfer coefficients $\kappa$ are defined as:

$$\kappa_{ij} = \frac{Đ_{ij}}{l} \tag{6.8}$$

$l$ is the length of the diffusion path that is assumed to be the film thickness in the film model. If temperature and concentration gradients within the film are neglected, the coefficients $c_t \kappa_{ij}$ and the matrix of thermodynamic factors [Γ] can be assumed constant. In gaseous systems, [Γ] is often omitted. Since the film thickness is usually not known, Taylor and Krishna (1993) suggest that the binary mass transfer coefficients $\kappa_{ij}$ be calculated from the binary Maxwell-Stefan diffusion coefficients using a mass transfer correlation (see Section 6.2). The binary Maxwell-Stefan diffusion coefficients can be estimated quite accurately using suitable correlations. In gas and vapor systems, the use of these correlations is straightforward. In liquid systems, the binary infinite dilution mass transfer coefficients are estimated first and then corrected for finite mole fractions. (Taylor and Krisna, 1993, chapter 3)

The molar fluxes $N$ are related to the diffusion fluxes $J$ by the following equation:

$$(N) = (J_B) + (x_B) N_t \tag{6.9}$$

Since only $n$ -1 diffusion fluxes $J$ are independent, but all fluxes $N$ are independent, and the total flux $N_t$ is not known *a priori* in the general case, additional information is needed. This additional condition is called the bootstrap condition. Typical bootstrap conditions are for example zero net flux or constant ratios of the mass transfer fluxes. If both energy and mass transfer through the interface are considered, the bootstrap condition is given by the energy equation.

A number of simplified methods have been developed as an alternative to the fairly complicated full Maxwell-Stefan matrix method. One of those simplified methods is the effective diffusivity method that is used in Publication [IV]. The aim of effective diffusivity methods is to avoid matrix algebra in calculating the mass transfer fluxes (leading to a decrease of about one order of magnitude in computation time). To derive the effective diffusivity method, it is assumed that the diffusion flux of a component depends only on its own concentration gradient, as in Fick's diffusion model: (Taylor and Krishna, 1993, chapter 6)

$$J_i = -c_t D_{i,eff} \nabla x_i \tag{6.10}$$

For the film model this means that the mass transfer flux is obtained directly from: (Taylor and Krishna, 1993, chapter 8.6)

$$J_{iB} = c_t k^{\bullet}_{i,eff} \left( y_{iB} - y_{iI} \right) \tag{6.11}$$

The equations for calculating the effective mass transfer coefficient are:

$$k^{\bullet}_{i,eff} = k_{i,eff} \Xi_{i,eff} \tag{6.11}$$

$$k_{i,eff} = \frac{D_{i,eff}}{l} \tag{6.12}$$

$$\Xi_{i,eff} = \frac{\Phi_{i,eff}}{\exp\left(\Phi_{i,eff}\right) - 1} \tag{6.13}$$

$$\Phi_{i,eff} = \frac{N_t l}{c_t \mathcal{D}_{i,eff}} \tag{6.14}$$

There are several alternative methods for estimating the effective diffusivities from the binary Maxwell-Stefan mass transfer coefficients. One method that is frequently used is the method of Wilke (1950):

$$D_{i,eff} = \frac{1 - x_i}{\sum_{\substack{j=1 \\ j \neq i}}^{n} \frac{x_j}{\mathcal{D}_{ij}}} \tag{6.15}$$

Other methods can be found in Taylor and Krishna (1993, chapter 6).

Effective diffusivity methods are accurate only when the case in question is close to one of the following limiting cases: (ibid)

- all binary diffusion coefficients equal
- dilute mixtures where one component is in large excess
- species $i$ diffuses through $n - 1$ stagnant gases

Wilke's equation (6.15) was originally intended for the third case, but it is often used even when this assumption is not valid. In Publication [IV], the use of Wilke's equation is justified since hydrogen is the only component that is transferred through the gas-liquid interface in notable quantities.

### *6.1.2 Double Film Model*

Nowadays, the double film model is the standard model for calculating mass and heat transfer fluxes across phase boundaries. The most fundamental assumption is that the bulk phases are perfectly mixed and all mass transfer resistance is located in two adjacent films of finite thickness. Figure 24 shows a schematic representation of the model. The interface between the films is in thermodynamic equilibrium. There is no accumulation of mass or energy in the films or at the interface. However, the double film model can also be used for most dynamic process equipment models, since the timescale of bulk flow is much larger than the time that is needed for the films to achieve equilibrium. This assumption is made for example in the continuous-contact separation model in Section 2.5.1.

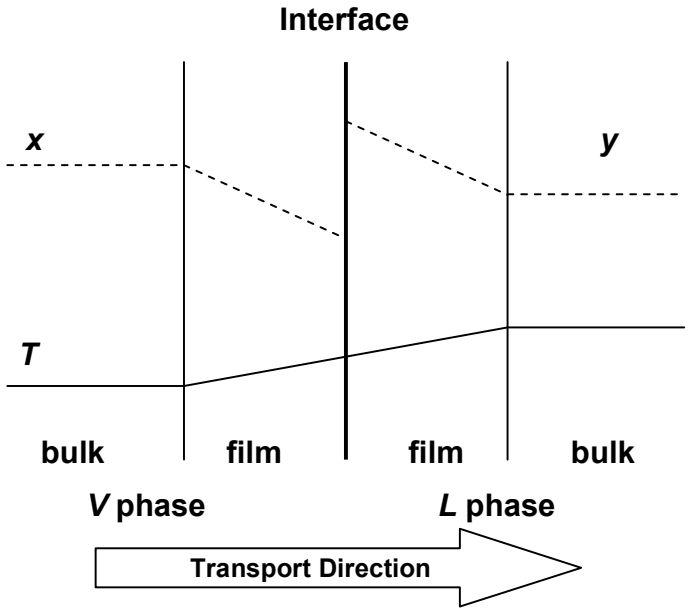


**Figure 24. Schematic representation of the double film model of mass transfer.**

When using the double film model for modeling of process equipment, such as continuous-contact distillation or trickle-bed reactors, all information about the complex flow patterns in the column packing or the catalyst bed is parameterized in the mass transfer coefficient. Because the film thickness is not known, a correlation for the mass transfer coefficient (briefly mass transfer correlation) is needed. Strictly speaking, the film concept is merely an abstraction, since in reality all mass transfer resistance cannot be located in a film of finite thickness. Consequently, the film thickness is not a real physical quantity, but should be rather understood as a model parameter. A reasonably accurate mass transfer correlation is crucial for obtaining meaningful results with the double film model. Some aspects of mass transfer correlations are discussed in Publication [IV] and Section 6.2.

The $(3nc + 1)$ variables to be solved are:

- $nc$ interface mole fractions in the $L$ phase ($x^I$)
- $nc$ interface mole fractions in the $V$ phase ($y^I$)
- $nc$ mass transfer fluxes ($N$)
- The interface temperature $T_I$

The equations for interphase mass and energy transfer in the double film model are: (Taylor and Krishna, 1993, chapter 11)

Mass transfer in the film in phase $V$ ($nc - 1$ eqs):

$$\left(R^V\right) \equiv c_t^V \left[k_V^{\bullet}\right]\left(y^V - y^I\right) + N_t(y^V) - (N) = (0) \tag{6.16}$$

Mass transfer in the film in phase $L$ ($nc - 1$ eqs):

$$\left(R^L\right) \equiv c_t^L \left[k_L^{\bullet}\right]\left(x^I - x^L\right) + N_t(x^L) - (N) = (0) \tag{6.17}$$

Thermodynamic equilibrium at the interface ($nc$ eqs):

$$Q_i^I \equiv K_i x_i^I - y_i^I = 0 \tag{6.18}$$

Energy equation (1 eq):

$$E^I \equiv q^V - q^L + \sum_{i=1}^{n} N_i \left(\overline{H}_i^V - \overline{H}_i^L\right) = 0 \tag{6.19}$$

Summation equations (2 eqs):

$$S^V = \sum_{i=1}^{n} y_i^I - 1 = 0 \tag{6.20}$$

$$S^L = \sum_{i=1}^{n} x_i^I - 1 = 0 \tag{6.21}$$

The system of equations (6.16) – (6.21) is usually solved with Newton's method.

## 6.2 Correlations for Mass Transfer Coefficients

### *6.2.1 Distillation and Absorption*

Onda's correlation is frequently used for randomly packed columns. The equations are, according to Taylor and Krishna (1993):

$$\frac{k_V}{a_p D_V} = A \,\mathrm{Re}_V^{0.7}\, \mathrm{Sc}_V^{0.333} \left(a_p d_p\right)^{-2} \tag{6.23}$$

$$\mathrm{Re}_V = \frac{\rho_t^V u_{SV}}{\mu_V a_p} \tag{6.23}$$

$$\mathrm{Sc}_V = \frac{\mu_V}{\rho_t^V D^V} \tag{6.24}$$

The parameter $A$ takes the value 2.0 if the nominal packing size $d_p$ is less than 0.012 m and 5.23 if $d_p$ is greater than or equal to 0.012 m.

$$k_L\left(\frac{\rho_t^L}{\mu_L g}\right)^{0.333} = 0.051\left(\mathrm{Re'}_L\right)^{0.667}\mathrm{Sc}_L^{-0.5}\left(a_p d_p\right)^{0.4} \tag{6.25}$$

$$\mathrm{Sc}_L = \frac{\mu_L}{\rho_t^L D^L} \tag{6.26}$$

$$\mathrm{Re'}_L = \frac{\rho_L u_{SL}}{\mu^L a'} \tag{6.27}$$

Onda's correlation for the interfacial area density $a$' (in $m^2/m^3$ of packing) is:

$$a' = a_p\left(1-\exp\left\{-1.45\left(\frac{\sigma_c}{\sigma}\right)^{0.75}\mathrm{Re}_L^{0.1}\,\mathrm{Fr}_L^{-0.05}\mathrm{We}_L^{0.2}\right\}\right) \tag{6.28}$$

$$\mathrm{Re}_L = \frac{\rho_t^L u_{SL}}{\mu^L a_p} \tag{6.29}$$

$$\mathrm{Fr}_L = \frac{a_p u_{SL}^2}{g} \tag{6.30}$$

$$\mathrm{We}_L = \frac{\rho_t^L u_{SL}^2}{a_p \sigma} \tag{6.31}$$

Bravo and Fair (1982) suggested an alternative correlation for the interfacial area density. In SI units, the correlation is: (Taylor and Krishna, 1993)

$$a' = 19.78 a_p\left(\mathrm{Ca}_L\,\mathrm{Re}_V\right)^{0.392}\sigma^{0.5}H^{-0.4} \tag{6.32}$$

$$\mathrm{Ca}_L = \frac{u_{SL}^2\mu^L}{\sigma} \tag{6.33}$$

Onda's correlation with Bravo and Fair's modification for the interfacial area density was used in [III]. Usually, the hydrodynamic and mass transfer correlations for specific packing types are interdependent. A comprehensive hydrodynamic and mass transfer model for structured packings is provided by Rocha *et al.* (1993, 1996) and for random packings by Wagner *et al.* (1997). New hydrodynamic and mass transfer models for novel packings, such as the catalytic packing KATAPAK-S, (Kołodziej *et al.*, 2004) are being developed constantly.

### 6.2.2 Gas-Liquid Mass Transfer in Trickle-Bed Reactors

Whereas the mass transfer correlations for packed and structured columns are well established, the validation data for different reactors and reaction systems, especially at industrial scale, are scarce. (Bhaskar *et al.*, 2004) Publication [IV] aims to meet this demand by comparing simulated trickle-bed temperature profiles to ones measured in industrial reactors and using the data for the validation of liquid film mass transfer correlations. For this purpose, an existing industrial trickle bed reactor for benzene hydrogenation was studied. Table 2 lists some well-known correlations for the different mass transfer coefficients needed in trickle-bed reactor modeling. Some of the correlations are flow regime specific, since trickle-bed reactors can operate in three different flow regimes: high interaction or pulsing flow regime, low interaction or trickle flow regime, and transition flow regime. More information on the use and the application areas of these correlations can be found in [IV].

In the base-case simulation, the correlations of Goto and Smith (1975) were used for the liquid film and liquid-solid mass transfer coefficients, and the correlation of Yaici *et al.* (1988) was used for the gas film mass transfer correlation. Figure 25 shows a comparison between measured and calculated liquid temperature profiles for two cases with different operating conditions (specified in [IV]). Toppinen *et al.* (1996) showed that the simulation results are most sensitive towards changes in the liquid film mass transfer coefficient $k_L a$. This result was also confirmed in [IV]. Figure 26 and Figure 27 show the effects of scaling the liquid-solid and liquid film mass transfer coefficients on the simulated temperature profiles. Scaling the gas film mass transfer coefficients did not have any noticeable effect on the simulation results. Figure 28 shows temperature profiles calculated with different correlations for the liquid film mass transfer coefficients. Clearly, the best results are obtained using the correlation of Goto and Smith (1975). Table 3 shows the numerical values calculated from the different correlations.

**Table 2. Mass transfer correlations for trickle-bed reactors (in SI units).**

| Reference | Correlation | Flow regime |
|---|---|---|
| Goto and Smith (1975) | $\frac{k_L a}{s^{-1}} = 10^4 \alpha_L \left( \frac{D}{m^2 s^{-1}} \right) \left( \frac{10^{-2}\, G_L / kg \cdot m^{-2} s^{-1}}{\mu_L / Pas} \right)^{n_L} (Sc_L)^{0.5}$<br>$\alpha_L = -2623 \left( \frac{d_p}{m} \right) + 13.63$ for $d_p > 0.0291 m$<br>$n_L = -8.197 \left( \frac{d_p}{m} \right) + 0.4339$<br>$\alpha_L = -759.8 \left( \frac{d_p}{m} \right) + 8.211$ for $d_p \le 0.0291 m$<br>$n_L = 8.442 \left( \frac{d_p}{m} \right) + 0.3854$ | All regimes |
| Wild *et al.* (1992) | $\mathrm{Sh}_L^{'} = 2.8 \cdot 10^{-4} \left[ \mathrm{X}_G^{0.5}\, \mathrm{Re}_L^{0.8}\, \mathrm{We}_L^{0.2} \mathrm{Sc}_L^{0.5} \left( \frac{a_S d_h}{1-\varepsilon} \right)^{0.25} \right]^{3.4}$ | Low interaction |
| | $\mathrm{Sh}_L^{'} = 0.091 \left[ \mathrm{X}_G^{0.25}\, \mathrm{Re}_L^{0.2}\, \mathrm{We}_L^{0.2} \mathrm{Sc}_L^{0.3} \left( \frac{a_S d_h}{1-\varepsilon} \right)^{0.25} \right]^{3.8}$ | Transition |
| | $\mathrm{Sh}_L^{'} = 0.45 \left[ \mathrm{X}_G^{0.5}\, \mathrm{Re}_L^{0.8}\, \mathrm{We}_L^{0.2} \mathrm{Sc}_L^{0.5} \left( \frac{a_S d_h}{1-\varepsilon} \right)^{0.25} \right]^{1.3}$ | High interaction |
| Turek and Lange (1981) | $\frac{k_L a}{s^{-1}} = 16.8 \cdot 10^4 \left( \frac{D}{m^2 s^{-1}} \right) \mathrm{Ga}_L^{-0.22}\, \mathrm{Re}_L^{0.25}\, \mathrm{Sc}_L^{0.5}$ | All regimes ($\mathrm{Re}_L < 1$) |
| Yaici *et al.* (1988) | $\frac{\mathrm{Sh}_G a d_p}{1-\beta} = 0.03 \phi^{-1.56}\, \mathrm{Re}_L^{0.33}\, \mathrm{Re}_G^{0.87}\, \mathrm{Sc}_G^{0.5} \left( \frac{d_p}{d_R} \right)^{-0.67}$ | All regimes |
| Goto and Smith (1975) | $\frac{k_{LS} a}{s^{-1}} = 10^4 \alpha_S \left( \frac{D}{m^2 s^{-1}} \right) \left( \frac{10^{-2}\, G_L / kg \cdot m^{-2} s^{-1}}{\mu_L / Pas} \right)^{n_S} (Sc_L)^{1/3}$<br>$\alpha_S = -57780 \left( \frac{d_p}{m} \right) + 184.3$<br>$n_S = -58.86 \left( \frac{d_p}{m} \right) + 0.7018$ | All regimes |

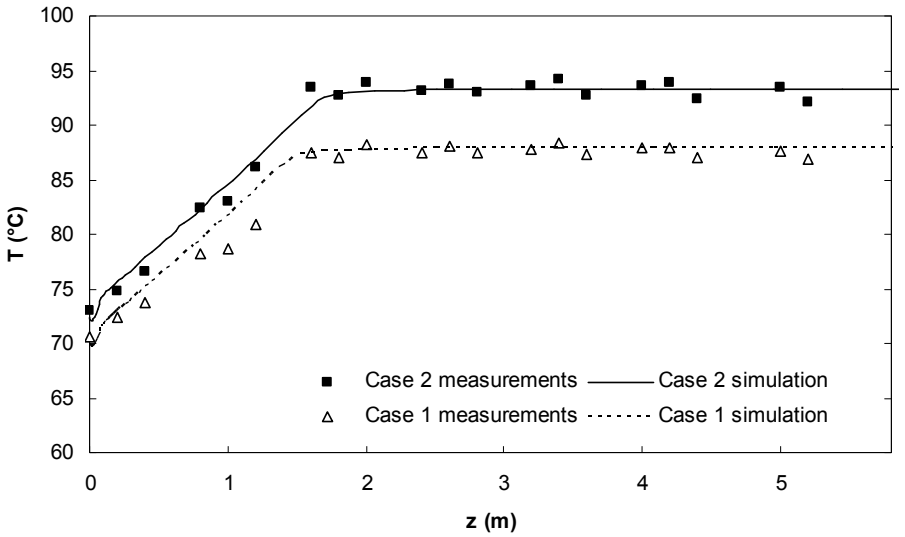


**Figure 25. Comparison of measured and simulated liquid temperature profiles in the trickle-bed reactor.**

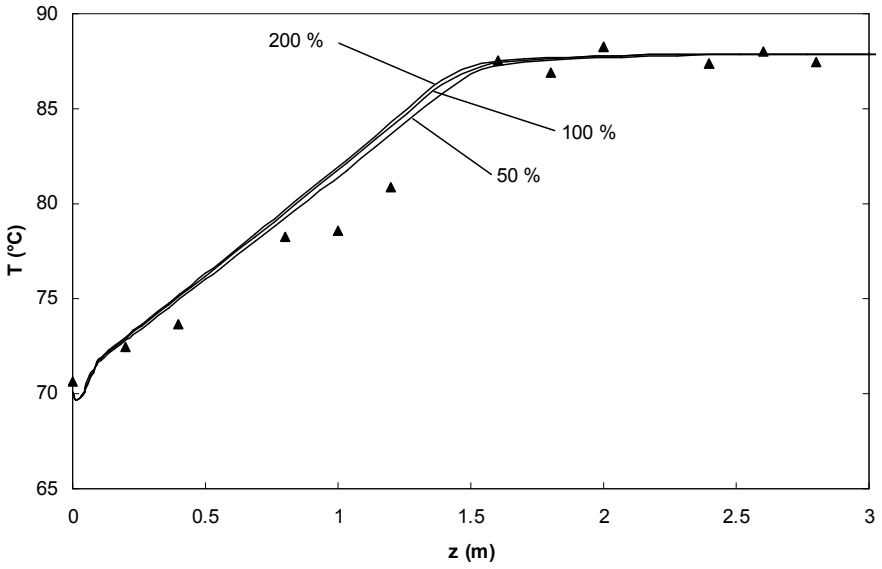


**Figure 26. Effect of $k_{LS}a$ values scaled to 50 % and 200 % of calculated value on the simulated temperature profile. (Case 1; ▲ measured values)**

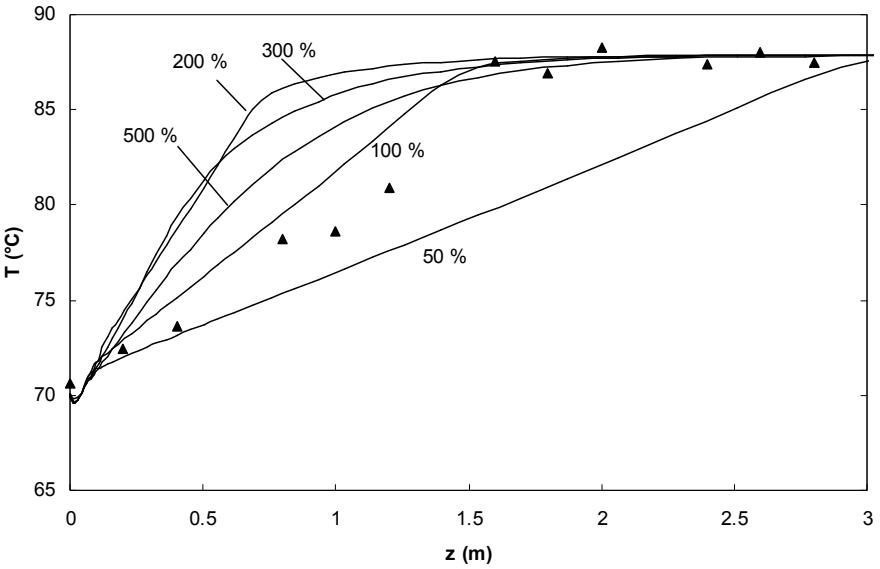


**Figure 27. Effect of $k_{Li}a$ values scaled to 50 %, 200 %, 300 %, and 500 % of calculated value on the simulated temperature profile. (Case 1; ▲ measured values)**

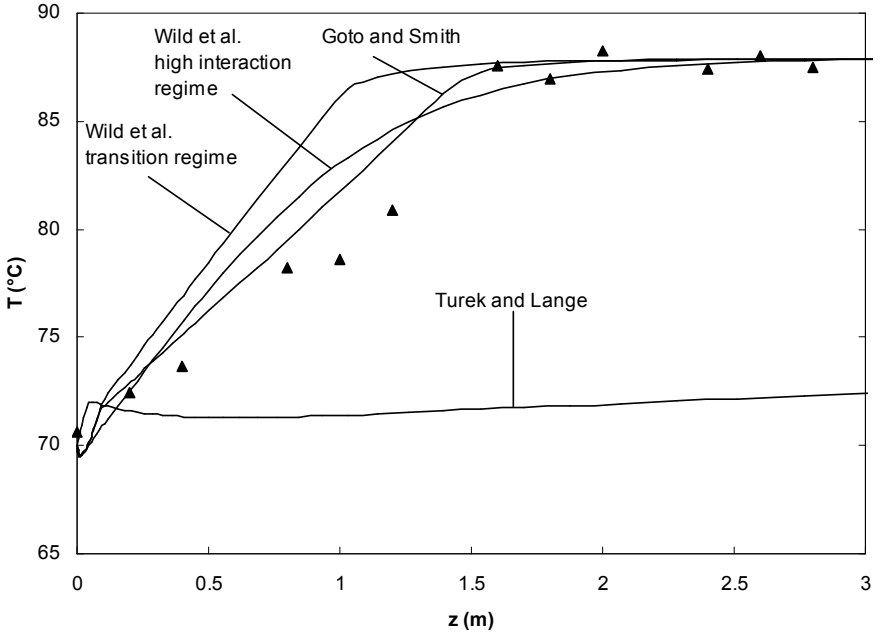


**Figure 28. Effect of the choice of different correlations for $k_{Li}a$ on the simulated temperature profile. (Case 1; ▲ measured values)**

**Table 3. Liquid film mass transfer coefficients calculated with different correlations in Case 1.**

| Correlation | Compound | $k_{Li,eff}a_{GL}$ (1/s) Inlet | Outlet |
|---|---|---|---|
| Goto and Smith | $H_2$ | 0.0428 | 0.0473 |
| | Benzene | 0.0326 | 0.0362 |
| | Cyclohexane | 0.0312 | 0.0356 |
| Wild *et al.* high interaction regime | $H_2$ | 1.03 | 1.15 |
| | Benzene | 0.852 | 0.956 |
| | Cyclohexane | 0.825 | 0.925 |
| Wild *et al.* transition regime | $H_2$ | 0.0473 | 0.0434 |
| | Benzene | 0.0511 | 0.0467 |
| | Cyclohexane | 0.0517 | 0.0473 |
| Turek and Lange | $H_2$ | 0.0017 | 0.0017 |
| | Benzene | 0.0013 | 0.0013 |
| | Cyclohexane | 0.0012 | 0.0013 |

## 6.3 Vapor-Liquid Equilibrium

Accurate vapor-liquid equilibrium (VLE) models are an important part of any chemical engineering model involving multiple phases. In this work, VLE models are needed for the trickle-bed reactor model in [IV] and the continuous-contact separation process model in [III]. In both cases a VLE model is needed for calculating the *K*-factor at the interface of the two films in the double film model. The *K*-factor appears explicitly in eq (6.18):

$$Q_i^I \equiv K_i x_i^I - y_i^I = 0 \tag{6.18}$$

Publications [V] and [VI] show how the model parameters for vapor-liquid equilibrium models can be obtained using measured VLE data.

$$K_i = \frac{y_i}{x_i} = \frac{\gamma_i \varphi_i^s p_i^s}{\varphi_i p} \exp\left( \int_{p_i^s}^{p} \frac{V_i^L}{RT} dp \right) \tag{6.34}$$

$\gamma_i$ is the activity coefficient for component *i*, $\varphi_i$ is the fugacity coefficient in the vapor phase for component *i*, and $\varphi_i^s$ is the saturated liquid fugacity coefficient for pure component *i* at system temperature. The exponential term is called the Poynting correction, which is often omitted since its contribution is negligible at low pressure. If the behavior of the liquid phase is near-ideal in the system under consideration, then the activity coefficient is usually neglected and eq (6.34) is reduced to:

$$\frac{y_i}{x_i} = \frac{\varphi_i^s p_i^s}{\varphi_i p} \tag{6.35}$$

This is the case in Publications [III] and [IV]. In [III], the fugacity coefficients were modeled with the Peng-Robinson (1976) equation of state. In [IV] the Graboski and Daubert (1978) modification of the Soave equation of state, which is supposed to be more accurate for hydrocarbon systems with hydrogen, was used.

The subjects of Publications [V] and [VI] are the VLE of *trans*-2-butene and *cis*-2-butene with 5 alcohols, respectively. Those components are relevant for example in the MTBE and iso-octene production processes, where they can be found either as reactants (methanol) or feed impurities. Reactive distillation of MTBE is an important industrial process that is also used as a prototype process for the modeling of reactive distillation. It can be used either for the production of the fuel component MTBE (Sundmacher and Hoffmann, 1996, Kenig *et al.*, 1999) or for the separation of a mixture of $C_4$-components. (Qi *et al.*, 2002) Another reactive distillation process with similar components is the dehydration of *tert*-butyl alcohol to produce isobutene. (Götze *et al.*, 2001, Qi and Sundmacher, 2006)

The components show unideal behavior in the liquid phase, and therefore an activity coefficient model, namely the Wilson (1964) model, was chosen to model the VLE. The experimental data were obtained using a total pressure apparatus and Barker's (1953) data reduction method. In the total pressure apparatus, total pressure, temperature, and the total volume of the components fed into the cell are recorded at each measurement point. The total number of moles and the total composition are then calculated from the feed volumes. Barker's method is based on the assumption that a VLE model can predict the bubble point pressure with smaller modeling error than the experimental error of the pressure measurements. More information on the apparatus, the experimental setup, and the data reduction procedure is given in Uusi-Kyyny *et al.* (2002). The data were first modeled using a Legendre polynomial with a variable number of coefficients, and then the Wilson model parameters were determined using the fitted Legendre polynomial. Details of the experimental setup and the data fitting procedure, as well as the data itself, can be found in [V] and [VI]. The fitted Wilson model parameters are given in Table 4. These parameters can be directly used for VLE estimation in process simulators.

**Table 4. Liquid activity coefficient model parameters for the Wilson model for *trans*-2-butene and *cis*-2-butene + alcohols.**

| *trans*-2-Butene (1) | + Methanol | + 1-Propanol | + 2-Propanol | + 2-Butanol | + 2-Methyl-2-propanol |
|---|---|---|---|---|---|
| Wilson $\lambda_{2,1}$/K | 896.7 | 639.8 | 540.3 | 449.3 | 395 |
| Wilson volume ratio | 2.197 | 1.193 | 1.165 | 0.971 | 0.943 |
| *cis*-2-Butene (1) | | | | | |
| Wilson $\lambda_{1,2}$/K | 168.4 | 101.4 | 90.30 | 76.64 | 53.11 |
| Wilson $\lambda_{2,1}$/K | 883.8 | 625.2 | 525.9 | 442.0 | 383.9 |
| Wilson volume ratio | 2.149 | 1.494 | 1.139 | 0.949 | 0.922 |

Figure 29 shows the measured pressure-composition diagrams for the *trans*-2-butene + alcohol –systems. Figure 30 shows the calculated activity coefficient-composition

diagram for the same systems. The measured VLE was also compared against predictions by the group contribution methods UNIFAC and UNIFAC-Dortmund. Figure 31 shows the measured pressure-composition diagram for the system *trans*-2-butene + methanol, compared to the model predictions with the UNIFAC and UNIFAC-Dortmund models. The corresponding figures for *cis*-2-butene + alcohols are very similar and can be found in [VI].

The results show that both the UNIFAC and UNIFAC-Dortmund models are able to predict the azeotrope in the *trans*-2-butene + methanol system, but UNIFAC-Dortmund does this more precisely. (The same applies for the *cis*-2-butene + methanol system; The UNIFAC models do not distinguish between the *trans*- and *cis*-forms.) A comparison of the accuracy of the UNIFAC models for the other systems is given in [V] and [VI]. The results show that the UNIFAC models can be used as a good estimate for the VLE in these systems when fitted model parameters are not available.

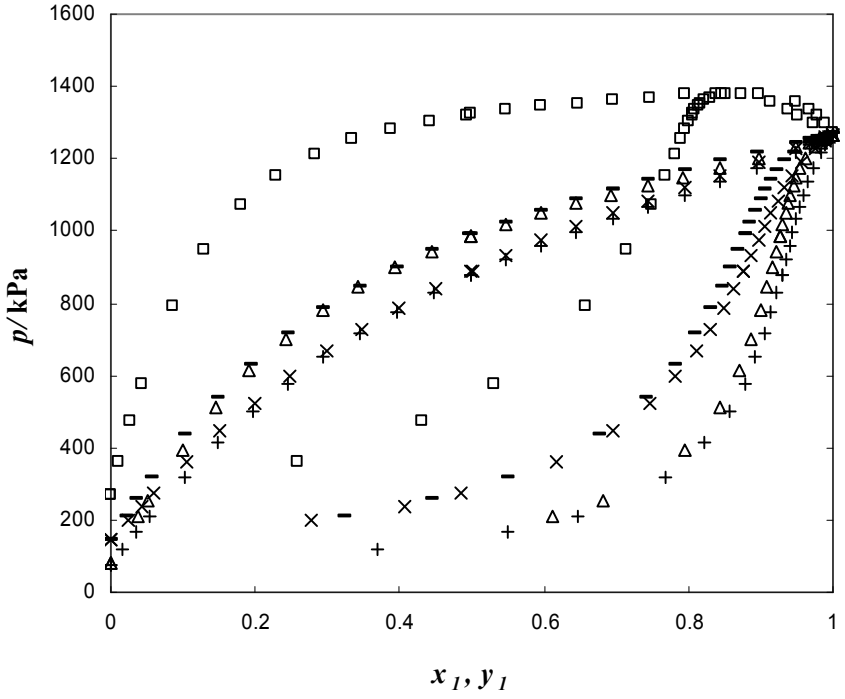


**Figure 29. Pressure-composition diagram for *trans*-2-butene (1) + alcohol (2) at 364.5 K: (□) trans-2-butene + methanol; (Δ) + 1-propanol; (-) + 2-propanol; (+) + 2-butanol; (×) + 2-methyl-2-propanol**

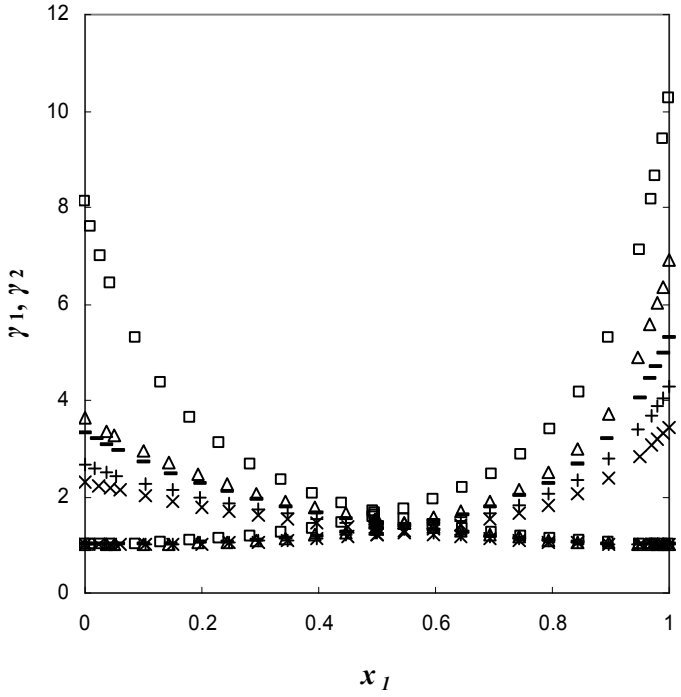


**Figure 30. Activity coefficient-composition diagram for *trans*-2-butene (1) + alcohol (2) at 364.5 K: (□) trans-2-butene + methanol; (Δ) + 1-propanol; (-) + 2-propanol; (+) + 2-butanol; (×) + 2-methyl-2-propanol**

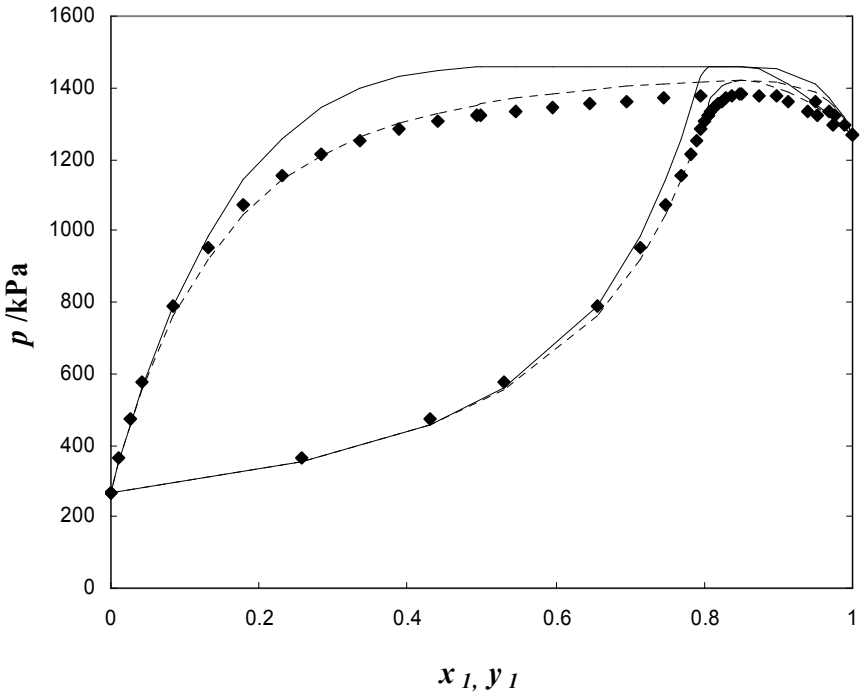


**Figure 31. Pressure-composition diagram for the *trans*-2-butene (1) + methanol (2) system at 364.5 K. ( ♦ ) experimental values; (—) UNIFAC results; (---) UNIFAC-Dortmund results**

# 7 Conclusions

This thesis presents the outline for modeling and simulation of chemical processes with the moment method, together with essential data that are needed for the closure models. It presents the fundamentals of the method and some important applications, such as catalyst deactivation and dynamic simulation of chemical reactors and continuous-contact separation processes.

The moment method may prove to be a viable alternative for the dynamic simulation of trickle-bed reactors and reactive distillation processes that are usually modeled using the nonequilibrium stage or similar models. The examples of closure models in Section 6 of this thesis are chosen such that they support especially the modeling of this type of processes.

The VLE and mass transfer correlation validation data can be directly used for the simulation of industrial processes. Although the purpose of this thesis is to deal with the fundamentals, the moment method as such is directly applicable to modeling and simulation of many industrial processes, such as chromatographic separation, packed-bed adsorption, or tubular reactors with axial dispersion. Further work needs to be done in order to make the moment method suitable for the simulation of distillation and absorption processes in more general cases. Especially the robustness and convergence issues associated with the method need to be improved. In its present form, the method works well in cases of simple distillation with near-ideal thermodynamics.

The goal is the development of a design tool, similar to DESIGNER, which is an integrated tool for reactive distillation based on the nonequilibrium stage model. (Kenig *et al.*, 1999) A tool like DESIGNER brings together all the physical properties data, the correlations, and the solvers needed for solving the process model under consideration. Clearly, the moment method has the potential to become a general solution method that can be used in such an integrated simulation environment.

## Notation

$A$ cross-sectional area ($m^2$), parameter in Onda's correlation, eq (6.23) ()

$[A]$ linear operator between moments and polynomial coefficients ()

$a$ interfacial mass transfer area ($m^2$ $m^{-3}$), mass transfer area on a stage in nonequilibrium stage model ($m^2$), parameter in Danckwert's expression for the concentration profile in a tubular reactor (), coefficient in WRM, parameter in trial function, lower domain boundary (), catalyst activity ()

$a_{GL}$ gas-liquid interfacial area ($m^2$ $m^{-3}$)

$a_p$ specific surface area of packing ($m^2$ $m^{-3}$)

$a_S$ solid-liquid interfacial area ($m^2$ $m^{-3}$)

$a_W$ reactor wall heat transfer area / reactor volume ($m^2$ $m^{-3}$)

$a'$ interfacial area density in a packed column ($m^2$ $m^{-3}$)

$B$ total molar buildup of a phase (mol $m^{-3}$ packing)

Bo Bodenstein number ($= D/uL$)

$b_i$ molar buildup of component $i$ in a phase (mol $m^{-3}$ packing),

$b$ weight of trial function (), upper domain boundary ()

$C$ concentration (mol $m^{-3}$)

$c$ polynomial coefficient ()

$c_p$ heat capacity (kJ $mol^{-1}$ $K^{-1}$)

$c_T$ total concentration (mol $m^{-3}$)

$Ca_L$ liquid capillary number ($= u_{SL}^2 \mu^L / \sigma$)

$D$ axial dispersion coefficient ($m^2$ $s^{-1}$)

$D_{AB}$ Fick diffusion coefficient in a binary mixture of A and B ($m^2$ $s^{-1}$)

$Đ_{ij}$ Maxwell-Stefan diffusion coefficient ($m^2$ $s^{-1}$)

$D_{i,eff}$ effective diffusivity ($m^2$ $s^{-1}$)

Da Damköhler number ($= kC_{ref}^{\alpha-1}\tau_S$)

$d_h$ Krischer and Kast hydraulic diameter ($= d_p \sqrt[3]{16\varepsilon^3/9\pi(1-\varepsilon)^2}$ , m)

$d_i$ driving force for mass diffusion ($m^{-1}$)

$d_p$ particle diameter, nominal packing diameter (m)

$d_R$ diameter of reactor in Yaici's correlation (m)

$E$ residence time distribution function ($s^{-1}$), energy buildup (kJ $m^{-3}$), energy transfer rate in nonequilibrium stage model (kW)

$\mathbf{E}$ energy balance equation in nonequilibrium stage model

$E_a$ activation energy (kJ $mol^{-1}$)

$E^I$ interface energy equation ()

$F$ flux (mol $m^{-2}$ $s^{-1}$, kW $m^{-2}$), feed stream in nonequilibrium stage model (mol $s^{-1}$)

$\overline{F}$ vector of equations in the moment method

$\vec{F}$ flux vector field in eq (3.27)

$F_j$ holdup discrepancy function in the moment method

$(\mathbf{F}_j)$ vector of equations for stage $j$ in nonequilibrium stage model

$f$ a function, normal flux in eq (3.28), component feed rate in nonequilibrium stage model (mol $s^{-1}$)

| | |
|---|---|
| $\mathrm{Fr}_L$ | liquid Froude number ($= u_{SL}^2 / d_p g$ in (2.37) or $= a_p u_{SL}^2 / g$ in eq (6.28)) |
| $G$ | superficial gas flow rate (mol $m^{-2}$ $s^{-1}$) |
| $G_L$ | liquid loading (kg $m^{-2}$ $s^{-1}$) |
| $\mathrm{Ga}_L$ | liquid Galileo number ($= d_p^3 g \rho_L^2 / \mu_L^2$) |
| $g$ | gravitational acceleration (m $s^{-2}$) |
| $H$ | enthalpy (kJ $mol^{-1}$), packing height in Bravo and Fair's correlation, eq (6.32) (m) |
| $\overline{H}$ | partial molar enthalpy (kJ $mol^{-1}$) |
| $\Delta H_R$ | heat of reaction (kJ $mol^{-1}$) |
| $h$ | heat transfer coefficient (kW $m^{-2}$ $K^{-1}$) |
| $h_L$ | liquid holdup ($m^3$ liquid/$m^3$ void) |
| $h_V$ | vapor holdup ($m^3$ vapor/$m^3$ void) |
| $\Delta h$ | height of packed bed section (m) |
| $[I]$ | identity matrix |
| $i$ | index () |
| $J$ | method order (), molar diffusion flux (mol $m^{-2}$ $s^{-1}$) |
| $(J)$ | vector of molar diffusion fluxes |
| $j$ | index () |
| $K$ | phase equilibrium coefficient () |
| $k$ | index (), reaction rate constant ($s^{-1}$) |
| $k_c$ | effective mass transfer coefficient in the adsorber model (m $s^{-1}$) |
| $k_i$ | mass transfer coefficient for component $i$ (m $s^{-1}$) |
| $k_{i,eff}$ | effective mass transfer coefficient for component $i$ (m $s^{-1}$) |
| $k_0$ | pre-exponential factor in reaction rate expression ($s^{-1}$) |
| $k_1$ | parameter in the fixed-bed adsorber model () |
| $k_2$ | parameter in the fixed-bed adsorber model () |
| $L$ | superficial liquid flow rate (mol $m^{-2}$ $s^{-1}$), liquid flow rate in nonequilibrium stage model (mol $s^{-1}$), domain length (m), differential equation |
| $l$ | index (), film thickness (m) |
| $\boldsymbol{M}$ | material balance equation in nonequilibrium stage model |
| $m$ | moment of a distribution () |
| $N$ | mass transfer flux (mol $m^{-2}$ $s^{-1}$), degree of trial function |
| $N_t$ | total mass transfer flux (mol $m^{-2}$ $s^{-1}$) |
| $(N)$ | vector of molar mass transfer fluxes |
| $n$ | number of components |
| $\dot{n}$ | molar flux (mol $s^{-1}$) |
| $\vec{n}$ | surface normal |
| $n_L$ | parameter in Goto and Smith's correlation () |
| $n_S$ | parameter in Goto and Smith's correlation () |
| nc | number of components () |
| $P$ | pressure (Pa), polynomial basis function () |
| $\boldsymbol{P}$ | pressure equation in nonequilibrium stage model |
| $\Delta P$ | pressure drop (Pa $m^{-1}$) |
| Pe | Péclet number ($= uL/D$) |
| $\mathrm{Pe}_h$ | mass Péclet number ($= uL/D$) |

| | |
|---|---|
| $\mathrm{Pe}_m$ | heat Péclet number ($= uL/\alpha$) |
| $Q$ | energy input or loss in nonequilibrium stage model (kW) |
| $Q^I$ | thermodynamic equilibrium equation () |
| $\mathsf{Q}$ | Interface equilibrium equation in nonequilibrium stage model |
| $q$ | concentration in bed material (mol $m^{-3}$), interphase heat flux (kW) |
| $R$ | radius (m), universal gas constant (kJ $mol^{-1}$ $K^{-1}$), residual () |
| $\mathsf{R}$ | mass transfer rate equation in nonequilibrium stage model |
| $R_0$ | shortcut notation for inflow boundary condition in moment method |
| $R_1$ | shortcut notation for outflow boundary condition in moment method |
| $R_d$ | retardation factor in packed-bed adsorber model () |
| $R_L$ | liquid phase reaction rate (mol $m^{-3}$ liquid $s^{-1}$) |
| $R_V$ | vapor phase reaction rate (mol $m^{-3}$ vapor $s^{-1}$) |
| $(R)$ | vector of mass transfer equations () |
| $[R]$ | matrix function of inverted binary mass transfer coefficients (s $m^{-1}$) |
| Re | Reynolds number ($= u_s \rho d_p / \mu$) |
| Re' | modified Reynolds number in Onda's correlation ($= u_s \rho / \mu a'$) |
| $r$ | ratio of side stream to interstage flow in nonequilibrium stage model () |
| $r_d$ | catalyst deactivation rate ($s^{-1}$) |
| $S$ | general source term (), surface area ($m^2$), sidestream flow rate in nonequilibrium stage model (mol $s^{-1}$), summation equation () |
| $S_i$ | control volume face in eqs (3.28) and (3.29) |
| $\mathsf{S}$ | summation equation in nonequilibrium stage model |
| $\overline{S}$ | solution vector in the moment method |
| Sc | Schmidt number ($= \mu / D\rho$) |
| Sh | Sherwood number ($= kad_p^2 / D$) |
| Sh' | modified Sherwood number ($= kad_h^2 / D$) |
| $T$ | temperature (K) |
| $t$ | time (s) |
| $t_m$ | mean residence time (s) |
| $u$ | interstitial velocity (m $s^{-1}$) |
| $u_s$ | superficial velocity (m $s^{-1}$) |
| $V$ | volume ($m^3$), superficial vapor flow rate (mol $m^{-2}$ $s^{-1}$), vapor flow rate in nonequilibrium stage model (mol $s^{-1}$) |
| $V_i^L$ | liquid molar volume of component $i$ ($m^3$ mol) |
| $V_\mathrm{r}$ | volume of a reactor ($m^3$) |
| $\dot{V}$ | volumetric flow rate ($m^3$ $s^{-1}$) |
| $W$ | weighting function () |
| $w$ | polynomial weight (), weighting function in the orthogonality condition () |
| $\mathrm{We}_L$ | liquid Weber number ($= u_{sL}^2 d_p \rho_L / \sigma_L$) |
| $X$ | conversion () |
| $\mathrm{X}_G$ | Lockhart-Martinelli number ($= u_{sG}\sqrt{\rho_G} / u_{sL}\sqrt{\rho_L}$) |
| $x$ | liquid mole fraction (), axial coordinate (m) |

$(x_j)$ vector of independent variables for stage *j* in nonequilibrium stage model
$y$ vapor or gas mole fraction (), trial function ()
$z$ axial coordinate (m)
$z_m$ collocation point (m)

Greek Symbols

$\alpha$ thermal axial dispersion coefficient ($m^2\ s^{-1}$), reaction order in eq (2.9) (), constant in eqs (3.7) – (3.9) ()
$\alpha_L$ parameter in Goto and Smith's correlation ()
$\alpha_S$ parameter in Goto and Smith's correlation ()
$\beta$ liquid holdup a trickle-bed reactor ()
$[\Gamma]$ matrix of thermodynamic factors
$\gamma_i$ activity coefficient of component *i* in solution ()
$\delta$ Dirac's delta function
$\delta(i,j)$ Kronecker delta
$\varepsilon$ void fraction ()
$\xi$ dimensionless axial coordinate
$\zeta$ dimensionless axial coordinate
$\eta$ dimensionless position within film
$[\Theta]$ matrix of rate factors for nonideal systems ()
$\theta$ dimensionless time
$\kappa$ binary Maxwell-Stefan mass transfer coefficient ($m\ s^{-1}$)
$\mu$ viscosity (Pas), molar chemical potential ($kJ\ mol^{-1}$)
$\nu$ stoichiometric coefficient ()
$\Xi_{i,eff}$ high-flux correction factor in effective diffusivity method ()
$[\Xi]$ matrix of high-flux correction factors ()
$\rho$ density ($kg\ m^{-3}$)
$\sigma$ standard deviation (), surface tension ($N\ m^{-1}$)
$\sigma_c$ critical surface tension ($N\ m^{-1}$)
$\tau$ reference time (s)
$\tau_S$ space time (s)
$\Phi_{i,eff}$ mass transfer rate factor in effective diffusivity method
$[\Phi]$ matrix of mass transfer rate factors ()
$\varphi_i$ fugacity coefficient of component *i* in vapor phase ()
$\varphi_i^s$ saturated liquid fugacity coefficient for pure component *i* ()
$\phi$ trial function
$\Psi$ general concentration ($mol\ m^{-3}$, $kJ\ m^{-3}$, other)
$\psi$ dimensionless concentration

Subscripts and Superscripts

| | |
|---|---|
| 0 | inflow, initial value |
| 1 | outflow |
| *B* | bulk phase |
| *corr* | value obtained from a correlation |
| *eff* | effective |
| *FS* | fluid-solid |
| *G* | gas phase |
| *GL* | gas-liquid |
| *I* | interface |
| *i* | index, component *i* |
| *j* | index, stage *j* in nonequilibrium stage model, $j^{th}$ moment in moment model |
| *L* | liquid phase, with reference to total domain length |
| *LS* | liquid-solid |
| *m* | index, polynomial degree, index of trial function |
| *n* | index |
| *ref* | reference value |
| *S* | solid (catalyst) phase |
| *t* | total |
| *V* | vapor phase |
| *VL* | vapor-liquid |
| *W* | reactor wall |
| * | dimensionless |
| ^ | calculated from polynomial approximation |
| ● | referring to finite transfer rates |
| + | downstream side of a boundary |
| − | upstream side of a boundary |

## References


Alopaeus, V., Hynynen, K., Aittamaa, J., 2006a. A Cellular Automata Model for Liquid Distribution in Trickle Bed Reactors. *Chemical Engineering Science,* 61, 4930-4943.

Alopaeus, V., Laakkonen, M., Aittamaa, J., 2006b. Solution of Population Balances with Breakage and Agglomeration by High Order Moment-Conserving Method of Classes. *Chemical Engineering Science,* 61, 6732-6752.

Alopaeus, V., Laakkonen, M., Aittamaa, J., 2007. Solution of Population Balances with Growth and Nucleation by High Order Moment-Conserving Method of Classes. *Chemical Engineering Science,* 62, 2277-2289.

Alopaeus, V., Laavi, H., Aittamaa, J., 2008. A Dynamic Model for Plug Flow Reactor State Profiles. *Computers & Chemical Engineering,* 32, 1494-1506.

Avraam, D. G., Vasalos, I. A., 2003. HdPro: A Mathematical Model of Trickle-Bed Reactors for the Catalytic Hydroprocessing of Oil Feedstocks. *Catalysis Today,* 79-80, 275-283.

Barker, J. A., 1953. Determination of Activity Coefficients from Total Pressure Measurements. *Australian Journal of Chemistry,* 6, 207-210.

Baten, J. M., Ellenberger, J., Krishna, R., 2001. Radial and Axial Dispersion of the Liquid Phase within a KATAPAK-S® Structure: Experiments vs. CFD Simulations. *Chemical Engineering Science,* 56, 813-821.

Bhaskar, M., Valavarasu, G., Sairam, B., Balamaran, K. S., Balu, K, 2004. Three-Phase Reactor Model to Simulate the Performance of Pilot-Plant and Industrial Trickle-Bed Reactors Sustaining Hydrotreating Reactions. *Industrial & Engineering Chemistry Research,* 43, 6654-6669.

Bird, R. B., Stewart, W. E., Lightfoot, E. N., 1960. *Transport Phenomena.* 2nd ed. New York: Wiley.

Birtill, J. J., 2007. Measurement and Modeling of the Kinetics of Catalyst Decay in Fixed Beds: The Eurokin Survey. *Industrial & Engineering Chemistry Research,* 46, 2392-2398.

Bischoff, K. B., 1961. A Note on Boundary Conditions for Flow Reactors. *Chemical Engineering Science,* 16, 131-133.

Bravo, J. L., Fair, J. R., 1982. Generalized Correlation for Mass Transfer in Packed Distillation Columns. *Industrial & Engineering Chemistry Process Design and Development,* 21, 162-170.

Buchanan, J. E., 1969. Pressure Gradient and Liquid Holdup in Irrigated Packed Towers. *Industrial & Engineering Chemistry Fundamentals,* 8, 502-511.

Buzzi-Ferraris, G., Facchi, E., Forzatti, P., Tronconi, E., 1984. Control Optimization of Tubular Catalytic Reactors with Catalyst Decay. *Industrial & Engineering Chemistry Process Design and Development,* 23, 126-131.

Chilton, T. H., Colburn, A. P., 1934. Mass Transfer (Absorption) Coefficients. *Industrial & Engineering Chemistry,* 26, 1183-1187.

Cho, Y. S., Joseph, B., 1983. Reduced-Order Steady-State and Dynamic Models for Separation Processes. *AIChE Journal,* 29, 261-276.

Churchill, S. W., 2007. Role of Universalities in Chemical Engineering. *Industrial & Engineering Chemistry Research,* 46, 7851-7869.

Cruz, P., Santos, J. C., Magalhães, F. D., Mendes, A., 2005. Simulation of Separation Processes Using Finite Volume Method. *Computers & Chemical Engineering,* 30, 83-98.

Danckwerts, P. V., 1953. Continuous Flow Systems. *Chemical Engineering Science,* 2, 1-13.

Davis, M. E., 1984. Numerical Methods and Modeling for Chemical Engineers. New York: John Wiley & Sons.

Deckwer, W. D., Mählmann, E. A., 1976. Boundary Conditions of Liquid Phase Reactors with Axial Dispersion. *Chemical Engineering Journal,* 11, 19-25.

Dorao, C. A., Jakobsen, H. A., 2006. A least squares method for the solution of population balance problems. *Computers and Chemical Engineering,* 30, 535-547.

Dunn, W. E., Vermeulen, T., Wilke, C. R., Word, T. T., 1977. Longitudinal Dispersion in Packed Gas-Absorption Columns. *Industrial & Engineering Chemistry Fundamentals,* 1, 116-124.

Ellenberger, J., Krishna, R., 1999. Counter-Current Operation of Structured Catalytically Packed Distillation Columns: Pressure Drop, Holdup and Mixing. *Chemical Engineering Science,* 54, 1339-1345.

Fan, L. T., Shen, B. C., Chou, S. T., 1995. Stochastic modeling of transient residence-time distributions during start-up. *Chemical Engineering Science,* 50, 211-221.

Feintuch, H. M., Treybal, R. E., 1978. The Design of Adiabatic Packed Towers for Gas Absorption and Stripping. *Industrial & Engineering Chemistry Process Design and Development,* 17, 505-513.

Ferziger, J. H., Perić, M., 2002. *Computational Methods for Fluid Dynamics.* 3rd ed. Berlin: Springer-Verlag.

Finlayson, B. A., 1972. *The Method of Weighted Residuals and Variational Principles.* New York: Academic Press.

Finlayson, B. A., 1980. *Nonlinear Analysis in Chemical Engineering.* New York: McGraw-Hill.

Fletcher, C. A. J., 1991. *Computational Techniques for Fluid Dynamics. Volume 1. Fundamental and General Techniques.* 2nd ed. Berlin: Springer-Verlag.

Fogler, H. S., 1999. *Elements of Chemical Reaction Engineering.* Upper Saddle River (NJ): Prentice-Hall.

Golz, W. J., 2003. *Solute Transport in a Porous Medium: A Mass-Conserving Solution for the Convective-Dispersion Equation in a Finite Domain.* Dissertation, Louisiana State University.

Golz, W. J., Dorroh, J. R., 2001. The Convection-Diffusion Equation for a Finite Domain with Time-Varying Boundaries. *Applied Mathematics Letters,* 14, 983-988.

Goto, S., Smith, J. M., 1975. Trickle-Bed Reactor Performance. Part I. Holdup and Mass Transfer Effects. *AIChE Journal,* 21, 706-713.

Götze, L., Bailer, O., Moritz, P., von Scala, C., 2001. Reactive distillation with KATAPAK®. *Catalysis Today,* 69, 201-208.

Graboski, M. S., Daubert, T. E., 1978. A Modified Soave Equation of State for Phase Equilibrium Calculations. 1. Hydrocarbon Systems. *Industrial & Engineering Chemistry Process Design and Development,* 17, 443-448.

Gunaseelan, P., Wankat, P. C., 2002. Transient Pressure and Flow Predictions for Concentrated Packed Absorbers Using a Dynamic Nonequilibrium Model. *Industrial & Engineering Chemistry Research,* 41, 5775-5788.

Guo, J., Jiang, Y., Al-Dahhan, M. H., 2008. Modeling of Trickle-Bed Reactors with Exothermic Reactions Using Cell Network Approach. *Chemical Engineering Science,* 63, 751-764.

Henry, H. C., Gilbert, J. B., 1973. Scale Up of Pilot Plant Data for Catalytic Hydroprocessing. *Industrial & Engineering Chemistry Process Design and Development,* 12, 328-334.

Higler, A., Taylor, R., Krishna, R., 1998. Modeling of a Reactive Separation Process Using a Nonequilibrium Stage Model. *Computers & Chemical Engineering,* 22, 111-118.

Hitch, D. M., Rousseau, R. W., Ferrell, J. K., 1986. Simulation of Continuous-Contact Separation Processes: Multicomponent, Adiabatic Absorption. *Industrial & Engineering Chemistry Research,* 25, 699-705.

Hitch, D. M., Rousseau, R. W., Ferrell, J. K., 1987. Simulation of Continuous-Contact Separation Processes: Unsteady-State, Multicomponent, Adiabatic Absorption. *Industrial & Engineering Chemistry Research,* 26, 1092-1099.

Iannibello, A., Marengo, S., Burgio, G., Baldi, G., Sicardi, S., Specchia, V., 1985. Modeling the Hydrotreating Reactions of a Heavy Residual Oil in a Pilot Trickle-Bed Reactor. *Industrial & Engineering Chemistry Process Design and Development,* 24, 531-537.

Iliuta, I., Larachi, F., Grandjean, B. P. A., 2003. Fines Deposition Dynamics in Gas-Liquid Trickle-Flow Reactors. *AIChE Journal,* 49, 485-495.

Kenig, E. Y., 2008. Complementary Modelling of Fluid Separation Processes. *Chemical Engineering Research and Design,* 86, 1059-1072.

Kenig, E., Jakobsson, K., Banik, P., Aittamaa, J., Górak, A., Koskinen, M., Wettmann, P., 1999. An Integrated Tool for Synthesis and Design of Reactive Distillation. *Chemical Engineering Science,* 54, 1347-1352.

King, C. J., 1980. *Separation Processes.* 2nd ed. New York: McGraw-Hill.

Kister, H. Z., Mathias, P. M., Steinmeyer, D. E., Penney, W. R., Crocker, B. B., Fair, J. R., 2008. Equiment for Distillation, Gas Absorption, Phase Dispersion, and Phase Separation. In *Perry's Chemical Engineers' Handbook,* 8th ed. Green, D. W., Perry, R. H. (eds.). New York: McGraw-Hill.

Kołodziej, A., Jaroszyński, M., Bylica, I., 2004. Mass Transfer and Hydraulics for KATAPAK-S. *Chemical Engineering and Processing,* 43, 457-464.

Kooijman, H. A., Taylor, R., 1995. A Nonequilibrium Model for Dynamic Simulation of Tray Distillation Columns. *AIChE Journal,* 41, 1852-1863.

Korsten, H., Hoffmann, U., 1996. Three-Phase Reactor Model for Hydrotreating in Pilot Trickle-Bed Reactors. *AIChE Journal,* 42, 1350-1360.

Krambeck, F. J., Shinnar, R., Katz, S., 1967. Stochastic Mixing Models for Chemical Reactors. *Industrial & Engineering Chemistry Fundamentals,* 6, 276-288.

Krishna, R., 2002. Reactive Separations: More Ways to Skin a Cat. *Chemical Engineering Science,* 57, 1491-1504.

Krishnamurthy, R., Taylor, R., 1985a. A Nonequilibrium Stage Model of Multicomponent Separation Processes. *AIChE Journal,* 31, 449-465.

Krishnamurthy, R., Taylor, R., 1985b. Simulation of Packed Distillation and Absorption Columns. *Industrial & Engineering Chemistry Process Design and Development,* 24, 513-524.

Langmuir, I., 1908. The Velocity of Reactions in Gases Moving through Heated Vessels and the Effect of Convection and Diffusion. *Journal of the American Chemical Society,* 30, 1742-1754.

Lappalainen, K., 2009. *Modelling Gas-Liquid Flow in Trickle-Bed Reactors*. Dissertation, Helsinki University of Technology.

Levenspiel, O., 1972. *Chemical Reactor Engineering.* 2nd ed. New York: John Wiley & Sons.

Liao, H.-T., Shiau, C.-Y., 2000. Analytical Solution to an Axial Dispersion Model for the Fixed-Bed Adsorber. *AIChE Journal,* 46, 1168-1176.

Macías-Salinas, R., Fair, J. R., 2000. Axial Mixing in Modern Packings, Gas, and Liquid Phases: II. Two-Phase Flow. *AIChE Journal,* 46, 79-91.

Noeres, C., Kenig, E. Y., Górak, A., 2003. Modelling of Reactive Separation Processes: Reactive Absorption and Reactive Distillation. *Chemical Engineering and Processing,* 42, 157-178.

Ogunye, A. F., Ray, W. H., 1970. Optimization of a Vinyl Chloride Monomer Reactor. *Industrial & Engineering Chemistry Process Design and Development,* 9, 619-624.

Parulekar, S. J., Ramkrishna, D., 1984a. Analysis of Axially Dispersed Systems with General Boundary Conditions – I. Formulation. *Chemical Engineering Science,* 39, 1571-1579.

Parulekar, S. J., Ramkrishna, D., 1984b. Analysis of Axially Dispersed Systems with General Boundary Conditions – II. Solution for Dispersion in the Appended Sections. *Chemical Engineering Science,* 39, 1581-1597.

Parulekar, S. J., Ramkrishna, D., 1984c. Analysis of Axially Dispersed Systems with General Boundary Conditions – III. Solution for Unmixed and Well-Mixed Appended Sections. *Chemical Engineering Science,* 39, 1599-1611.

Patankar, S. V., 1980. *Numerical Heat Transfer and Fluid Flow.* New York: Hemisphere.

Peng, D.-Y., Robinson, D. B., 1976. A New Two-Constant Equation of State. *Industrial & Engineering Chemistry Fundamentals,* 15, 59-64.

Qi, Z., Sundmacher, K., 2006. Multiple Product Solutions of *tert*-Butyl Alcohol Dehydration in Reactive Distillation. *Industrial & Engineering Chemistry Research*, 45, 1613-1621.

Qi, Z., Sundmacher, K., Stein, E., Kienle, A., Kolah, A., 2002. Reactive Separation of Isobutene from C4 Crack Fractions by Catalytic Distillation Processes. *Separation and Purification Technology,* 26, 147-163.

Rice, R. G., Do, D. D., 1995. *Applied Mathematics and Modeling for Chemical Engineers*. New York: John Wiley & Sons.

Rocha, J. A., Bravo, J. L., Fair, J. R., 1993. Distillation Columns Containing Structured Packings: A Comprehensive Model for Their Performance. 1. Hydraulic Models. *Industrial & Engineering Chemistry Research,* 32, 641-651.

Rocha, J. A., Bravo, J. L., Fair, J. R., 1996. Distillation Columns Containing Structured Packings: A Comprehensive Model for Their Performance. 2. Mass-Transfer Model. *Industrial & Engineering Chemistry Research,* 35, 1660-1667.

Ruivo, R., Paiva, A., Mota, J. P. B., Simões, P., 2004. Dynamic Model of a Countercurrent Packed Column Operating at High Pressure Conditions. *Journal of Supercritical Fluids,* 32, 183-192.

Sereno, C., Rodrigues, A., Villadsen, J., 1991. The Moving Finite Element Method with Polynomial Approximation of Any Degree. *Computers & Chemical Engineering,* 15, 25-33.

Sereno, C., Rodrigues, A., Villadsen, J., 1992. Solution of Partial Differential Equations Systems by the Moving Finite Element Method. *Computers & Chemical Engineering,* 16, 583-592.

Srivastava, R. K., Joseph, B., 1984. Simulation of Packed-Bed Separation Processes Using Orthogonal Collocation. *Computers & Chemical Engineering,* 8, 43-50.

Sundmacher, K., Hoffmann, U., 1996. Development of a New Catalytic Distillation Process for Fuel Ethers Via a Detailed Nonequilibrium Model. *Chemical Engineering Science,* 51, 2359-2368.

Taylor, R., Krishna, R., 1993. *Multicomponent Mass Transfer*. New York: John Wiley & Sons.

Taylor, R., Krishna, R., 2000. Modelling Reactive Distillation. *Chemical Engineering Science,* 55, 5183-5229.

Toppinen, S., Aittamaa, J., Salmi, T., 1996. Interfacial Mass Transfer in Trickle-Bed Reactor Modelling. *Chemical Engineering Science,* 51, 4335-4345.

Trefethen, L. N., 2000. *Spectral Methods in MATLAB*. Philadelphia: SIAM.

Turek, F., Lange, R., 1981. Mass Transfer in Trickle-Bed Reactors at Low Reynolds Number. *Chemical Engineering Science,* 36, 569-579.

Uusi-Kyyny, P., Pokki, J.-P., Laakkonen, M., Aittamaa, J., Liukkonen, S., 2002. Vapor Liquid Equilibrium for the Binary Systems 2-Methylpentane + 2-Butanol at 329.2 K and *n*-Hexane + 2-Butanol at 329.2 and 363.2 K with a Static Apparatus. *Fluid Phase Equilibria,* 201, 343-358.

Villadsen, J., Michelsen, M. L., 1978. *Solution of Differential Equation Models by Polynomial Approximation.* Englewood Cliffs, NJ: Prentice-Hall.

Wagner, I., Stichlmair, J., Fair, J. R., 1997. Mass Transfer in Beds of Modern, High-Efficiency Random Packings. *Industrial & Engineering Chemistry Research,* 36, 227-237.

Wehner, J. F., Wilhelm, R. H., 1956. Boundary Conditions of Flow Reactor. *Chemical Engineering Science,* 6, 89-93.

Wild, G., Larachi, F., Charpentier, J. C., 1992. Heat and Mass Transfer in Gas-Liquid-Solid Fixed Bed Reactors. In Quintard, M., Todorovic, M. (eds.), *Heat and Mass Transfer in Porous Media.* Amsterdam: Elsevier.

Wilke, C. R., 1950. Diffusional Properties of Multicomponent Gases. *Chemical Engineering Progress,* 46, 95-104.

Wilson, G. M., 1964. Vapor-Liquid Equilibrium. XI. A New Expression for the Excess Free Energy of Mixing. *Journal of the American Chemical Society,* 86, 127-130.

Yaici, W., Laurent, A., Midoux, N., Charpentier, J.-C., 1988. Determination of Gas-Side Mass Transfer Coefficients in Trickle-Bed Reactors in the Presence of an Aqueous or an Organic Liquid Phase. *International Chemical Engineering,* 28, 299-305.

Zhang, W. W., Liu, C. J., Yuan, X. G., Yu, G. C., 2008. Prediction of Axial Mixing for a Structured Packed Column Using a Two-Equation Model. *Chemical Engineering & Technology,* 31, 208-214.

Zheng, Y., Gu, T., 1996. Analytical Solution to a Model for the Startup Period of Fixed-Bed Reactors. *Chemical Engineering Science,* 51, 3773-3779.